AD_____

CONTRACT NO.: DAMD17- 92-C-2071

TITLE: Mechanisms of Cutaneous Vesication

PRINCIPAL INVESTIGATOR: Nancy A. Monteiro-Riviere, Ph.D.
CO-AUTHORS: Jason Z. Zhang, B.M.
Alfred O. Inman, M.S.
Jim E. Riviere, D.V.M., Ph.D.

CONTRACTING ORGANIZATION: North Carolina State University
Raleigh, North Carolina 27606

REPORT DATE: December 16, 1995

TYPE OF REPORT: Final

PREPARED FOR: U.S. Army Medical Research and Materiel Command
Fort Detrick, Frederick, Maryland 21702-5012

REPORT DOCUMENTATION PAGE

Form Approved
OMB No. 0704-0188

1. AGENCY USE ONLY (Leave blank)	2. REPORT DATE	3. REPORT TYPE AND DATES COVERED
	December 16, 1995	Final (17 Jul 92 - 30 Nov 95)

4. TITLE AND SUBTITLE
Mechanisms of Cutaneous Vesication

5. FUNDING NUMBERS
DAMD17-92-C-2071

6. AUTHOR(S)
Nancy A. Monteiro-Riviere, Ph.D., Jason Z. Zhang, B.M., Alfred O. Inman, M.S., Jim E. Riviere, DVM, Ph.D.

7. PERFORMING ORGANIZATION NAME(S) AND ADDRESS(ES)
North Carolina State University
Raleigh, North Carolina 27606

8. PERFORMING ORGANIZATION REPORT NUMBER

9. SPONSORING/MONITORING AGENCY NAME(S) AND ADDRESS(ES)
U.S. Army Medical Research and Materiel Command
Fort Detrick, MD 21702-5012

10. SPONSORING/MONITORING AGENCY REPORT NUMBER

11. SUPPLEMENTARY NOTES

12a. DISTRIBUTION/AVAILABILITY STATEMENT
Approved for public release; distribution unlimited

12b. DISTRIBUTION CODE

13. ABSTRACT *(Maximum 200 words)*

This project investigated the mechanism of bis (2-chloroethyl) sulfide [sulfur mustard, HD] induced cutaneous vesication using the isolated perfused porcine skin flap (IPPSF) and *in vitro* cell cultures. Treatment of IPPSFs with 5.0 mg/ml of HD results in a characteristic increase in vascular resistance, decrease in glucose utilization, and the formation of gross and microblisters. The first study demonstrated that the vascular changes associated with HD vesication are accompanied by increases in the efflux of prostaglandins PGE_2 and $PGF_{2\alpha}$. Additionally, studies were designed to evaluate the protective effects of sodium thiosulfate, cysteine, niacinamide and indomethacin. Treatments with niacinamide and indomethacin resulted in an inhibition of the vascular response and microvesicles were partially prevented with indomethacin. These data suggested that none of these agents alone would be successful antivesicant and different mechanisms are involved in the production of dark basal cells, microvesicles, and the vascular response. Unfortunately, blocking of the cellular toxicity as evidenced by dark basal cell formation did not prevent vesication, suggesting

14. SUBJECT TERMS	15. NUMBER OF PAGES
Pig;Skin;Porcine;Percutaneous Absorption;Pharmacology; Vesicants; Sulfur Mustard;Laminin;Prostaglandins;Toxicokinetics; Chemical Warfare;Morphology;Immunohistochemistry;ElectronMicroscopy	160
	16. PRICE CODE

17. SECURITY CLASSIFICATION OF REPORT	18. SECURITY CLASSIFICATION OF THIS PAGE	19. SECURITY CLASSIFICATION OF ABSTRACT	20. LIMITATION OF ABSTRACT
Unclassified	Unclassified	Unclassified	Unlimited

GENERAL INSTRUCTIONS FOR COMPLETING SF 298

The Report Documentation Page (RDP) is used in announcing and cataloging reports. It is important that this information be consistent with the rest of the report, particularly the cover and title page. Instructions for filling in each block of the form follow. It is important to ***stay within the lines*** to meet ***optical scanning requirements***.

Block 1. Agency Use Only *(Leave blank)*.

Block 2. Report Date. Full publication date including day, month, and year, if available (e.g. 1 Jan 88). Must cite at least the year.

Block 3. Type of Report and Dates Covered. State whether report is interim, final, etc. If applicable, enter inclusive report dates (e.g. 10 Jun 87 - 30 Jun 88).

Block 4. Title and Subtitle. A title is taken from the part of the report that provides the most meaningful and complete information. When a report is prepared in more than one volume, repeat the primary title, add volume number, and include subtitle for the specific volume. On classified documents enter the title classification in parentheses.

Block 5. Funding Numbers. To include contract and grant numbers; may include program element number(s), project number(s), task number(s), and work unit number(s). Use the following labels:

C	- Contract	**PR**	- Project
G	- Grant	**TA**	- Task
PE	- Program Element	**WU**	- Work Unit Accession No.

Block 6. Author(s). Name(s) of person(s) responsible for writing the report, performing the research, or credited with the content of the report. If editor or compiler, this should follow the name(s).

Block 7. Performing Organization Name(s) and Address(es). Self-explanatory.

Block 8. Performing Organization Report Number. Enter the unique alphanumeric report number(s) assigned by the organization performing the report.

Block 9. Sponsoring/Monitoring Agency Name(s) and Address(es). Self-explanatory.

Block 10. Sponsoring/Monitoring Agency Report Number. *(If known)*

Block 11. Supplementary Notes. Enter information not included elsewhere such as: Prepared in cooperation with...; Trans. of...; To be published in.... When a report is revised, include a statement whether the new report supersedes or supplements the older report.

Block 12a. Distribution/Availability Statement. Denotes public availability or limitations. Cite any availability to the public. Enter additional limitations or special markings in all capitals (e.g. NOFORN, REL, ITAR).

- **DOD** - See DoDD 5230.24, "Distribution Statements on Technical Documents."
- **DOE** - See authorities.
- **NASA** - See Handbook NHB 2200.2.
- **NTIS** - Leave blank.

Block 12b. Distribution Code.

- **DOD** - Leave blank.
- **DOE** - Enter DOE distribution categories from the Standard Distribution for Unclassified Scientific and Technical Reports.
- **NASA** - Leave blank.
- **NTIS** - Leave blank.

Block 13. Abstract. Include a brief *(Maximum 200 words)* factual summary of the most significant information contained in the report.

Block 14. Subject Terms. Keywords or phrases identifying major subjects in the report.

Block 15. Number of Pages. Enter the total number of pages.

Block 16. Price Code. Enter appropriate price code *(NTIS only)*.

Blocks 17. - 19. Security Classifications. Self-explanatory. Enter U.S. Security Classification in accordance with U.S. Security Regulations (i.e., UNCLASSIFIED). If form contains classified information, stamp classification on the top and bottom of the page.

Block 20. Limitation of Abstract. This block must be completed to assign a limitation to the abstract. Enter either UL (unlimited) or SAR (same as report). An entry in this block is necessary if the abstract is to be limited. If blank, the abstract is assumed to be unlimited.

*U.S.GPO:1993-0-358-779

DISCLAIMER NOTICE

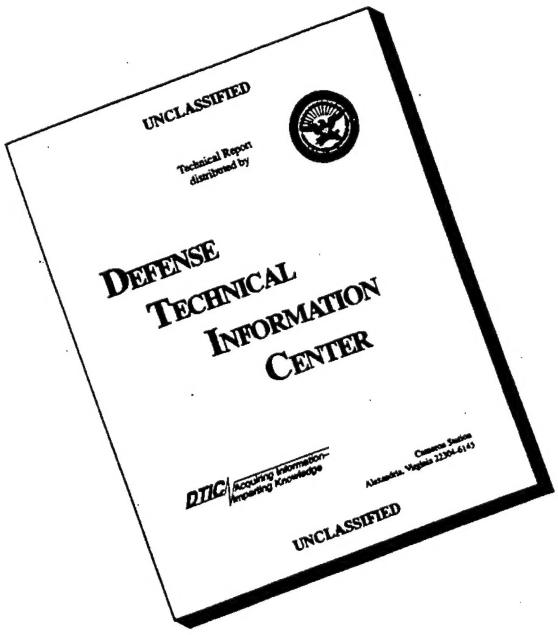

THIS DOCUMENT IS BEST QUALITY AVAILABLE. THE COPY FURNISHED TO DTIC CONTAINED A SIGNIFICANT NUMBER OF PAGES WHICH DO NOT REPRODUCE LEGIBLY.

13. **ABSTRACT (continued)**

that other mechanisms must be operative and that there is a multistep, biochemical process that leads to the blister. The flux of HD through the skin was investigated to determine if metabolites are formed due to epidermal metabolism. These experiments showed that little, if any HD, appears in the venous perfusate and that epidermal metabolism of HD does occur to a significant degree in the IPPSF. Assessment of extracellular and intravascular space using radiolabeled inulin and albumin infusions, respectively, demonstrated that HD primarily produced an increase in intravascular space. Thus, these studies unequivocally demonstrate a vascular component to HD vesication directly mediated by cutaneous elements, since the IPPSF is an isolated system not associated with a systemic immune response. A second study probed the molecular basis of HD interaction with laminin, a basement membrane component previously implicated by our group to be primarily involved in HD-induced epidermal-dermal separation. HD directly alkylated laminin and reduced its cell adhesive activity through a non-cytotoxic mechanism This is a significant finding, since not only does it offer insight into HD-induced epidermal-dermal separation, but it also suggests hypotheses as to the reasons for delayed epidermal regeneration and healing in HD wounds. To further probe the molecular basis of HD-induced basement membrane damage, the effect of HD treatment on six epidermal-dermal epitopes (laminin, type IV collagen, bullous pemphigoid antigen (BPA), epidermolysis bullosa acquisita antigen (EBA), fibronectin and GB3) was characterized using indirect immunohistochemistry and immunoelectron microscopy. These studies confirmed the laminin alkylation data by localizing the HD-induced blister cleavage plane to be within the upper lamina lucida, above the type IV collagen, EBA and GB3, but below the BPA sites. Finally, in an effort to get a better understanding of the relationship between HD absorption and toxicologic effect, a toxicokinetic model of ^{14}C-HD percutaneous absorption and intra-cutaneous disposition was formulated. This study demonstrated rapid penetration of HD and confirmed the direct vascular toxicity by characterizing the physiologic volume changes produced as assessed by albumin and inulin studies. It also suggests that a great deal of the variability encountered in HD vesication research is secondary to the large variability inherent to the penetration process. We also confirmed the cutaneous metabolism of HD which is associated with its transit through skin. We believe that the studies reported herein have made significant progress in probing the mechanism of cutaneous vesication, characterizing the use of the IPPSF to study this phenomenon, and identifying the molecular targets of HD in the basement membrane which leads to epidermal-dermal separation.

FOREWORD

Opinions, interpretations, conclusions, and recommendations are those of the author and are not necessarily endorsed by the U.S. Army.

N/A Where copyrighted material is quoted, permission has been obtained to use such material.

N/A Where material from documents designated for limited distribution is quoted, permission has been obtained to use the material.

N/A Citations of commercial organizations and trade names in this report do not constitute an official Department of Army endorsement or approval of the products or services of these organizations.

N/A In conducting research using animals, the investigator(s) adhered to the "Guide for the Care and Use of Laboratory Animals," prepared by the Committee on Care and Use of Laboratory Animals of the Institute of Laboratory Resources, National Research Council (NIH Publication No. 86-23, Revised 1985).

N/A For the protection of human subjects, the investigator(s) adhered to policies of applicable Federal Law 45 CFR 46.

N/A In conducting research utilizing recombinant DNA technology, the investigator(s) adhered to current guidelines promulgated by the National Institutes of Health.

N/A In the conduct of research utilizing recombinant DNA, the investigator(s) adhered to the NIH Guidelines for Research Involving Recombinant DNA Molecules.

N/A In the conduct of research involving hazardous organisms, the investigator(s) adhered to the CDC-NIH Guide for Biosafety in Microbiological and Biomedical Laboratories.

Nancy A Montes Rivera 12/15/95

PI - Signature DATE

ACKNOWLEDGMENTS

The technical assistance of Becky Vaughn and Dawn Chasse is deeply appreciated in the surgical procedure, caring, and histological preparation of the skin flaps. The prostaglandins release, protective effects and assessment of HD alkylation of laminin represents partial fulfillment of the requirements for the Doctor of Philosophy (Ph.D.) degree in toxicology for Jason Zili Zhang under the direction of Dr. Nancy Monteiro-Riviere. We appreciate the expertise and data analysis by Jim Brooks for the HD disposition study. Thanks are also given to Drs. Patrick Williams and Barry Peters for assistance. Only with the dedication and conscientiousness of all these individuals was this project possible.

TABLE OF CONTENTS

TABLE OF CONTENTS (continued)

TABLE OF CONTENTS (continued)

TABLE OF CONTENTS (continued)

List of Tables

List of Figures

TABLE OF CONTENTS (continued)

TABLE OF CONTENTS (continued)

INTRODUCTION

The purpose of this final report was to summarize our study of the mechanism of action of the cutaneous vesicant sulfur mustard, bis (2-chloroethyl) sulfide (HD), in the isolated perfused porcine skin flap (IPPSF), an *in vitro* model previously shown to be a useful system to investigate the actions of topically applied vesicants on skin. The morphological, biochemical, and physiological changes induced by HD in the IPPSF have been fully described previously in the final report of the USAMRDC contract (DAMD17- 87-C-7139), during which the model was developed (Monteiro-Riviere et al., 1991). Based on this previous research, a number of interesting phenomena were noted and a hypothesis developed that is the subject of the present contract.

These previous studies generated two relatively independent lines of research related to the mechanism and pathogenesis of HD blisters in the skin: the inflammatory reaction and the molecular mechanism of HD damage to the basement membrane zone. These were independently investigated in the present proposal in Sections 1 through 6.

A characteristic physiological change seen with HD treatment in the IPPSF is an increase in total flap vascular resistance (VR) shortly after exposure. In fact, compared to all historical IPPSF data collected to date ($\approx$ 2,155 IPPSFs), this increase in VR is a hallmark of chemical vesication. Similar manifestations of vascular changes (e.g. erythema, edema, etc.) have also been reported by other investigators. What is the mechanism of this change which precedes morphological evidence of vesication? Section 1 of this report characterizes the inflammatory mediator profile of prostaglandin E_2 (PGE_2), prostaglandin $F_{2\alpha}$ ($PGF_{2\alpha}$), and interleukin 1α (IL-1α), and provides data which strongly suggest that the mechanism is mediated by the release of prostaglandins. Section 6 further documents an HD-induced increase in intravascular volume as assessed by albumin space which suggests an increase in capillary permeability. Since these changes occur in the IPPSF, an *in vitro* model which lacks

a functional immune system, the mediators responsible must be produced by cutaneous elements via a mechanism triggered by HD.

Section 2 evaluates the protective effects in the IPPSF, pharmacological agents with different mechanisms of action, including HD scavengers (sodium thiosulfate and cysteine), poly (ADP-ribose) polymerase inhibitor (niacinamide), and prostaglandin inhibitor (indomethacin) were used to characterize HD toxicity.

Earlier studies demonstrated that HD-induced vesication occurred at the level of the lamina lucida of the epidermal-dermal junction (EDJ; basement membrane). Additional studies reported in Section 3 have further defined the molecular epitope mapping by indirect immunohistochemistry and immunoelectron microscopy of the EDJ zone antigens (laminin, Type IV collagen, fibronectin, GB3 (Nicein), BP (bullous pemphigoid), EBA (epidermolysis bullosa acquita), L3d and 19-DEJ (Uncein) after HD treatment which localized the precise cleavage plane to the upper lamina lucida. What specific molecular components of this structure are involved, and is HD capable of directly interacting with these components? The results documented in Sections 4 of the present report strongly suggest that laminin may be directly alkylated by HD. Furthermore, after a blister is formed, laminin remaining on the dermis is altered and may be directly responsible for the delayed wound healing that is characteristic of HD-induced vesication. This altered laminin, which normally serves as a scaffold for epidermal regeneration, is now deficient in this function. Addition studies in Section 5 were performed to study the flux of HD through the skin and to determine if the metabolites formed are due to the epidermal metabolism of HD.

The final component in Section 6 of this report deals with our attempts to develop an integrated toxicokinetic-toxicodynamic (TK-TD) model of HD vesication in the IPPSF. Such a model would be useful in tying together the multiple toxicologic end points observed after HD treatment and correlating them to the disposition of HD and its metabolites within the skin. For example, what is the concentration of HD seen in the basement membrane of HD-treated flaps? Also, these studies shed light on the source of the variability seen after HD

treatment since a great deal of variability in HD penetration and absorption was documented. In this report, the IPPSF venous efflux and intra-cutaneous disposition profiles of ^{14}C - HD are reported. A TK model based on individual flaps which is integrated with the previously mentioned changes in vascular volume seen with HD.

1. TOPICAL SULFUR MUSTARD INDUCES CHANGES IN PROSTAGLANDINS AND INTERLEUKIN-1_α IN ISOLATED PERFUSED PORCINE SKIN

Zili Zhang, Jim E. Riviere, and Nancy A. Monteiro-Riviere

Published in *In Vitro Toxicology* 8 (2):149-158, 1995

Abstract

Sulfur mustard (bis (2-chloroethyl) sulfide, HD) is an alkylating agent which causes severe cutaneous injury. The isolated perfused porcine skin flap (IPPSF) is an *in vitro* model that has been utilized in cutaneous toxicity research. The objective of this study was to characterize the local IPPSF inflammatory response after topical exposure to 5.0 and 10.0 mg/ml of HD (n= 5/treatment, n= 5/control). Biochemical markers of viability (cumulative glucose utilization (CGU)), vascular resistance (VR), morphological parameters, and venous flux of prostaglandin E_2 (PGE_2), prostaglandin $F_{2\alpha}$ ($PGF_{2\alpha}$), and interleukin 1_α (IL-1_α) were determined. HD caused a dose-related response in the formation of gross blisters, and epidermal-dermal separation. Decreases in CGU and an increase in VR were seen in all HD-treated IPPSFs. Increase of both PGE_2 and $PGF_{2\alpha}$ was only observed in 5.0 mg/ml HD treatment which showed the greatest increase in VR, while the 10.0 mg/ml concentration of HD enhanced the release of IL-1_α. These results suggest that HD is a potent dermal toxic agent which induces alterations in glucose metabolism and vascular resistance which resulted in dose-specific patterns of PGE_2, $PGF_{2\alpha}$ and IL-1_α release.

Introduction

Sulfur mustard bis (2-chloroethyl) sulfide (HD), an old warfare chemical, is well-documented for its severe cutaneous damage as well as systemic toxicity (Papirmeister et al., 1991). At the molecular level, HD represents a classical alkylating agent, which forms a DNA

adduct and can cause mutagenesis and carcinogenesis (Boberts, 1978). Derivatives of mustard have been used as antineoplastic drugs (Calabresi and Chabner, 1992).

Traditional *in vitro* models used to study skin toxicity usually do not contain an intact anatomic structure, and therefore fail to mimic the complicated physiological responses seen after *in vivo* exposure. The isolated perfused porcine skin flap (IPPSF), developed in our laboratory as a novel *in vitro* model for percutaneous absorption and cutaneous toxicity has been shown to be a rational tool to evaluate dermally toxic compounds, especially vesicants. This model responded with biochemical, vascular, and morphological changes that were identical to human cutaneous exposure to HD, including the formation of macroscopic blisters (Monteiro-Riviere and King, 1989; Monteiro-Riviere et al., 1990; 1991).

Recent studies have shown a complex immune network in the skin, and it is now evident that the keratinocyte profoundly influences the course of immune and inflammatory responses in skin by producing cytokines and prostaglandins. Thus, determination of inflammatory mediators may offer a unique and early insight into the evaluation of dermal toxicity (Rheins, 1992). Since the IPPSF is an *in vitro* system isolated from systemic immune responses yet maintains normal anatomical structure, and a functional microcirculation, it may provide a better approach to study the immunological response to HD localized in the skin. The role of this dimension of cutaneous immunology caused by chemical vesicants has not been studied.

The objective of this study was to characterize HD effects in the IPPSF by topical exposure to 5.0 mg/ml and 10.0 mg/ml of HD, and to determine the changes in viability, vascular resistance, and morphology. To assess the cutaneous immune response, venous fluxes of two inflammatory mediators, prostaglandin E_2 (PGE_2) and prostaglandin $F_{2\alpha}$ ($PGF_{2\alpha}$), and a cytokine, interleukin 1_α (IL-1_α) were evaluated in HD-treated IPPSFs.

Materials and Methods

IPPSF preparation and dosing

Weanling, female Yorkshire pigs (18-24 kg) were given atropine sulfate (0.04 mg/kg) and anesthetized with an intramuscular injection of ketamine hydrochloride (10.0 mg/kg) and xylazine hydrochloride (4.0 mg/kg), and maintained during surgery with halothane via tracheal intubation. The first stage involves creation of two skin flaps, one on either side of the midline in the inguinal region of the pig (Figure 1-1). Two days later, the arterial supply to each flap was cannulated and the flaps were harvested for perfusion. Each flap was flushed with heparinized saline to remove excess blood from the vasculature and placed in a perfusion chamber within a specially designed fume hood (Figure 1-2) (Riviere et al., 1986; Monteiro-Riviere et al.,1987; Monteiro-Riviere 1990; Bowman et al., 1991).

Each flap was perfused in a nonrecirculating manner with a media consisting of bovine serum albumin (BSA) and glucose in a Kreb's-Ringer bicarbonate buffer solution. The conditions of the chamber parameters are as follows: temperature, 36-38 $^{\circ}$C; relative humidity, 50-65%; and media flow rate, 1.5 ml/min. Media were gassed with 95% O_2/5% CO_2 via a silastic tube oxygenator. Flaps are perfused for 1 hour prior to dosing to ensure perfusion viability and stability.

Each IPPSF was fitted with a 7.5 cm^2 nonoccluded template (Stomahesive, ConvaTec-Squibb, Princeton, NJ) adhered with Skin Bond (Pfizer Hospital Products, Inc., Largo, FL). A dosing solution of 300 µl was applied using a positive displacement pipette (Gilson Microman, Gilson Medical Electronics, France). Fifteen IPPSFs were treated with either 5.0 mg/ml, 10.0 mg/ml or 0 mg/ml (control) of HD in ethanol (n=5/treatment) and perfused for 8 hours. Stock HD in ethanol was obtained from the U.S. Army Medical Research and Development Command. Concentrations greater than 10.0 mg/ml could not be used in this study because greater concentrations would exceed the surety limits presently established for university laboratories.

Biochemical and vascular parameters

Arterial and venous media samples were collected hourly throughout the perfusion period and analyzed for glucose. Hourly glucose utilization was the primary biochemical marker of flap viability during perfusion (King and Monteiro-Riviere, 1990; Riviere and Monteiro-Riviere, 1991). A plateau in CGU was used as a retrospective indicator of a loss in flap viability.

The physiological parameter vascular resistance (VR) is defined as the ratio of arterial pressure to media flow rate and has been used as an indirect measure of vascular activity in previous IPPSF studies (Monteiro-Riviere et al., 1990; 1991).

Tissue preparation and morphological parameters

After 8 hours of perfusion, skin from the dosed region of each IPPSF was excised and samples fixed in 10% neutral buffered formalin, processed through a graded series of alcohols and embedded in paraffin for light microscopy (LM). Sections (6 μm) were stained with hematoxylin and eosin (H&E) and then examined by LM.

Inflammatory mediator and cytokine production

PGE_2 and $PGF_{2\alpha}$ were measured with a competitive enzyme-linked immunosorbent assay (ELISA) and IL-1α was determined with enzyme immunometric assay.

To purify prostaglandin samples, 8 ml of 0.1 M KH_2PO_4 solution was added in each of the 250 μl hourly venous effluent samples. PGE_2 and $PGF_{2\alpha}$ were extracted from the diluted IPPSF medium sample using a Sep-Pak Plus^R extraction cartridge (Waters, Milford, MA), then washed with ethyl acetate (EA) (8 ml EA for each column). After the EA was evaporated, the remaining PGE_2 and $PGF_{2\alpha}$ was dissolved in an enzyme immunosorbent assay (EIA) buffer (1 ml), and ready for assay. For IL-1α assay, non-specific mouse immunoglobulin (IgG) was added to block the effect of anti-mouse IgG which may be present in the samples. Samples were measured for PGE_2, $PGF_{2\alpha}$, and IL-1_α by EIA (Caymen Chemical, Ann Arbor, MI), and analyzed on a Fisher Biotech ELISA Reader (Fisher Scientific, Pittsburgh, PA).

Statistical methods

Statistical comparisons were made for all parameters by carrying out an analysis of variance on responses separately for each hour after HD treatment. Where significant ($p < 0.05$) treatment effects were noted, multiple comparison tests were conducted using Fisher's protected lsd procedure.

Results

Viability parameters

All HD-treated IPPSF (5.0 mg/ml and 10.0 mg/ml) showed a significant decrease ($p < 0.05$) in CGU compared to the ethanol-treated control group (Figure 1-3) by 6 hours after HD dosing.

Vascular resistance parameters

At 4 hours, all HD-treated IPPSFs demonstrated a higher VR response than the control, and the 5.0 mg/ml of HD had a higher VR than did the 10.0 mg/ml of HD (Figure 1-4). Although differences between 10.0 mg/ml HD and ethanol or 5.0 mg/ml of HD treatment were not statistically significant ($p > 0.05$), VR of the 5.0 mg/ml of HD was significantly greater than the ethanol controls.

Morphological parameters

Morphological findings are summarized in Table 1-I. Macroscopically, approximately 30% of the HD-treated IPPSFs demonstrated the formation of gross blisters. One out of 6 IPPSFs treated with 5.0 mg/ml of HD developed macroscopic blisters, while 3 out of 6 developed macroscopic blisters with the 10.0 mg/ml of HD. In general, blisters on the dosing surface started as small vesicles at 5.5 hours after dosing and then coalesced into larger bullae. However, LM observations showed that microvesicles occurred in 100% of all the HD-treated IPPSFs. (Figures 1-5 and 1-6). In addition, lymphocyte infiltration, pyknotic basal cells, and intracellular and intercellular epidermal edema were noted at 5.0 mg/ml and 10.0 mg/ml of HD. No lesions were found in the ethanol control flaps (Figure 1-7).

Inflammatory mediator and cytokine production

In the ethanol-control, the PGE_2 level did not increase until after 6 hours (Figure 1-8). However, the 5.0 mg/ml of HD demonstrated a significant increase ($p < 0.05$) of PGE_2 release by 6 hours and continued to increase until 7 hours. Interestingly, PGE_2 was unaffected in the flaps treated with the 10.0 mg/ml of HD (Figure 1-8). Similarly, we did not find any significant changes of $PGF_{2\alpha}$ levels in the ethanol or 10.0 mg/ml of HD IPPSFs. However, the 5.0 mg/ml of HD caused an increase in $PGF_{2\alpha}$ by 6 hours while the ethanol controls or 10.0 mg/ml of HD had no significant effect (Figure 1-9). Venous efflux profiles of IL-1_α after 5.0 mg/ml of HD did not show a significant increase in IL-1_α, however IL-1_α level was significantly increased ($p < 0.05$) in the 10.0 mg/ml of HD at 6 hours (Figure 1-10).

Table 1-I. Frequency of Morphological Lesions with HD.

Treatment	Blisters	Microvesicles
Ethanol	0/5	0/5
5.0 mg/ml HD	1/5	5/5
10.0 mg/ml HD	3/5	5/5

Discussion

Sulfur mustard is a highly reactive electrophilic molecule and reacts with DNA, RNA, protein and other biological macromolecules. As a result, HD interferes with a variety of critical biochemical processes (Boursnell, 1951; Levy, 1946; Singer, 1975; Fox and Scott, 1980; Smith et al., 1992). Many studies have demonstrated that HD damages vital cellular organelles and membranes (Ray et al., 1990). In this regard, HD has been shown to cause degeneration of mitochondria which can lead to inhibition of cellular metabolism and energy production. Also, HD has been shown to disrupt the intracellular calcium homeostasis and release of proteinases, leading to cellular injury (Orrenius and Nicotera, 1987; Nicotera et al. 1989; Higuchi et al., 1988).

In HD-induced cutaneous toxicity studies, most *in vitro* models show HD affecting only the epidermal cells, with no reports of gross blisters. Blister formation has been reported in *in vivo* studies with HD (Mitcheltree et al., 1989; Wade et al., 1989; Marlow et al., 1990; Petrali et al., 1990). The IPPSF has been shown to be a useful model for studying cutaneous toxicity because it maintains a viable anatomical structure identical to that of human skin and simultaneously provides information on the biochemical, vascular, and morphological changes; therefore, it is possible to analyze the relationship of these responses over a time course. In this study, all HD-treated flaps developed microvesicles and/or gross blisters in a dose-dependent response. Further, these morphological alterations were consistent with that of human skin exposed to HD (Ginzler and Davis, 1943; Momeni et al.,1992; Requena et al., 1988). Our previous transmission electron microscopy studies of the mustard analog 2-chloroethyl methyl sulfide (CEMS) (King and Monteiro-Riviere, 1990), HD and lewisite (L) (Monteiro-Riviere et al., 1990) also revealed these morphological changes which consisted of epidermal-dermal separation.

Previous IPPSF studies have evaluated glucose utilization as a measure of flap viability and alterations in cutaneous metabolism (Riviere et al., 1986). In this study, the CGU decreased in all IPPSFs treated with HD, consistent with a dose-dependent loss of cell

viability. Other IPPSF studies have demonstrated a decrease in glucose utilization in flaps treated with L (King et al, 1992), a potent organic arsenical, and with CEMS (King and Monteiro-Riviere, 1990). A decrease in CGU was correlated to the degeneration of the mitochondria, site of the citric acid cycle, based on the time course studies Monteiro-Riviere et al., 1990). Inhibition of glucose metabolic pathways was proposed as a mechanism of HD-induced cytotoxicity by other groups (Dixon and Needham, 1946; Holzer, 1964). Therefore, these effects may contribute to the change in CGU caused by HD toxicity.

Despite the rather extensive studies conducted on direct HD epidermal toxicity, little work has been focussed on the inflammatory aspects of HD toxicity. This is the purpose of this study. Some studies have demonstrated that HD can release certain vasoactive substances (e.g., prostaglandins) and cause an increase in proteinases after HD exposure (Rudin, 1953; Rikimaru et al., 1991). These factors could affect the vascular permeability and vascular tone. VR was used in this study to measure the potential activity of the cutaneous vasculature in response to HD exposure. All IPPSFs had an increase in VR with the 5.0 mg/ml HD, resulting in a higher vascular response than the 10.0 mg/ml of HD. A separate toxicokinetic modeling study showed that the enhancement of VR was primarily due to an increase vascular permeability and imblance of intercellular pressure (Riviere et al. 1994). Some inflammatory mediators (e.g., PGE_2, and $PGF_{2\alpha}$) were found to alter the vascular permeability and activity. The levels of both PGE_2 and $PGF_{2\alpha}$ increased only in the 5.0 mg/ml rather than in the 10.0 mg/ml of HD. The consistency of change between these vasoactive mediators and VR after HD exposure indicates that PGE_2 and $PGF_{2\alpha}$ may be involved in the HD-induced VR change seen during this study.

Products of arachidonic acid (AA) metabolism by cyclooxygenase and lipoxygenase enzymes are known to be potent inflammatory mediators present in many skin diseases and the skin can display a highly active metabolism of AA (Ziboh, 1992). High levels of PGE_2, $PGF_{2\alpha}$, and LTB_4 have been shown to elicit a cutaneous inflammatory reaction. Injection of these prostaglandins resulted in erythema and edema by either altering the vascular responses

or by chemotaxis (Willis and Cornelson, 1973). Although the specific cell type responsible for the release of prostaglandins in the skin is uncertain, the epidermal cells and endothelial cells are likely candidates since these cells possess an enzyme system that is needed to convert prostaglandins (Dahlen, 1987; Grabbe et al., 1985) and inflammatory cells are not present in the IPPSF perfusion media. Treatment with indomethacin, a cyclooxygenase inhibitor, prevented an increase in PGE_2 as well as reducing the inflammatory reaction caused by ultraviolet light (Snyder, 1975).

In this study, we attempted to assess changes in AA metabolism in HD-treated IPPSFs and the role of these prostaglandins in vesication by examining the production of PGE_2 and $PGF_{2\alpha}$. In the control group, PGE_2 levels only begin to increase at 7 hours. The 5.0 mg/ml of HD increased in both PGE_2 and $PGF_{2\alpha}$ as early as 5 hours. However, we detected no increase in PGE_2 or $PGF_{2\alpha}$ levels in the flaps treated with 10.0 mg/ml of HD compared to the controls, although this high dose group produced the most severe morphological evidence of cutaneous vesication. Similar paradoxical results were also reported after HD exposure to human skin cultures (Rikimaru et al., 1991). Our laboratory showed no changes in LTB_4, a major lipoxygenase metabolite in the skin, after HD treatment (unpublished studies). Thus, the lack of effect of 10.0 mg/ml of HD on the production of PGE_2 and $PGF_{2\alpha}$ and a resultant attenuation in the VR response, is a true manifestation of HD vesication. It would appear unlikely that 10.0 mg/ml of HD switches the AA metabolism from cyclooxygenase to lipoxygenase pathways. Thus, it is reasonable to postulate that 10.0 mg/ml of HD produces severe vesication but either inhibits both AA metabolism enzymes, produces other mediating factor(s), or causes cell death which prevents both PGE_2 and $PGF_{2\alpha}$ release.

Recently, many cytokines have been found to be produced in skin, and mediate diverse biological responses to injury and infection. These molecules may play an important role in the inflammatory and immune responses. In addition, cytokines are involved in the tissue remodeling during wound healing (Durum et al., 1985). Among these cytokines, IL-1 has been well studied. Two forms of IL-1; IL-1_α and IL-1_β, have been identified (March et al., 1985).

Although both IL-1 genes encode for 31 kD proteins, IL-1β is biologically inactive until it is proteolytically processed to a 17 kD molecule. It has become clear that the keratinocytes may be a major source of epidermal IL-1α, since these cells have been shown to produce IL-1α mRNA and protein (Kupper et al., 1986; Schmitt et al., 1989). Biological activity of IL-1β cannot be demonstrated in either normal epidermis or in cultured keratinocytes because of the absence of IL-1β proteolytical enzymes (Kostura et al., 1989). Therefore, we chose IL-1α as a biomarker to assess the immune response elicited by HD in the IPPSF.

In this study, 5.0 mg/ml of HD did not change the venous efflux of IL-1α compared to controls, whereas 10.0 mg/ml of HD increased the release of IL-1α at 5 hours. Controversy exists on how keratinocytes secrete IL-1, but it generally thought that lysis of cells release a preformed IL-1. Therefore, it is feasible that 10.0 mg/ml of HD destroys more cells, causing an increase in IL-1α release. Also, this supports the explanation that cell death may be responsible for the lack of increase in prostaglandins after the 10.0 mg/ml of HD. Alternatively, the higher release of PGE_2 seen with the lower dose may downregulate IL-1α release. When PGE_2 is low at the high HD dose, IL-1α release may occur (Knudsen et al., 1986; Kunkel et al., 1986). In conclusion, HD is a potent cutaneous vesicant causing severe toxicity, and dose dependent release profiles of the inflammatory mediators PGE_2 and $PGF_{2\alpha}$ and the cytokine IL-1α. Based on these results, prostaglandin release may be involved in low dose exposure to HD and may modulate an inflammatory response as assessed by a change in VR. However, release of a cytokine such as IL-1α may correlate better to the formation of epidermal-dermal separation which is more severe at higher doses.

References

Boberts, J.J. (1978). The repair of DNA modified by cytotoxic, mutagenic, and carcinogenic chemicals. Adv. Radiat. Biol. 9:211-435.

Boursnell, J.C. (1951). Some reactions of mustard gas with protein. Biochem. Soc. Symp. 2:8-15.

Bouzon, M., Dussert, C., Lissitzky, J.C., and Martin, R.M. (1990). Spreading of B16F1 cells on laminin and its proteolytic fragments P1 and E8: Involvement of laminin carbohydrate chains. Exp. Cell Biol. 190:47-56.

Bowman, K.F., Monteiro-Riviere, N.A., and Riviere, J.E. (1991). Development of surgical techniques for preparation of *in vitro* isolated perfused porcine skin flaps for percutaneous absorption studies. Am. J. Vet. Res. 52:75-82.

Calabresi, P., and Chabner, B.A. (1992). Antineoplastic agents. In The Pharmacological Basis of Therapeutics. (Eds. A.G. Gilman, T.W. Rall, A.S. Nies, and P. Taylor). Elmsford, NY, pp. 1209-1223.

Dahlen, S.E. (1987). Prostaglandins and leukotrienes. In Dermatology in General Medicine, Vol.1. (Ed. T.B. Fitzpatrick), McGraw-Hill, New York.

Dixon, M., and Needham, D.M. (1946). Biochemical research on chemical warfare agents: A review. Cancer Res. 22:651-688.

Durum, S.K., Schmidt, J.A., and Oppenheim, J.J. (1985). Interleukin 1: An immunological perspective. Annu. Rev. Immunol. 31:263-287.

Fox, M., and Scott, D. (1980). The genetic toxicology of nitrogen and sulfur mustard. Mutat. Res. 75:131-168.

Ginzler, A.M., and Davis, M.I.J. (1943). The pathology of mustard burns of human skin. U.S. Army Medical Research Laboratory, Edgewood Arsenal, Maryland, Report No.3.

Grabbe, J., Rosenbach, T., and Czarnetzki, B.M. (1985). Production of LTB_4-like chemotactic arachidonate metabolites from human keratinocytes. J. Invest. Dermatol. 86:527-530.

Higuchi, K., Kajiki, A., Nakamura, M., Harada, S., Pula, P.J., Scott, A.L., and Dannenberg, A.M. (1988). Proteases released in organ culture by acute dermal inflammatory lesions produced *in vivo* in rabbit skin by sulfur mustard: Hydrolysis of synthetic peptide substrates for trypsin-like and chymotrypsin-like enzymes. Inflammation. 12:311-333.

King, J.R., and Monteiro-Riviere, N.A. (1990). Cutaneous toxicity of 2-chloroethyl methyl sulfide in isolated perfused porcine skin. Toxicol. Appl. Pharmacol. 104:167-179.

King, J.R., Riviere, J.E., and Monteiro-Riviere, N.A. (1992). Characterization of lewisite toxicity in isolated perfused skin. Toxicol. Appl. Pharmacol. 116:189-201.

Knudsen, P.J., Dinarello, C.A., and Strom, T.B. (1986). Prostaglandins posttranscriptionally inhibit monocyte expression of interleukin 1 activity by increasing intracellular cyclic adenosine monophosphate. J. Immunol. 137:3189-3194.

Kostura, M.J., Tocci, G.L., Chin, J., Cameron, P., Hillman, A., Chartrain, N., and Schmidt, J. (1989). Identification of a monocyte specific pre-interleukin 1 beta convertase activity. Proc. Natl. Acad. Sci. USA. 86:6171-6175.

Kunkel, S.L., Chensue, S.W., and Phan, S.H. (1986). Prostaglandins as endogenous mediators of interleukin 1 production. J. Immunol. 136:186-192.

Kupper, T.S., Ballard, D., and Chua, A,O. (1986). Human keratinocytes contain mRNA indistinguishable from monocyte interleukin 1 and mRNA: Keratinocyte epidermal cell-derived thymocyte activating factor is identical to identical to interleukin 1. J. Exp. Med. 164:2095-2100.

Levy, M. (1946). Effects of sulfur and nitrogen mustards on proteins, enzymes, and cells. In Chemical Warfare Agents and Related Chemical Problems - Parts III-VI. Summary Technical Report of Division 9, National Defense Research Committee of the Office of Scientific Research and Development, Washington, D.C. DTIC No.AD-234 249.

March, C.J., Mosely, B., and Larsen, A. (1985). Cloning, sequencing, and expression of two distinct human interleukin 1 complemetary DNA's. Nature (London). 315:641-647.

Marlow, D.D., Mershon, M.M., Mitcheltree, L.W., Petrali, J.P., and Jaax, G.P. (1990). Sulfur mustard-induced skin injury in hairless guinea pigs. J. Toxicol. Cut. & Ocular Toxicol. 9:179-192.

Mitcheltree, L.W., Mershon, M.M., Wall, H.G., Pulliam, J.D., and Manthei, J.H. (1989). Microblister formation in vesicant-exposed pig skin. J. Toxicol. Cut. & Ocular Toxicol. 8:309-319.

Momeni, A., Enshaeih, S., Meghdadi, M., and Amindjavaheri, M. (1992). Skin manifestations of mustard gas. Arch. Dermatol. 128:775-780.

Monteiro-Riviere, N.A., Bowman, K.L., Scheidt, V.J., and Riviere, J.E. (1987). The isolated perfused porcine skin flap (IPPSF). II. Ultrastructural and histological characterization of epidermal viability. In Vitro Toxicol. 1:241-252.

Monteiro-Riviere, N.A., and King, J.R. (1989). The dermatotoxicity of 2-chloroethyl methyl sulfide and solvent vehicles in isolated perfused porcine skin. In Proceedings of the Medical Defense Bioscience Review, U.S.Army Research Institute of Chemical Defense, Aberdeen Proving Ground, MD. pp. 53-56.

Monteiro-Riviere, N.A., King, J.R., and Riviere, J.E. (1990). Cutaneous toxicity of mustard and lewisite on the isolated perfused porcine skin flap. DAMD17-87-C-7139; NTIS, ADA229922, pp. 1-144.

Monteiro-Riviere, N.A. (1990). Specialized technique: The isolated perfused porcine skin flap (IPPSF). In Methods for Skin Absorption. (Eds. B.W. Kemppainen and W.G. Reifenrath). CRC Press, Boca Raton, FL, pp. 175-189.

Monteiro-Riviere, N.A., King, J.R., and Riviere, J.E. (1991). Mustard induced vesication in isolated perfused skin: biochemical, physiological, and morphological studies. In Proceedings of the Medical Defense Bioscience Review, U.S. Army Medical Research Institute of Chemical Defense, Aberdeen Proving Ground, MD. pp. 159-162.

Nicotera, P., Mcconkey, D.J., Dypbukt, J.M., Jones, D.P., and Orrenius, S. (1989). Ca^{2+}-activated mechanisms in cell killing. Drug Metabol. Res. 20:193-201.

Orrenius, S., and Nicotera, P. (1987). On the role of calcium in chemical toxicity. Arch. Toxicol. Suppl. 11:11-19.

Papirmeister, B., Feister, A.J., Robinson, S.I., and Ford, R.D. (1991). Medical Defense Against Mustard Gas: Toxic Mechanisms and Pharmacological Implications, CRC Press, Boca Raton, FL.

Petrali, J.P., Oglesby, S.B., and Mills, K.R. (1990). Ultrastructural correlates of sulfur mustard toxicity. J. Toxicol. Cut. & Ocular Toxicol. 9:193-214.

Ray, R., Legere, R.H., and Broomfield, C.A. (1990). Membrane composition and fluidity changes due to alkylating agents. J. Cell Biol. 3:73A.

Requena, L., Requena, C., Sanchez, M., Jaqueti, G., Aguilar, A., Sanchez-Yus, E., and Hernandez-Moro, B. (1988). Chemical warfare. Cutaneous lesions from mustard gas. J. Amer. Acad. Dermatol. 19:529-536.

Rheins, L.A. (1992). What's new in cutaneous toxicity? J. Toxicol. Cut. & Ocular Toxicol. 11:225-238.

Rikimaru, T., Nakamura, M., Yano, T., Beck, G., Habicht, G.S., Rennie, L.L., Widra, M., Hirshman, C.A., Boulay, M.G., Spannhake, E.W., Lazarus, G.S., Pula, P.J., and Dannenberg, A.M. (1991). Mediators, initiating the inflammatory response, released in organ culture by full-thickness human skin explants exposed to the irritant, sulfur mustard. J. Invest. Dermatol. 96:888-897.

Riviere, J.E., Bowman, K.F., Monteiro-Riviere, N.A., Carver, M.P., and Dix, L.P. (1986). The isolated perfused porcine skin flap (IPPSF). I. A novel *in vitro* model for percutaneous absorption and cutaneous toxicology studies. Fundam. Appl. Toxicol. 7:444-453.

Riviere, J.E. and Monteiro-Riviere, N.A. (1991). The isolated perfused porcine skin flap as an *in vitro* model for percutaneous absorption and cutaneous toxicology. CRC Crit. Rev. Toxicol. 21:329-344.

Riviere, J.E. and Williams, P.L. (1992). On the pharmacokinetic implications of changing blood flow in skin. J. Pharm. Sci. 81:601-602.

Riviere, J.E., Williams, P.L., Zhang, Z., and Monteiro-Riviere, N.A. (1994). Toxicokinetics of sulfur mustard cutaneous disposition and percutaneous absorption in isolated perfused porcine skin. Toxicologist 14:184.

Rudin, D.O. (1953). A review of the biological action of mustard as a basis for therapy. U.S. Army Chemical Corps Medical Laboratories, Army Chemical Center, Maryland, Special Report No. 21. DTIC No. AD-15 565.

Schmitt, A., Hauser, C., and Jaunin, F. (1989) Normal epidermis contains high amounts of natural tissue IL-1: Biochemical analysis by HPLC identifies a MW approximately 17 kD form with a pI 5.7 and a MW approximately 30 kD form. Lymphokine Res. 5:105-118.

Singer, B. (1975). The chemical effects of nucleic acid alkylation and their relation to mutagenesis and carcinogenesis. Prog. Nucleic Acid Res. Mol. Biol. 15:219-284.

Smith, W.J., Sanders, K.M., Caulfield, J.E., and Gross, C.L. (1992). Sulfur mustard-induced biochemical alterations in proliferating human cells in culture. J. Toxicol. Cut. & Ocular Toxicol. 11:293-304.

Snyder, D.S. (1975). Cutaneous effects of topical indomethacin, an inhibitor of prostaglandin synthesis on UV-damaged skin. J. Invest. Dermatol. 64:322-326.

Wade, J.V., Mershon, M.M., Mitcheltree, L.W., and Woodard, C.L. (1989). The hairless guinea pig model and vesicant vapor exposures for bioassay purposes. In Proceedings of the Medical Defense Bioscience Review, U.S.Army Research Institute of Chemical Defense, Aberdeen Proving Ground, MD. pp. 569-575.

Willis, A.L., and Cornelson, M. (1973). Repeated injection PGE_2 in rat paws induces chronic swelling and a marked decrease in pain threshold. Prostaglandin. 3:353-355.

Ziboh, V.A. (1992). Prostaglandins, leukotrienes, and hydroxy fatty acids in epidermis. Dermatol. 11:114-120.

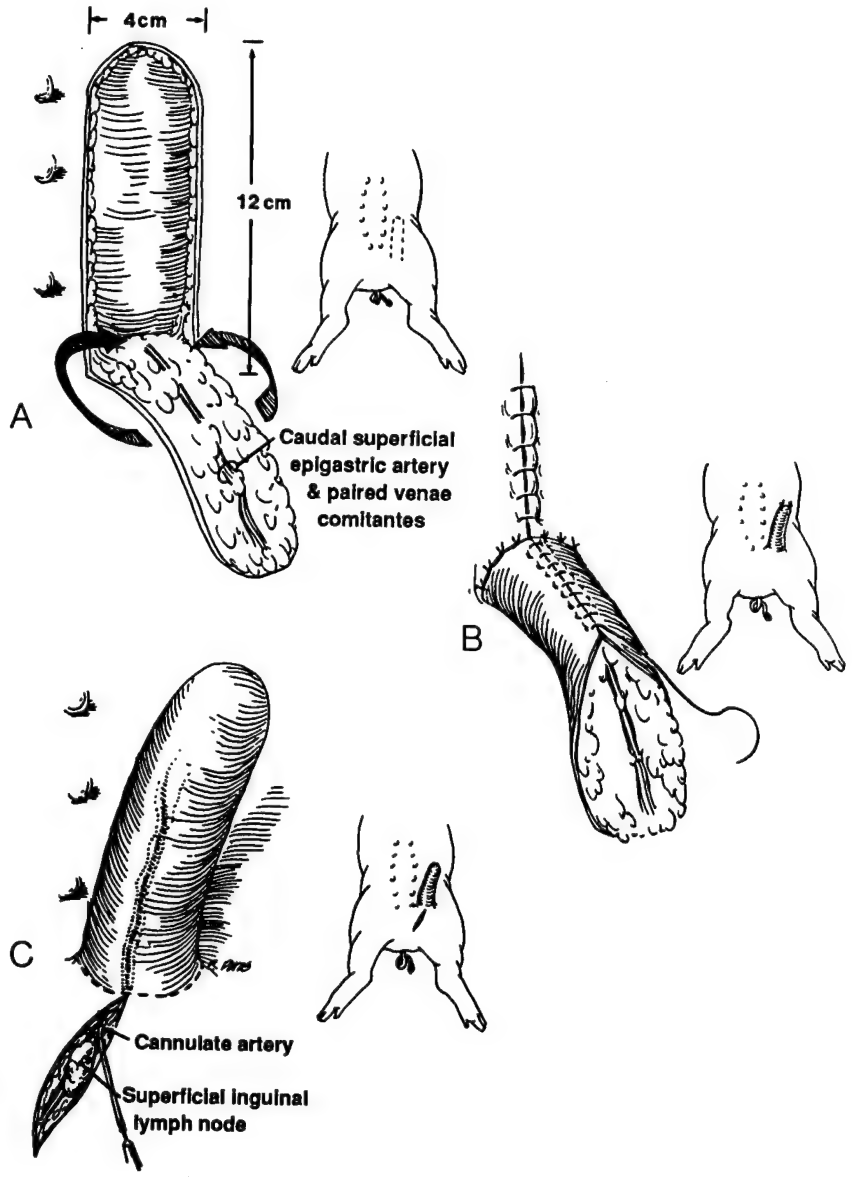

Figure 1-1. Surgical procedure for creating the IPPSF. (A) A single pedicle axial pattern skin flap is raised and (B) tubed completing stage I. Two days later, (C) the superficial epigastric artery is cannulated during stage II.

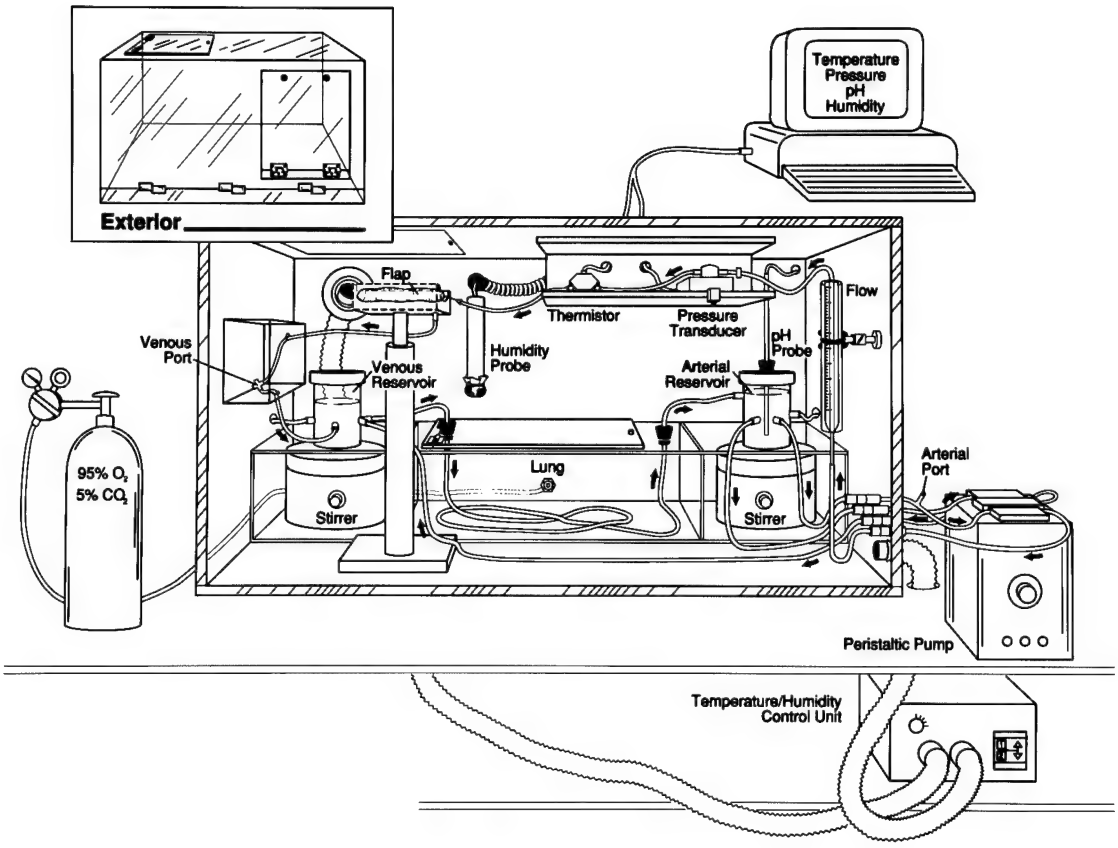

Figure 1-2. Schematic of the IPPSF perfusion chamber.

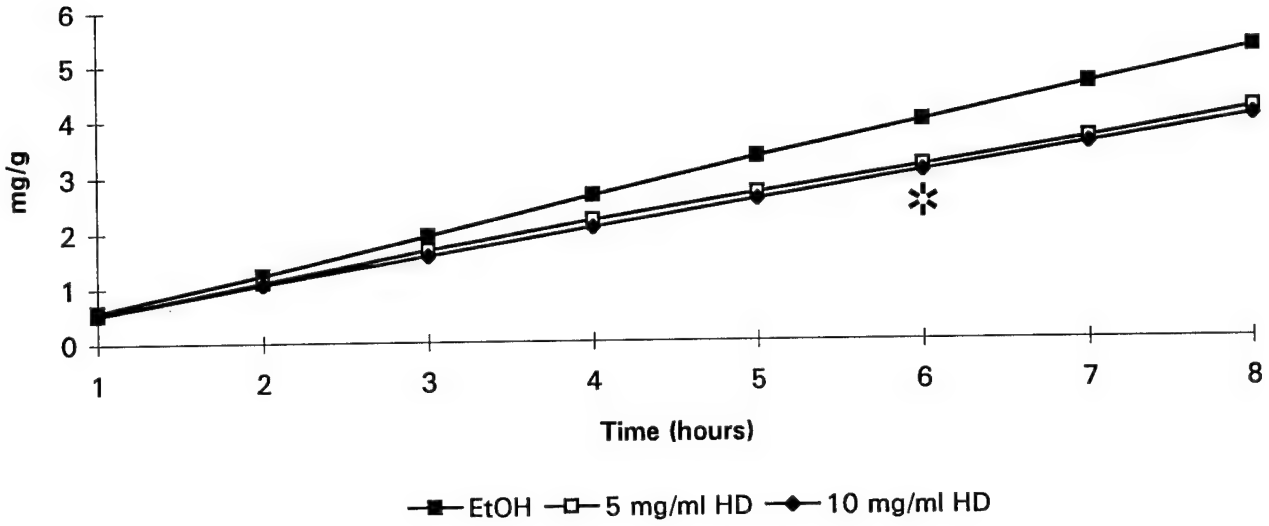

Figure 1-3. Cumulative glucose utilization in IPPSFs exposed to 5.0 mg/ml and 10.0 mg/ml of HD for 8 hours and ethanol controls (n = 5/treatment). (*) Mean CGU for treatment of 5.0 mg/ml HD is significantly different from that of EtOH control.

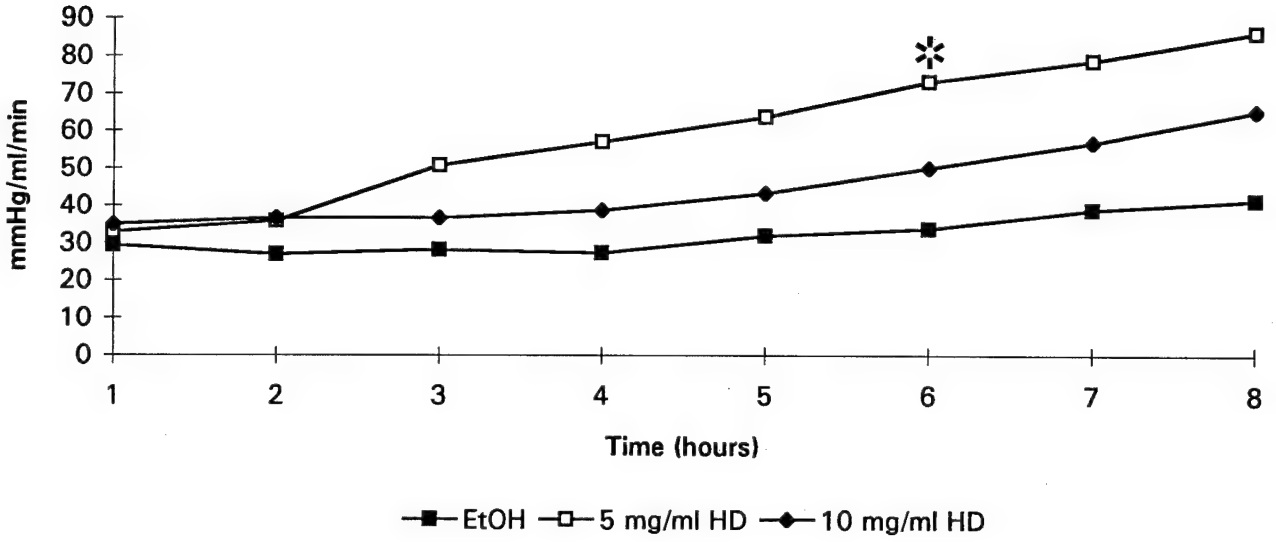

Figure 1-4. Vascular resistance of IPPSFs exposed to 5.0 mg/ml and 10.0 mg/ml of HD for 8 hours and ethanol controls (n = 5/treatment). (*) Mean VR for EtOH control is significantly different from that of 5.0 and 10.0 mg/ml of HD.

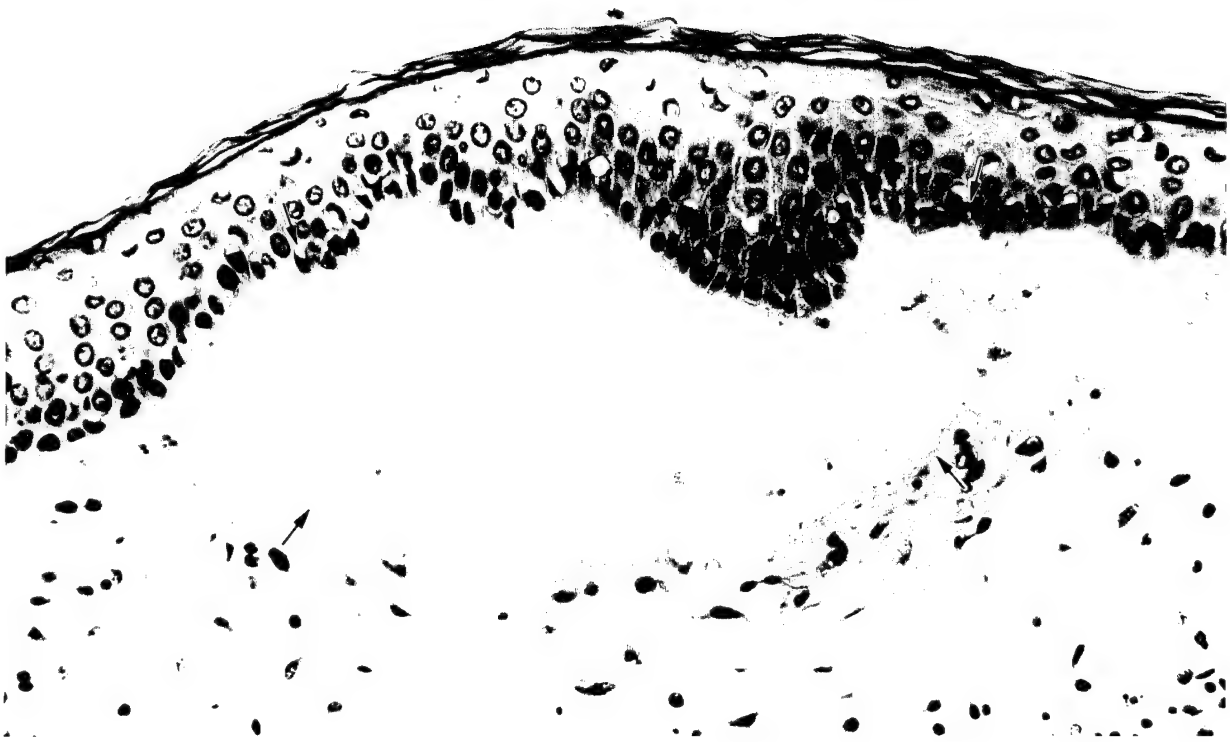

Figure 1-5. Light micrograph of an IPPSF exposed to 10.0 mg/ml of HD showing typical epidermal-dermal separation (arrows). H&E (X700).

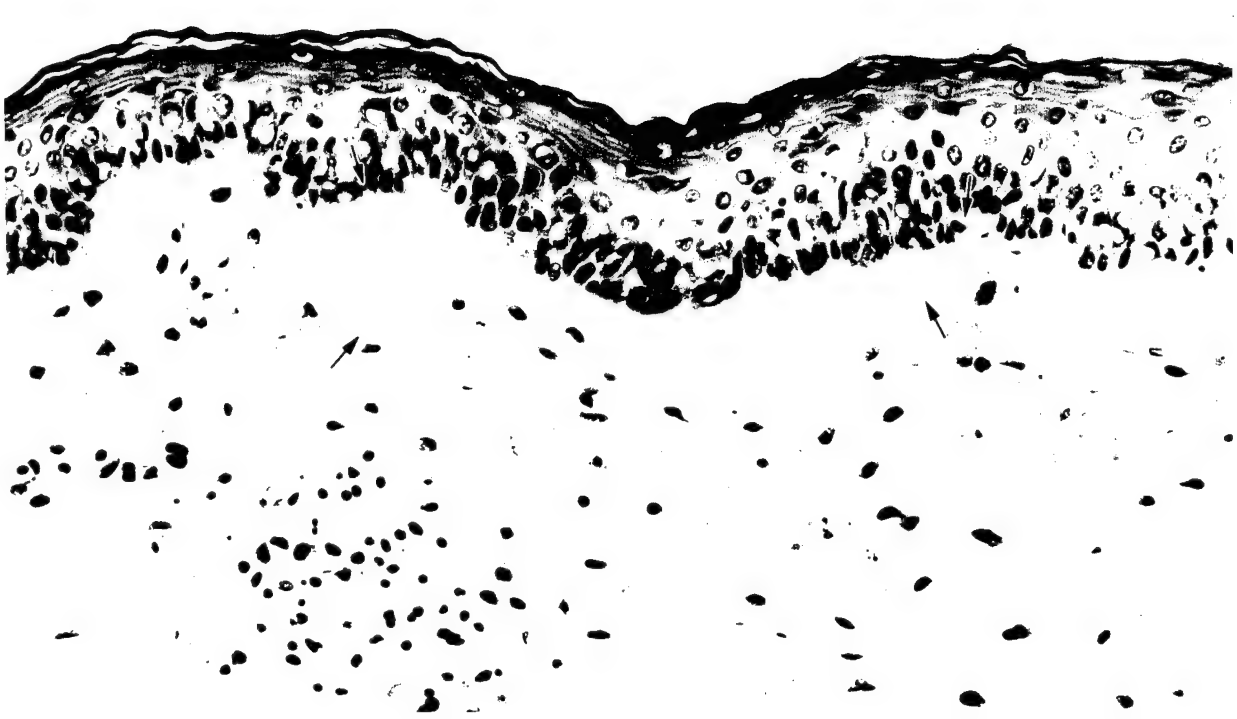

Figure 1-6. Light micrograph of an IPPSF exposed to 5.0 mg/ml of HD depicting epidermal-dermal separation (arrows). H&E (X600).

Figure 1-7. Light micrograph of an IPPSF dosed with ethanol, showing normal morphology. H&E (X700).

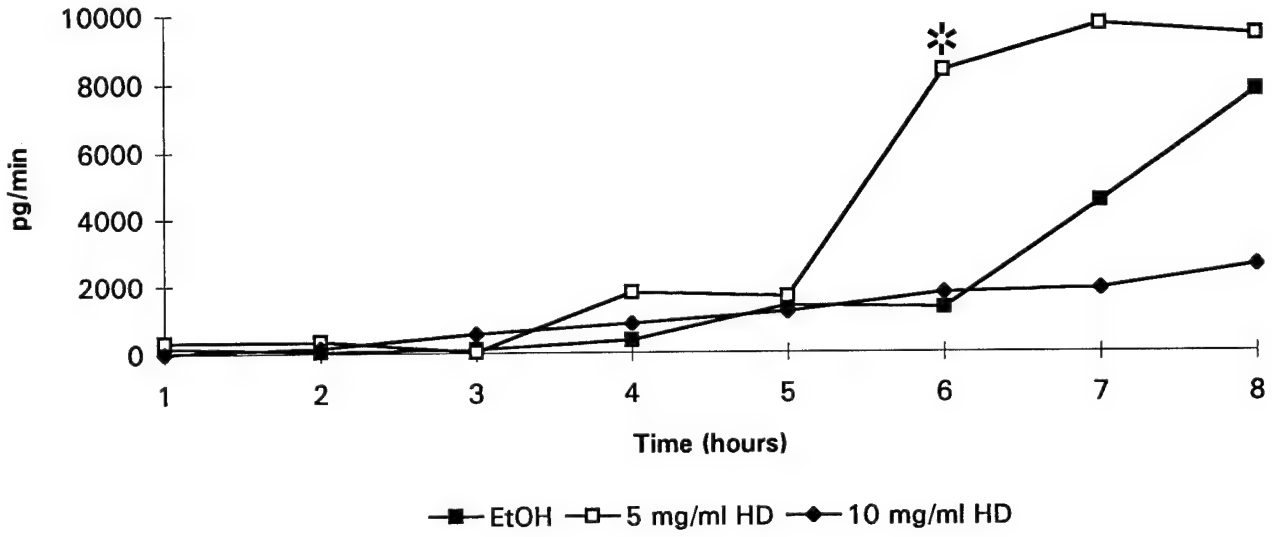

Figure 1-8. IPPSF venous efflux profiles of PGE_2 for 5.0 mg/ml and 10.0 mg/ml of topically applied HD and ethanol controls (n = 5/treatment). (*) Mean PGE_2 venous efflux for treatment of topical 5.0 mg/ml of HD is significantly different from that of EtOH control and 10.0 mg/ml of HD.

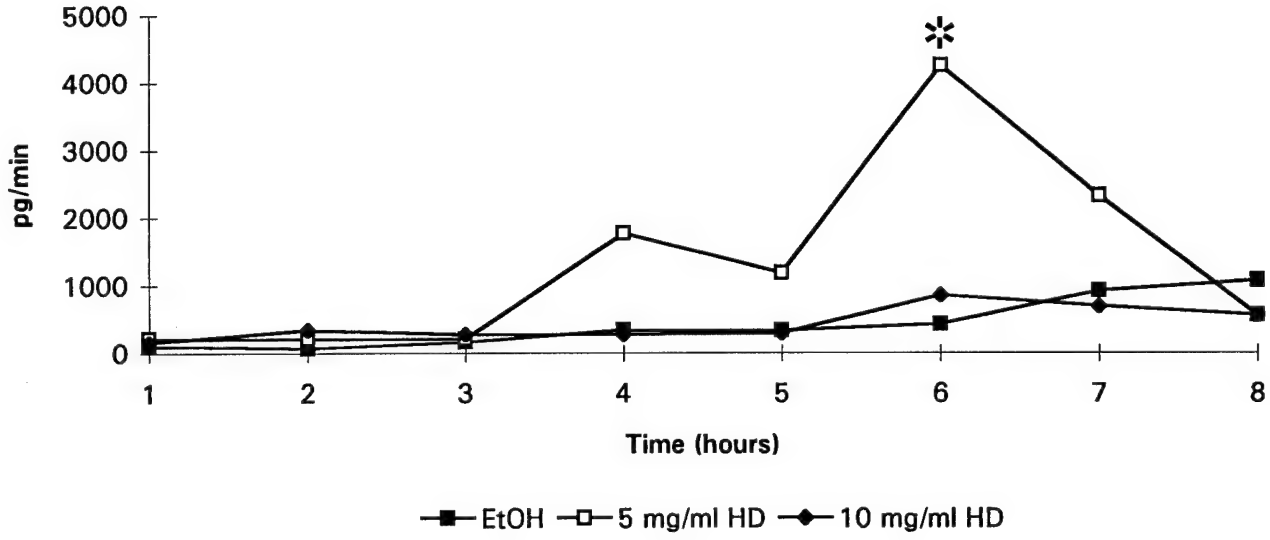

Figure 1-9. IPPSF venous efflux profiles of $PGF_{2\alpha}$ for 5.0 mg/ml and 10.0 mg/ml of topically applied HD and ethanol controls (n = 5/treatment). (*) Mean $PGF_{2\alpha}$ venous efflux for treatment of topical 5.0 mg/ml of HD is significantly different from that of EtOH control and 10.0 mg/ml of HD.

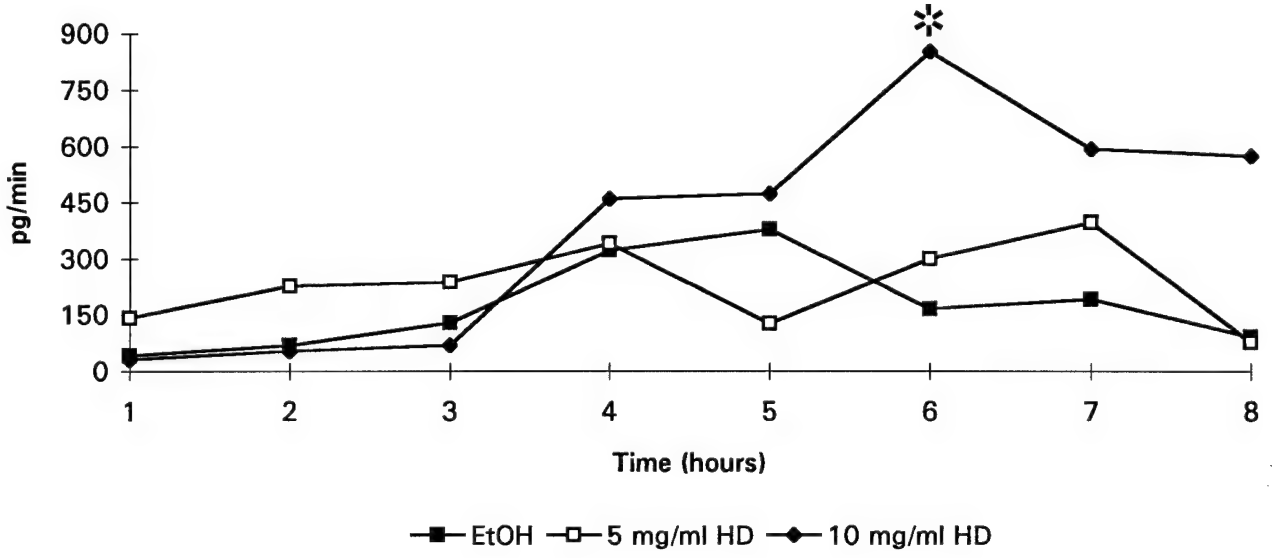

Figure 1-10. IPPSF venous efflux profiles of IL-1_α for 5.0 mg/ml and 10.0 mg/ml of topically applied HD and ethanol controls (n = 5/treatment). (*) Mean IL-1_α venous efflux for treatment of topical 5.0 mg/ml of HD is significantly different from that of EtOH control and 10.0 mg/ml of HD.

2. EVALUATION OF PROTECTIVE EFFECTS OF SODIUM THIOSULFATE, CYSTEINE, NIACINAMIDE, AND INDOMETHACIN ON SULFUR MUSTARD-TREATED ISOLATED PERFUSED PORCINE SKIN

Zili Zhang, Jim E. Riviere, and Nancy A. Monteiro-Riviere

Published in *Chemico-Biological Interactions* 96:249-262, 1995

Abstract

Sulfur mustard (bis (2-chloroethyl) sulfide, HD), a bifunctional alkylating agent, causes severe cutaneous injury, including cell death, edema, and vesication. However, the mechanisms underlying HD-induced cutaneous toxicity remain undefined. The isolated perfused porcine skin flap (IPPSF) has been utilized to investigate dermal toxic compounds and pharmacological intervention. In this study, four compounds with different pharmacological mechanisms were tested for their ability to prevent the dark basal cell formation, vesication, and vascular response characteristic of exposure to HD in the IPPSF. Reduction of HD-induced dark basal cells was observed in IPPSFs perfused with sodium thiosulfate and cysteine, which are HD scavengers; niacinamide, a possible NAD^+ stabilizer and an inhibitor of poly (ADP-ribose) polymerase; or indomethacin, a cyclooxygenase inhibitor, respectively. Treatments with niacinamide and indomethacin, but not sodium thiosulfate or cysteine, resulted in a inhibition of the vascular response in IPPSF exposed to HD. Microvesicles caused by HD were only partially prevented in the indomethacin-perfused IPPSFs. These data suggest that none of these agents alone would be successful antivesicant agents and different mechanisms are involved in production of HD-induced dark basal cells, microvesicles, and the vascular response; unfortunately, blocking of the cellular toxicity as evidenced by dark basal cell formation did not prevent vesication, suggesting that other

mechanisms must be operative, and that there is a multistep, biochemical process that lead to a final lesion.

Introduction

Sulfur mustard, bis (2-chloroethyl) sulfide, (HD) is a bifunctional alkylating agent which is highly reactive with nucleophilic molecules, such as DNA and proteins. Since this property may affect diverse aspects of cellular metabolism, a wide variety of manifestations of HD-induced toxicity has been documented, including mutagenenesis, cytotoxicity, and vesication (Papirmeister et al., 1991). However, neither a clear mechanism of HD action nor an effective antidote is known. As a consequence of its high chemical reactivity, HD predominantly effects exposed epithelial tissues at the site of exposure, namely the skin, the eye, and the respiratory tract. At higher doses, HD may be absorbed and cause direct systemic toxicity. Because of this diversity of actions, it is important to choose an appropriate model to precisely evaluate specific endpoints of HD-induced toxicity.

HD effects have been evaluated in three different ways. The first has been to measure HD-induced local epithelial injuries (Petrali et al., 1990); the second to assess cell lesions in tissue culture models (Rikimaru et al., 1991; Smith et al., 1992); and the third is to determine systemic toxicity in animals after percutaneous or parenteral administration of HD (Maisonneuve et al., 1993). In order to explore the potential mechanisms of HD toxicity and to develop a therapeutic rationale, several pharmacological compounds have been tested for their ability to protect against the systemic toxic effects (Vojvodic et al., 1985). However, despite the predominant epithelial toxicity of HD, only a few studies have been conducted. Part of this may be due to the lack of an *in vitro* model that can blister upon exposure of a vesicant. The isolated perfused porcine skin flap (IPPSF), developed in our laboratory, has been shown to be a useful tool for percutaneous absorption (Riviere et al., 1986), and pharmacological intervention (Riviere and Monteiro-Riviere, 1991). The IPPSF maintains a normal anatomical structure, a functional vascular system, and an intact local immune

network. Our previous studies have shown that exposure to HD or lewisite (dichloro(2-chlorovinyl)arsine), another highly toxic vesicant, resulted in cytotoxicity, alteration of the vascular response, gross blister formation, and other cutaneous injuries similar to that reported after human exposure to HD (Monteiro-Riviere et al., 1990; 1991).

The present study was undertaken in the IPPSF to determine the potential mechanisms of HD-induced cytotoxicity, vascular response, and vesication, and to examine the protective effects to these toxic endpoints by using pharmacological agents with different mechanisms of action, including sodium thiosulfate and cysteine (which are HD scavengers), niacinamide (a NAD^+ stabilizer and an inhibitor of poly (ADP-ribose) polymerase) and indomethacin (a nonsteroidal antiinflammatory drug and protaglandin inhibitor).

Materials and Methods

Procedures

The procedure of IPPSF preparation is described in detail elsewhere (Riviere et al., 1986). Briefly, weanling, female, Yorkshire pigs were chosen for the study. Two stages of surgery were conducted to create two IPPSFs on each pig. The Stage 1 surgery consisted of the formation of two, axial pattern, tubed skin flaps which are vascularized primarily by the caudal superficial epigastric artery and its paired venae comitantes. Two days later, in Stage 2 surgery the flaps are removed from the pig and their arterial supply cannulated. The flaps are then flushed with heparinized saline to clear the vasculature of blood, and placed in a skin flap chamber for perfusion. The perfusion chambers were housed in a specifically designed fumehood. The IPPSFs were perfused with a medium containing bovine serum albumin, glucose, and Kreb's-Ringer bicarbonate buffer. The media were oxygenated during perfusion with 95% O_2/5% CO_2 via a silastic oxygenator. Media temperature, flow rate, pH, and chamber humidity were monitored and controlled throughout the experiment. Samples of the arterial media and the venous effluent were taken on an hourly basis, and these were analyzed

for glucose utilization as an indicator of biochemical viability of IPPSF elsewhere (Riviere et al., 1986; Monteiro-Riviere, 1990).

Sodium thiosulfate, cysteine, niacinamide, and indomethacin were commercially obtained from Sigma Chemical Co. (St. Louis, MO). The IPPSF perfusion medium was prepared to contain 10^{-3} M of sodium thiosulfate, 10^{-2} M of cysteine, 10^{-3} M of niacinamide, or $2X10^{-4}$ M of indomethacin, respectively, by directly dissolving these compounds. Although indomethacin has a low solubility in aqueous solutions, it has a high affinity to albumin in the IPPSF perfusion medium, thereby dissolving readily. The criteria of choosing these dosages was based on the reported efficacy and side effect of these compounds in the literature and previous pilot IPPSF studies (Vojvodic et al., 1985; Mol et al., 1991; Yourick et al., 1991). For each compound studied, the chemical was administered to the IPPSFs by perfusion for 2 hours before HD exposure. After this 2 hour preinfusion, the IPPSFs were dosed with 300 µl of a 5.0 mg/ml of HD (total dose of 1.5 mg HD) in ethanol within a 7.5 cm^2 dosing area defined by a flexible, plastic template (Stomahesive, ConvaTec-Squibb, Princeton, NJ), then the IPPSFs were placed in the chambers and perfusion continued for an additional 6 hours. In our previous study, 5.0 mg/ml concentration of HD was shown to cause microvesication in the treated IPPSFs, and elicit the maximal vascular response associated with the release of prostaglandins (PGE_2 and $PGF_{2\alpha}$) compared to 10.0 mg/ml (Fitzpatrick et al., 1986; Monteiro-Riviere et al., 1994). IPPSFs without perfusion of any of the four pharmacological compounds were dosed with the same amount and concentration of HD in ethanol, or ethanol alone served as controls.

Vascular resistance (VR), dark basal cells, and microvesication were assessed to determine the pharmacological effects of these compounds on preventing HD cutaneous toxicity. Our previous studies have shown that these three endpoints were reproducible characteristics of HD-induced toxicity (Monteiro-Riviere et al., 1991; 1994). An increase in VR is a physiological parameter indicative of the vascular response of the IPPSF (Monteiro-Riviere, 1990). The formation of dark stratum basale cells caused by the accumulation of the

chromatin into a dense homogeneous shrunken mass, is representative of HD-induced cellular toxicity. HD-induced blistering was assessed by formation of epidermal-dermal separation.

Arterial pressure and media flow rate were monitored throughout the perfusion period, and the VR was calculated as the ratio of arterial pressure to media flow rate. After the experiment, the HD dosed region of the skin was excised, and tissue samples were taken for light microscopy (LM). LM samples were fixed in 10% neutral-buffered formalin for 24-48 hours, and routinely processed and embedded in paraffin. Sections cut at 6 μm were stained with Harris's hematoxylin and eosin (H&E) for microscopic evaluations. To determine dark basal cell number in IPPSFs treated with or without HD, five 2.8 μm long segments of epidermal-dermal junction were randomly chosen in each IPPSF tissue sample, and all dark basal cells and normal basal cells in these areas were counted under LM. The resultant development of dark basal cell was expressed by the ratio of total dark basal cells to all normal basal cells assessed in each IPPSF tissue. Microvesicles were scored as either being present or absent as a graded response is not seen.

The pharmacological effect of indomethacin (prostaglandin inhibitor) was assessed by inhibition of PGE_2 synthesis in IPPSFs. PGE_2 was extracted from hourly venous effluent samples collected from IPPSFs using a Sep-Pak Plus^R extraction cartridge (Waters, Milford, MA), then washed with ethyl acetate (EA). After the EA was evaporated, the remaining PGE_2 was dissolved in an enzyme immunosorbent assay (EIA) buffer (1 ml). The samples were then measured with an enzyme-linked immunosorbent assay using PGE_2 EIA kits (Caymen Chemical, Ann Arbor, MI). The EIA kits were developed according to the manufacturer's instructions and the samples were assayed on a Fisher Biotech ELISA Reader (Fisher Scientific, Pittsburgh, PA).

Statistical methods

Statistical comparisons were made for all parameters by carrying out an analysis of variance on responses separately for each hour after HD treatment. Where significant

($p < 0.05$) treatment effects were noted, multiple comparison tests were conducted using Fisher's protected lsd procedure.

Results

Protective effects of drugs on dermal cytotoxicity by HD. The effects of pharmacological agents on the cytotoxicity of HD exposure are shown in Tables 2-I and 2-II, and Figures 2-1 through 2-5. The HD-treated control IPPSFs developed a mean of 19.7% dark basal cells compared to the total basal cells in epidermal-dermal junction. Dark basal cells were found in one out of four IPPSFs perfused with either 10^{-3} M sodium thiosulfate or 10^{-2} M cysteine, and total ratios of dark basal cells were 3.9% and 4.2% in these two treated groups, respectively. Two out of four 10^{-3} M niacinamide-treated IPPSFs, elicited dark basal cells. Similarly, perfusion of $2X10^{-4}$ M indomethacin prevented development of dark basal cells in two out of four IPPSFs after HD treatment. The formation of dark basal cells decreased to 5.8% and 1%, respectively, in these two groups after HD treatment. Since the typical HD-lesion is homogeneous, and not focal, the tissue samples taken represent the entire dosing area. Therefore, the partial protective effect of these drugs suggests that there are several mechanisms for HD action which can contribute to cytotoxicity of the skin. For two of these drugs, the mechanism maybe chemical scavenging which reduces the effective HD tissue dose.

Table 2-I. Frequency of Morphological Lesion Noted with HD Exposure.

Topical	Perfused	Dark Basal Cells	Microvesication
HD		4/4	4/4
HD	Thiosulfate (10^{-3} M)	1/4	4/4
HD	Cysteine (10^{-2} M)	1/4	4/4
HD	Niacinamide (10^{-3} M)	2/4	4/4
HD	Indomethacin ($2X10^{-4}$ M)	2/4	2/4

Table 2-II. Protective Effect of Sodium Thiosulfate, Cysteine, Niacinamide, and Indomethacin on the Severity of HD-Induced Dark Basal Cells in IPPSFs.

Topical Perfused	EtOH -	HD -	HD Thiosulfate	HD Cysteine	HD Niacinamide	HD Indomethacin
Mean	0.0%	19.7%	3.9%	4.2%	5.8%	1.0%
SEM	±0.0%	±6.7%	±3.9%	±4.2%	±3.3%	±0.6%

Protective effects of drugs on HD-induced microvesicle. The effect of these compounds on preventing blister formation is presented in Table 2-I, and Figures 2-1 through 2-5. In the control HD-treatments, all of the four IPPSFs developed microvesicles. HD-induced microvesicles were also observed in all of the IPPSFs perfused with 10^{-3} M sodium thiosulfate, 10^{-2} M cysteine, or 10^{-3} M niacinamide, but the microvesicles were less numerous and less severe. The $2X10^{-4}$ M of indomethacin partially inhibited HD microvesication, however the epidermal-dermal separations were still noted in two out of the four IPPSFs.

Protective effects of drugs on the vascular response of IPPSF to HD. Alteration of the vascular response in the skin is usually a consequence of cutaneous injury after receiving a variety of detrimental stimuli. Furthermore, a change of the vascular response may initiate or promote other pathological reactions (Fitzpatrick et al., 1986). Therefore, we examined the cause and the role of the vascular response in HD-induced dermal lesions by using different pharmacological agents. As shown in Figure 2-6, the VR of the IPPSFs progressively increased after HD treatment. Perfusion of both 10^{-3} M niacinamide and $2X10^{-4}$ M indomethacin significantly inhibited and decreased the VR caused by HD ($p < 0.05$). VR was not affected with sodium thiosulfate and cysteine pretreatment. The antiinflammatory effect of indomethacin inhibited the increase of prostaglandin E_2 release in IPPSFs after HD exposure (Figure 2-7).

Discussion

The toxic effects of HD is mainly attributed to its highly reactive alkylating properties. However, the biochemical mechanisms leading to HD injury, such as cytotoxicity, vesication, and vascular response, are not well understood. It was thought that alkylation of DNA with subsequent DNA cross-links or breaks was the primary and initial event responsible for HD cutaneous toxicity (Papirmeister et al., 1991). Thus, a hypothesis regarding DNA alkylation, metabolic disruption, and proteolytic activity has been proposed. In this scenario, after HD exposure, DNA repair processes are induced, including the activation of poly (ADP-ribose) polymerase which uses NAD^+ as a substrate. As repair continues, NAD^+ is depleted which decreases epidermal glycolysis, and thus stimulates activation of the $NADP^+$ dependent hexose monophosphate shunt, resulting in protease release. Extracellular proteases attack dermal tissue causing cell death, inflammation, and blister formation. Recently, results from several laboratories did not support this initial hypothesis (Mol et al., 1991; Gray, 1989). It has been shown that other inhibitors of NAD^+ synthesis did not cause vesication. Additionally, using nicotinamide to increase NAD^+ levels resulted in normal glycolysis levels, however cell death and microblister formation were not inhibited. Previous studies in our laboratory have shown that gross blisters and microvesicles were present at 5 hours after HD exposure (Monteiro-Riviere et al., 1990; Zhang et al., 1995). Also, epidermal-dermal separation occured at the upper lamina lucida of the basement membrane, where a majority of HD or its metabolites penetrated (Riviere et al., 1994). Additionally, other DNA alkylating agents do not cause vesication yet cause other pathological changes characterized by HD (Zhang et al., 1995). Therefore, based on all of these arguments, alkylation of DNA may not be a primary biochemical event in acute cutaneous injury of HD, and HD may have its own unique molecular targets in the basement membrane zone of the skin, such as laminin, a thiol-rich adhesive protein (Zhang et al., 1994; Zhang et al., 1995).

To date, there are two possible strategies for the prevention of HD toxicity. The first is to prevent HD from alkylating the critical target molecules; the second, is to attempt to reverse

the subsequential biochemical events following HD alkylation, such as NAD^+ depletion and inflammation. The efficacy of the first class of pharmacological agents mainly depends on their reactive speed and concentration with HD compared to other molecular targets in cells or tissues. These two categories of compounds have been widely used systemically or in tissue cultures to determine the potential mechanism of HD action (Papirmeister et al., 1991). Other studies have been limited due to model systems which have only evaluated the protective effects of some pharmacological agents only on one aspect of HD-induced changes. Further, there has been conflicting results due to the fact that different endpoints of HD toxicity were evaluated. The advantage of the IPPSF over existing models is that the biochemical, physiological, and morphological alterations can be evaluated and integrated in one system. We employed the IPPSF model to evaluate the antagonistic effects of the different pharmacological agents on three defined endpoints of HD-induced dermal toxicity; formation of dark basal cells, vesication, and altered vascular resistance.

In this study, 10^{-3} M of sodium thiosulfate, 10^{-2} M of cysteine, 10^{-3} M of niacinamide, and $2X10^{-4}$ M of indomethacin partially prevented the appearance of dark basal cells in the IPPSFs exposed to HD. The reduction of HD-induced cytotoxicity by different compounds is consistent with their known activities. Sodium thiosulfate and cysteine provide alternative competitive reactive sites for HD, acting as scavengers and thereby preventing chemical modification of cellular molecules by HD (Papirmeister et al., 1991). It has been proposed that HD indirectly activates poly (ADP-ribose) polymerase by alkylation of DNA. During the repair process of alkylated DNA, activation of poly (ADP-ribose) polymerase results in the depletion of cellular NAD^+, which initiates a consequent pathological changes. Niacinamide has been postulated to inhibit poly (ADP-ribose) polymerase and prevent the depletion of NAD^+, thus inhibiting the induction of proteolytic activity according to the Papirmeister hypothesis (Papirmeister et al., 1991). However, studies conducted in hairless guinea pigs showed that only pretreatment of niacinamide reduced microvesication induced by HD. The reduction in microvesicles was not correlated with cellular NAD^+ content (Yourick

et al., 1991). This evidence seems to indicate that niacinamide might block HD toxicity by a mechanism other than NAD^+ depletion. In addition, both HD toxicity and the partial protective effects of niacinamide were seen at 5 hours after HD treatment in our IPPSF model. It is unlikely that toxicity initiated by alkylation of DNA occurs in such a short time window. Thus, our results suggests other possible mechanisms involved in HD dermal toxicity. Chemical alkylation which disrupts normal metabolic activities, and inflammation may contribute to cytotoxicity induced by HD.

Unlike the protective effects of these compounds on cytotoxicity, sodium thiosulfate, cysteine, and niacinamide did not prevent microvesicle formation caused by HD. Our previous studies have demonstrated that all HD-induced epidermal-dermal separation was exclusively localized at the upper lamina lucida of the basement membrane (Monteiro-Riviere et al., 1991; (Monteiro-Riviere and Inman, 1993; Monteiro-Riviere et al., 1993), and that several key basement membrane components, such as fibronectin, laminin, and heparan sulfate proteoglycan, were shown to be molecular targets for direct chemical modification of HD. Further, alkylation of the basement membrane by HD destroyed its cell adhesive activity, suggesting that HD may weaken the epidermal-dermal junction by alkylation of basement membrane constituents during the process of vesication (Zhang et al., 1994; Zhang et al., 1995). Our previous study showed that 30% of the thiol group in laminin, an adhesive protein in the basement membrane is available for alkylation (King et al., 1994). In this study, sodium thiosulfate and cysteine were not able to compete with these thiol-rich proteins at the basement membrane for HD alkylation, leading to the failure of vesicle prevention. Also, it is possible that we did not have a higher enough concentration of HD scavengers at the basement membrane. Additional studies could be performed to test the efficacy of more potent scavengers that could have a higher reactivity to HD and/or better diffusivity in skin. In this study, indomethacin partially prevented epidermal-dermal separation, indicating a partial role of inflammation in HD-induced blister formation. In addition, the vascular response,

intercellular and intracellular edema, the consequences of inflammation, may increase the pressure in the interstitial spaces of the tissue to promote the epidermal-dermal separation.

Neither sodium thiosulfate nor cysteine blocked an increase in vascular resistance. As mentioned above, failure to prevent the key molecular targets from HD alkylation may be responsible for cell injury caused by HD, leading to inflammation and a vascular response. An increase in prostaglandin E_2 and prostaglandin $F_{2\alpha}$ release after HD treatment has been reported in several different study models, including the IPPSF (Monteiro-Riviere et al., 1994; Zhang et al., 1995). Based on our toxicokinetic study, the vascular response of the IPPSF to HD may be explained by the increase in vascular permeability (Riviere et al., 1994). Also, we exogenously infused the IPPSF with prostaglandin E_2 and prostaglandin $F_{2\alpha}$, demonstrating that prostaglandins can cause a similar increase in VR, suggesting a possible role of inflammatory mediators in the dermal vascular response. In this study, indomethacin blocked both the vascular response of HD and the efflux of PGE_2, further confirming the role of prostaglandins in HD-induced vascular response. Finally, niacinamide also prevented HD-induced increase of vascular resistance in the IPPSFs, however, its mechanism is not well understood.

In conclusion, none of the previously postulated potential anti-vesicant agents tested were effective in blocking HD toxicity. Based on this information presented so far, it is reasonable to postulate that a multistep mechanism is involved in the development of HD-induced cutaneous toxicity with at least three components (cytotoxicity, microvesication and inflammation) interacting to produce the lesion. Alkylation of intracellular and extracellular key molecules seems to be an initial and determining factor for dark basal cells and microvesicles. Secondary biochemical events such as inflammation may promote an increase in the severity of HD-induced toxicity.

References

Fitzpatrick, T.B., Eisen, A.Z., Wolff, K., Freedberg, I.M., and Austen, K.F. (1986). Dermatology in General Medicine. McGraw-Hill, Inc. Pp. 321-322.

Gray, P.J. (1989). A literature review on the mechanism of action of sulfur and nitrogen mustard. Report No. MRL-TR-89-24.

King, J.R., Peters, B.P., and Monteiro-Riviere, N.A. (1994). Laminin in the cutaneous basement membrane as a potential target in lewisite vesication. Toxicol. Appl. Pharmacol. 126:164-173.

Maisonneuve, A., Callebat, I., Debordes, L., and Coppet, L. (1993). Distribution of [14C] sulfur mustard in rats after intravenous exposure. Toxicol. Appl. Pharmacol. 125:281-287.

Mol, M.A.E., De Vries, R., and Kluivers, A.W. (1991). Effects of nicotinamide on biochemical changes and microblistering induced by sulfur mustard in human skin organ cultures. Toxicol. Appl. Pharmacol. 107:439-449.

Monteiro-Riviere, N.A. (1990). Specialized technique: The isolated perfused porcine skin flap (IPPSF). In Methods for Skin Absorption, (Eds. B.W. Kemppainen and W.G. Reifenrath). CRC Press, Boca Raton, FL., pp. 175-189.

Monteiro-Riviere, N.A., King, J.R., and Riviere, J.E. (1990). Cutaneous toxicity of mustard and lewisite on the isolated perfused porcine skin flap. DAMD17-87-C-7139; NTIS, ADA229922, pp. 1-144.

Monteiro-Riviere, N.A., King, J.R., and Riviere, J.E. (1991). Mustard induced vesication in isolated perfused skin: Biochemical, physiological, and morphological studies. In Proceedings of the Medical Defense Bioscience Review, U.S.Army Medical Research Institute of Chemical Defense, Aberdeen Proving Ground, MD. pp. 159-162.

Monteiro-Riviere, N.A., and Inman, A.O. (1993). Histochemical localization of three basement membrane epitopes with sulfur mustard induced toxicity in porcine skin. Toxicologist 13:58.

Monteiro-Riviere, N.A., Inman, A.O., Spoo, J.W., Rogers, R.A., and Riviere, J.E. (1993). Studies on the pathogenesis of bis (2-chloroethyl) sulfide (HD) induced vesication in porcine skin. The Proceedings of the Medical Defense Bioscience Review, U.S.Army Medical Research Institute of Chemical Defense, Aberdeen Proving Ground, MD. 1:31-40.

Monteiro-Riviere, N.A., Zhang, Z., Williams, P.L., and Riviere, J.E. (1994). Sulfur mustard causes vascular and inflammatory changes in isolated perfused porcine skin. Toxicologist, 14:104.

Papirmeister, B, Feister, A.J., Robinson, S.I., and Ford, R.D. (1991). Medical Defense Against Mustard Gas: Toxic Mechanisms and Pharmacological Implications, CRC Press, Boca Raton, FL.

Petrali, J.P., Oglesby, S.B., and Mills, K.R. (1990). Ultrastructural correlates of sulfur mustard toxicity. Cut. Ocular Toxicol. 9:193-214.

Rikimaru, T., Nakamura, M., Yano, T., Beck, G., Habicht, G.S., Rennie, L.L., Widra, M., Hirshman, C.A., Boulay, M.G., Spannhake, E.W., Lazarus, G.S., Pula, P.L., and Dannenberg, A.M. Jr. (1991). Mediators, initiating the inflammatory response, released in organ culture by full-thickness human skin explants exposed to the irritant, sulfur mustard. J. Invest. Dermatol. 96:888-897.

Riviere, J.E., Bowman, K.F., Monteiro-Riviere, N.A., Dix, L.P., and Carver, M.P. (1986). The isolated perfused porcine skin flap: A novel *in vitro* model for percutaneous absorption and cutaneous toxicology studies. Fundam. Appl. Toxicol. 7:444-453.

Riviere, J.E., and Monteiro-Riviere, N.A. (1991). The isolated perfused porcine skin flap as an *in vitro* model for percutaneous absorption and cutaneous toxicology. CRC Crit. Rev. Toxicol. 21:329-344.

Riviere, J.E., Williams, P.L., Zhang, Z., and Monteiro-Riviere, N.A. (1994). Toxicokinetics of sulfur mustard cutaneous disposition and percutaneous absorption in isolated perfused porcine skin. Toxicologist 14:184.

Smith, W.J., Sanders, K.M., Caulfield, J.E., and Gross, C.L. (1992). Sulfur mustard-induced biochemical alterations in proliferating human cells in culture. Cut. Ocular Toxicol. 11:293-304.

Vojvodic, V., Milosavljevic, Z., Boskovic, B., and Bojanic, N. (1985). The protective effect of different drugs in rats poisoned by sulfur and nitrogen mustards. Fundam. Appl. Toxicol. 5: S160-S168.

Yourick, J.J., Clark, C.R., and Mitcheltree, L.W. (1991). Niacinamide pretreatment reduces microvesicle formation in hairless guinea pigs cutaneously exposed to sulfur mustard. Fundam. Appl. Toxicol. 17:533-542.

Zhang, Z., Peters, B.P., and Monteiro-Riviere, N.A. (1994). Assessment of the cutaneous basement membrane in sulfur mustard-induced toxicity. Toxicologist 14:428.

Zhang, Z., Peters, B.P., and Monteiro-Riviere, N.A. (1995). Assessment of sulfur mustard interaction with basement membrane components. Cell Biol. Toxicol. 11:89-101.

Zhang, Z., Riviere, J.E., and Monteiro-Riviere, N.A. (1995). Topical sulfur mustard induces changes in prostaglandins and interleukin-1_α in isolated perfused porcine skin. In Vitro Toxicol. 8:149-158.

Figure 2-1. Light micrograph of an IPPSF exposed to 5.0 mg/ml of HD depicting dark basal cells (small arrows) and epidermal-dermal separation (large arrows). H&E (X600).

Figure 2-2. Light micrograph of a sodium thiosulfate-perfused IPPSF exposed to 5.0 mg/ml of HD depicting less severe epidermal-dermal separation (large arrows), and a decrease in the number of dark basal cells (small arrows). H&E (X600).

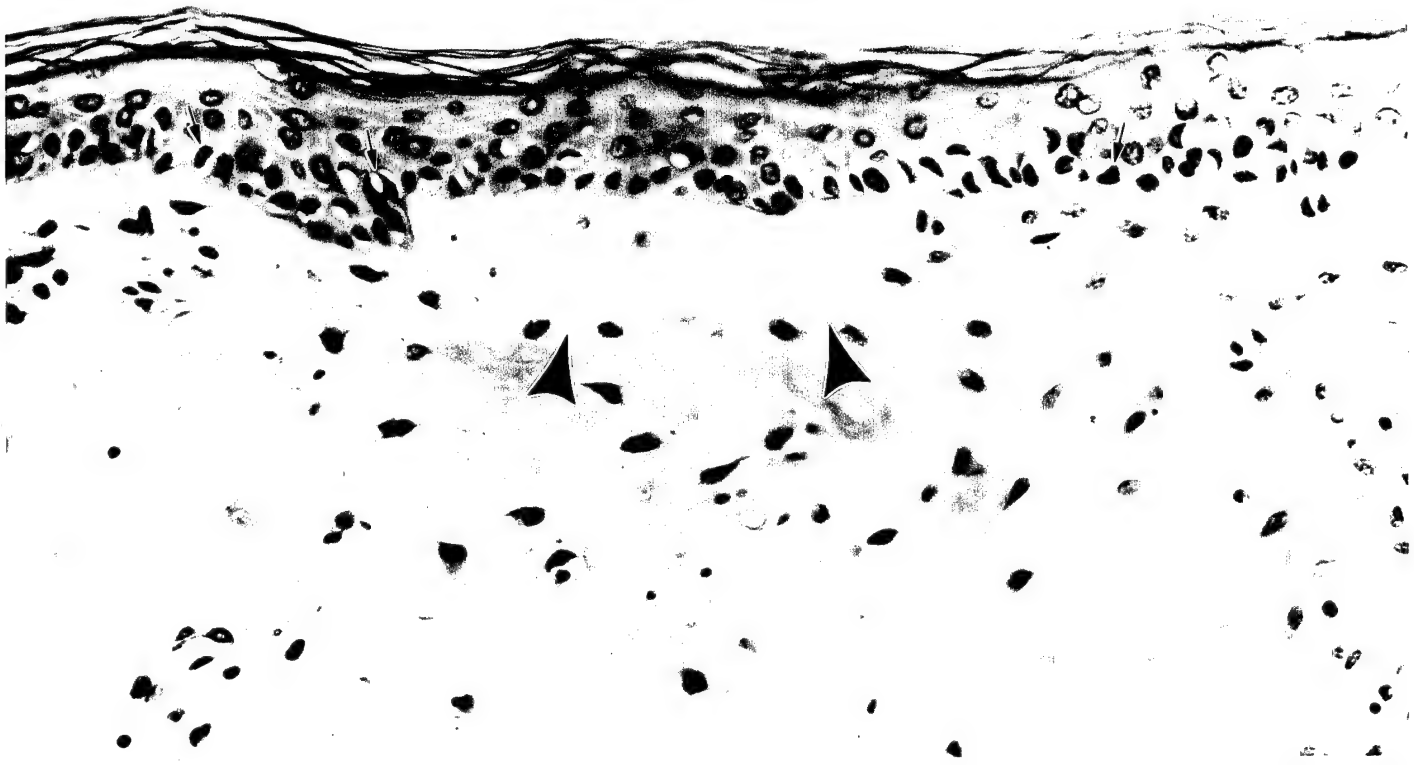

Figure 2-3. Light micrograph of an cysteine-perfused IPPSF exposed to 5.0 mg/ml of HD depicting a less severe epidermal-dermal separation (large arrows), and a few dark basal cells (small arrows). H&E (X700)

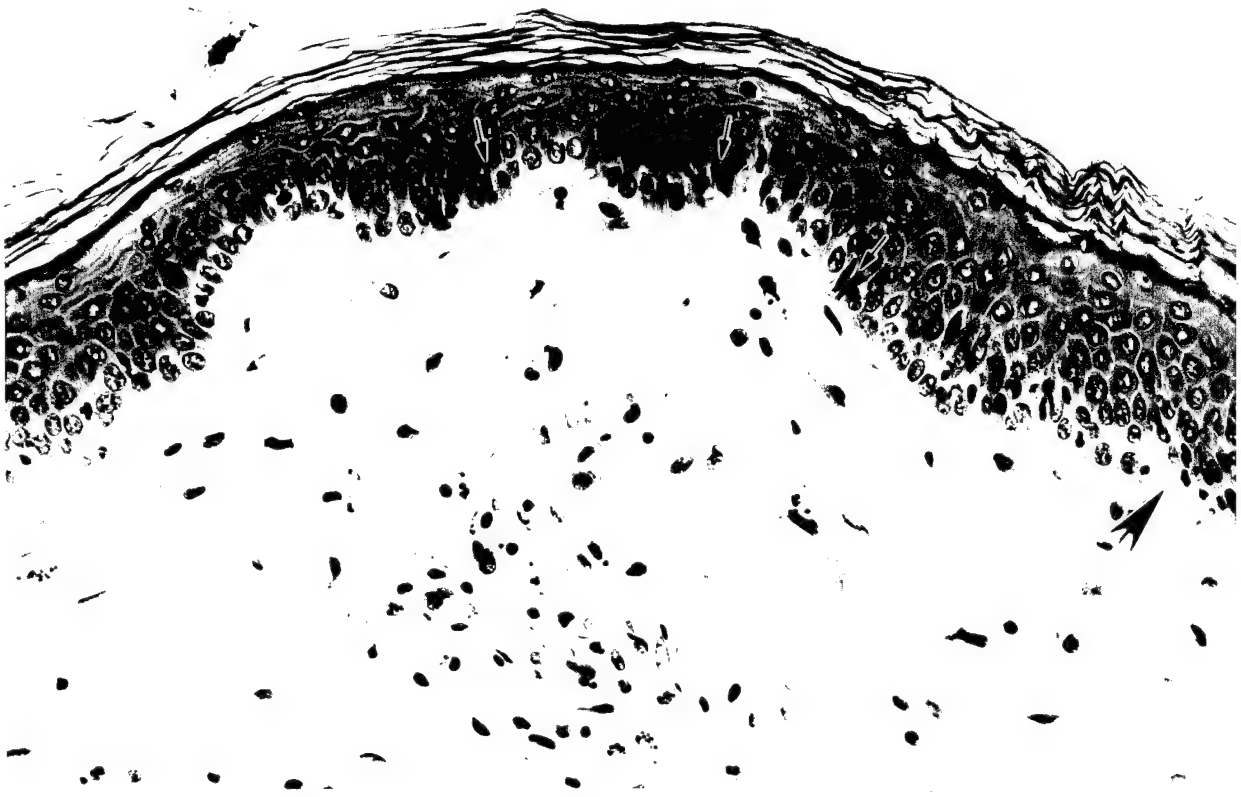

Figure 2-4. Light micrograph of an niacinamide-perfused IPPSF exposed to 5.0 mg/ml of HD showing a slight separation of the epidermal-dermal junction (large arrow), and a few dark basal cells (small arrows). H&E (X600).

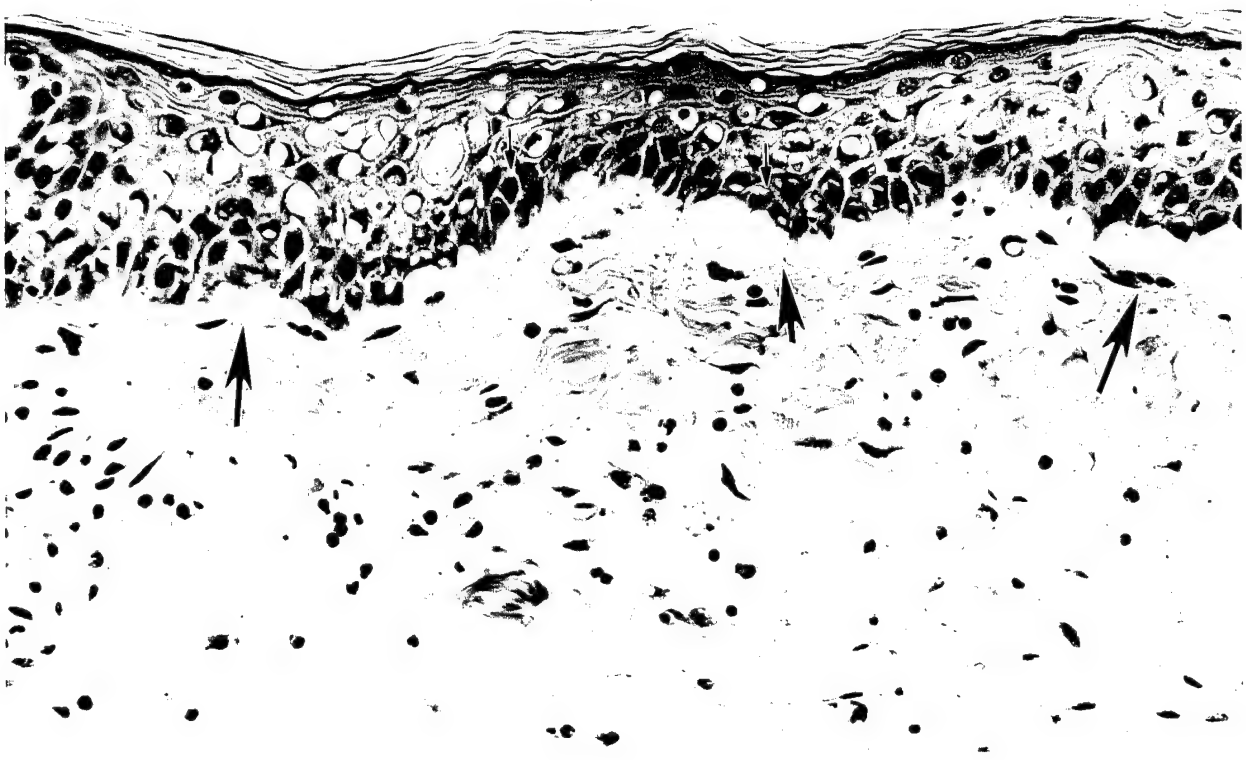

Figure 2-5. Light micrograph of an indomethacin-perfused IPPSF exposed to 5.0 of mg/ml HD showing epidermal-dermal separation (large arrows), and only a few dark basal cells (small arrows). H&E (X600).

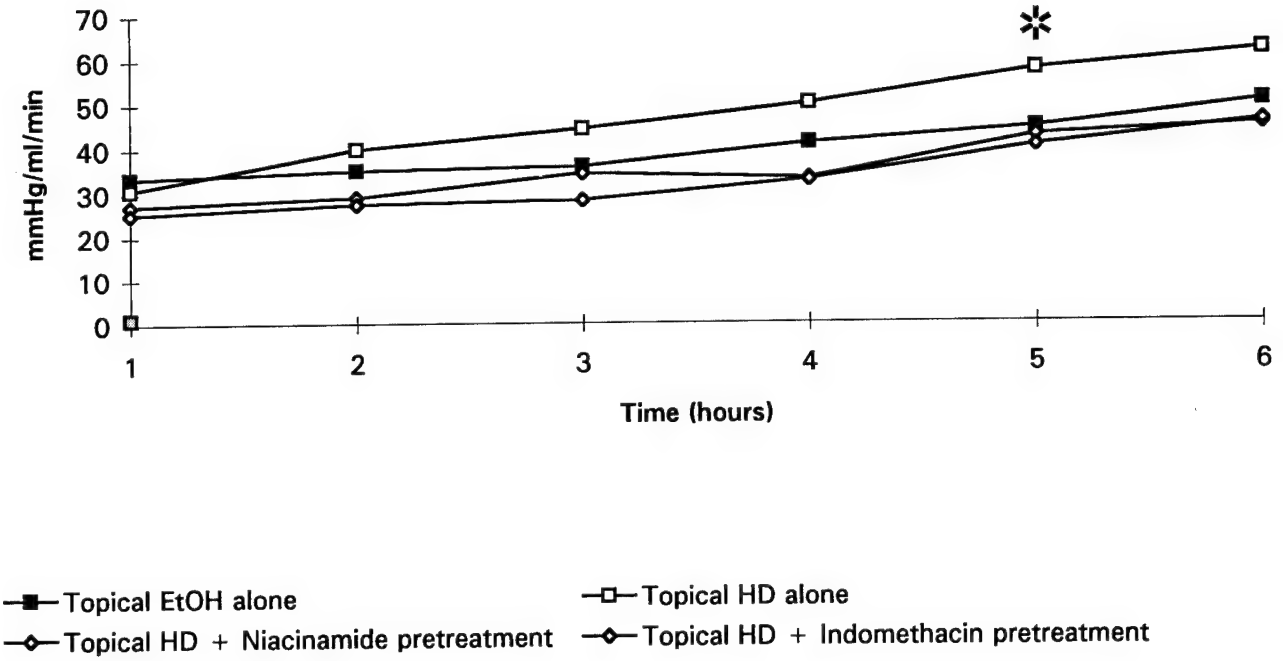

Figure 2-6. Vascular resistance of IPPSFs treated with 5.0 mg/ml of HD topically for 6 hours. (■) IPPSF treated with only topical EtOH as the control; (□) IPPSF treated with 5.0 mg/ml of topical HD; (◆) IPPSF perfused with 10^{-3} M niacinamide; (◊) IPPSF perfused with 10^{-4} M indomethacin. (*) Mean VR for topical HD treatment is significantly different from EtOH control, niacinamide, and indomethacin perfusion.

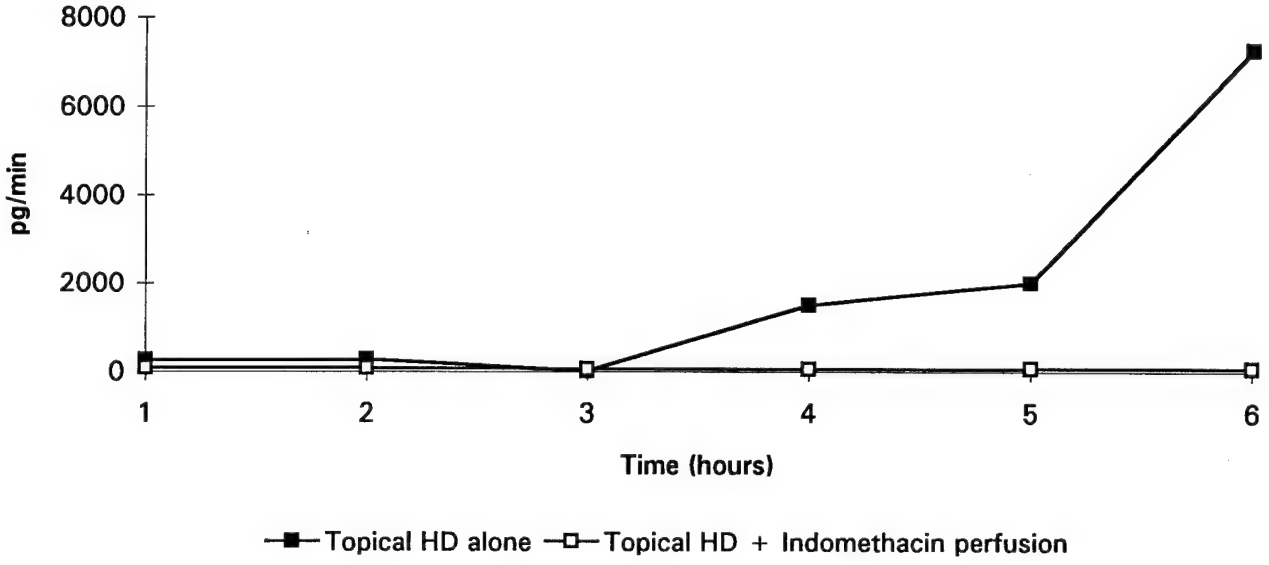

Figure 2-7. Venous efflux profile of PGE_2 for 5.0 mg/ml of HD-topically treated IPPSFs perfused with (□) and without (■) indomethacin.

3. INDIRECT IMMUNOHISTOCHEMISTRY AND IMMUNOELECTRON MICROSCOPY DISTRIBUTION OF EIGHT EPIDERMAL-DERMAL JUNCTION EPITOPES IN THE PIG AND IN ISOLATED PERFUSED SKIN TREATED WITH BIS (2-CHLOROETHYL) SULFIDE

Nancy A. Monteiro-Riviere and Alfred O. Inman

Published in *Toxicologic Pathology* 23:313-325, 1995

Abstract

Sulfur mustard (bis (2-chloroethyl) sulfide, HD) is a potent cutaneous vesicant that causes gross blisters by separation of the epidermal-dermal junction (EDJ). The EDJ of the skin is a highly specialized and complex structure composed of several components and plays a major role in the integrity of the skin. The isolated perfused porcine skin flap (IPPSF) was dosed with 0.2 mg/ml (n=4), 5.0 mg/ml (n=4), and 10.0 mg/ml (n=5) HD or ethanol (n=4) for 8 hr (dose response study) and 10.0 mg/ml HD or ethanol for 1, 3, 5, and 8 hr (n=4/treatment) (time response study). Successful EDJ mapping was carried out in normal pig skin (NPS), ethanol-treated IPPSFs, and HD-treated IPPSFs using the following antibodies: laminin, type IV collagen, fibronectin, GB3 (Nicein), bullous pemphigoid (BP), and epidermolysis bullosa acquisita (EBA). Two mouse anti-human monoclonal antibodies, L3d and 19-DEJ-1 (Uncein), did not cross-react with the EDJ of the pig. Antibody staining in NPS, ranging from very intense for laminin and type IV collagen to weak for fibronectin, was generally more discrete than in the IPPSF. No differences in staining were noted between the ethanol and nonblistered areas of the HD-treated IPPSFs. In HD-blistered areas, BP stained only the epidermal hemidesmosomes and laminin, fibronectin, and GB3 stained primarily the dermis with fragments attached to the basal pole of the stratum basale cells, while type IV collagen and EBA stained only the dermis. Mapping of these epitopes determined the precise

plane of EDJ separation in the HD-treated skin occurred beneath the hemidesmosomes within the upper portion of the lamina lucida. The conservation of human epitopes in the EDJ of the pig further emphasizes the similarities between human skin and pig skin. Therefore, pig skin and the IPPSF may be used to study HD-induced vesication and blistering diseases.

Introduction

Sulfur mustard (bis (2-chloroethyl sulfide), HD) is a potent cutaneous vesicant. Human skin exposed to HD causes severe cutaneous lesions manifested by erythema and gross blisters (Renshaw, 1946; Requena et al., 1988; Willems, 1989). Microvesicles are formed in a number of animal species in response to cutaneous exposure to HD. However, no known *in vitro* model except the isolated perfused porcine skin flap (IPPSF) produces gross blisters.

Porcine skin is morphologically (Meyer et al., 1986; Montagna and Yun, 1964; Monteiro-Riviere, 1986; Monteiro-Riviere, 1990) and histochemically (Meyer et al., 1978; Rigal et al., 1991; Woolina et al., 1991) similar to human skin and has been utilized as a model for the study of percutaneous absorption and toxicity (Bartek et al., 1972; Renshaw, 1946). The IPPSF, an alternative *in vitro* model, is morphologically similar to human skin (Monteiro-Riviere et al., 1987) and correlates well to *in vivo* (Carver et al., 1989; Williams et al., 1990) and human absorption (Riviere and Monteiro-Riviere, 1991) data. The advantages of this system over other *in vitro* systems include a viable full thickness skin preparation, an intact vasculature, a relatively large surface area for dosing, ease in sample collection, ease of measuring and manipulating experimental parameters, and the lack of systemic immune system mediation. The *in vivo* and *in vitro* models employed to study vesicant exposure either lack the structural and functional similarities to human skin or fail to produce gross blisters. Micheltree et al. (Mitcheltree et al., 1989) showed that cutaneous exposure to HD and lewisite (L) in pigs resulted in microvesicle formation but not gross blisters. Studies utilizing other *in vivo* models such as rabbit, guinea pig, hairless guinea pig, and human skin graft/nude mouse model (Marlow et al., 1990; Papirmeister et al., 1984a; 1984b; Petrali et al., 1990; Vogt et al.,

1984; Wade et al., 1989) have reported similar results. The IPPSF is the only *in vitro* model that produces gross fluid filled blisters in response to the analog 2-chloroethyl methyl sulfide and other vesicants (King et al., 1990; 1992; Monteiro-Riviere et al., 1991; 1993).

The effects of cutaneous exposure of HD and L on the epidermal-dermal junction (EDJ) antigens has been briefly explored (King et al., 1992; Monteiro-Riviere et al., 1991; 1993; Monteiro-Riviere and Stromberg, 1985). The purpose of this study was to investigate: (1) the cross reactivity of eight epitopes in pig skin that are present within the epidermal-dermal junction of normal human skin; (2) the cross reactivity of these epitopes in the IPPSF; (3) the effects of HD on these epitopes in the IPPSF; and (4) the EDJ cleavage plane within blistered HD-treated flaps.

Materials and Methods

Female weanling Yorkshire pigs (18-23 kg) purchased commercially were allowed to acclimate for a minimum of one week prior to surgery. They were housed at 72°F on elevated pen floors with a 12 hr light/12 hr dark cycle. The pigs were provided *ad libitum* with water and 15% protein pig and sow pellets (Wayne Feeds Division, Chicago, IL).

The surgical procedure (Stage I and Stage II) is described in detail elsewhere (Bowman et al., 1991; Monteiro-Riviere and Inman, 1993). Briefly, Stage I surgery involves the formation of two axial pattern, tubed skin flaps on the ventral abdomen of the pig. The flaps, removed from the pig 48 hr later during Stage II surgery, were cannulated, flushed with heparinized saline, and each placed in a skin flap perfusion chamber maintained in a specially designed fume hood.

The flaps were perfused with a modified Kreb's-Ringer buffer containing bovine serum albumin and electrolytes. The oxygen concentration, temperature, and humidity in the chamber and the pH and flow rate of the media were continuously monitored by computer and maintained throughout the entire perfusion period. Media flow, pressure, and glucose were

recorded to determine the glucose utilization (GU) and vascular resistance (pressure/flow) of the flap.

Each flap was perfused 1 hr prior to dosing to assess biochemical (GU) and morphological viability. All flaps were dosed with 200 µl of absolute ethanol or HD within a 5.0 cm^2 Stomahesive (ConvaTec-Squibb, Princeton, NJ) dosing template using a Microman positive displacement pipette (Gilson Medical Electronics S.A., Villers-le-Bel, France). In the dose response study, flaps were dosed with absolute ethanol (n=4) or HD (0.2 mg/ml (n=4), 5.0 mg/ml (n=4), or 10.0 mg/ml (n=5)) and perfused for 8 hrs. For the time response study, flaps were dosed with absolute ethanol or HD (10.0 mg/ml) and perfused for 1, 3, 5, and 8 hrs (n=4/group).

Following flap perfusion, tissue samples were taken from the dosed area for light microscopy (LM). LM samples were fixed in 10% neutral buffered formalin, processed routinely through graded ethanols, and embedded in paraffin. Sections (6 µm) were cut on a Reichert-Jung 820 rotary microtome, stained with Periodic acid-Schiff (PAS), and photographed on an Olympus BH-2 photomicroscope (Olympus Optical, Ltd., Tokyo, Japan). Tissue for immunochemistry was harvested and immediately oriented in an aluminum foil boat, quenched and embedded in OCT Compound (Tissue-Tek, Miles Inc., Elkhart, IN) in an isopentane well immersed in liquid nitrogen.

Indirect immunohistochemistry (or immunofluorescence) and immunoelectron microscopy were performed using rabbit anti-mouse Engelbreth-Holm-Swarm (EHS) tumor laminin, rabbit anti-mouse EHS tumor type IV collagen (Dr. H. Furthmayr, Stanford University), rabbit anti-human fibronectin (Biogenex Laboratories, San Ramone, CA), monoclonal mouse anti-human GB3, human bullous pemphigoid antibody (BP, IgG titer $>$1:2560), and human epidermolysis bullosa acquisita antibody (EBA, IgG titer 1:320) on all ethanol and HD-treated flaps. In addition, skin dissected from the ventral abdomen of the pig acted as normal controls for the flaps. The mouse anti-human monoclonal antibodies L3d and 19-DEJ-1 did not cross-react to EDJ epitopes in pig skin.

Indirect immunohistochemistry (IH) was carried out using routine biotin/streptavidin methodology. Cryosections (8 μm) were cut on a cryostat (Histostat, AO Reichert Scientific Instruments, Buffalo NY), mounted on poly-l-lysine coated slides, and air dried for 20 min. Sections were then incubated in 3% hydrogen peroxide and rinsed in 0.1M phosphate buffered saline (pH 7.6). The sections were incubated in 3% normal goat serum for 30 min, followed by the primary antibody (laminin, type IV collagen, fibronectin, BPA, or EBA) or the control (normal rabbit or human serum). Biotinylated IgG conjugate (goat anti-rabbit or goat anti-human) (Boehringer-Mannheim Biochemica) was applied for 1 hr followed by a 30 min incubation in the streptavidin-peroxidase conjugate label (Boehringer-Mannheim Biochemica). The tissue was then fixed in formol saline for 15 min and the reaction product developed in the substrate 3'3 diaminobenzidine tetrahydrochloride (DAB, Polysciences Inc., Warrington, PA). The sections were dehydrated through a graded ethanol series, cleared, mounted unstained, and screened on a microscope equipped with bright field optics. Indirect immunofluorescence (IF) was performed in a manner similar to the IH. The cryosections were incubated in the primary (GB3 or normal mouse serum control) and secondary (FITC labeled goat anti-mouse IgG) (Sigma ImmunoChemicals, Sigma Chemical Co., St. Louis, MO) antibodies for 30 min each and mounted in glycerin. Micrographs were taken on a Zeiss IM 35 inverted microscope equipped with epifluorescence (Carl Zeiss, Inc., West Germany).

Indirect immunoelectron microscopy (IEM) was performed using a modification of the method described by Yaoita et al. (45). Cryosections (20 μm) were mounted on chrome alum coated slides, air dried, and incubated in normal goat serum. The sections were incubated for 30-60 min in the primary antibody or the corresponding control. The secondary antibody (biotinylated goat anti-rabbit IgG, anti-mouse IgG, or anti-human IgG) was applied to the sections for 1 hr and followed by a 45 min incubation of the streptavidin-peroxidase conjugate label. The sections were fixed in half-strength Karnovsky's fixative (22) at 4°C and the reaction product developed in DAB. The tissue was post-fixed in 1% osmium tetroxide, dehydrated through a graded ethanol series, cleared in acetone, and infiltrated in Spurr resin

(Polysciences, Inc., Warrington, PA). Each section was topped with resin and polymerized overnight at 60°C. Tissue sections (600-900 Å) were cut on a Reichert Ultracut E ultramicrotome (Leica, Nussloch, Germany) and mounted on 75 x 200 mesh copper grids. Unstained sections were screened and photographed on a Philips EM 410LS transmission electron microscope (Philips Electronic Instruments, Inc., Mahwah, NJ).

Results

Morphological characterization of HD-induced blisters (EDJ separation) was reported elsewhere in detail (Monteiro-Riviere et al., 1991; 1993). HD-induced vesicles within the dose site coalesced to form large bullae (gross blisters). Blisters were localized to the EDJ in PAS stained pig skin (Figure 3-1). Gross blisters and microvesicles were present in the 0.2 mg/ml, 5.0 mg/ml, and 10.0 mg/ml HD dosed IPPSFs (Table 3-I). No gross blisters or microvesicles were noted in the ethanol controls. Indirect IH and IEM were conducted on all samples from each flap in the dose response and time response studies. Since EDJ epitope localization within the flaps of the dose response and time response studies were identical, only the dose response study will be described.

Table 3-I. Frequency of Gross Blisters and Microvesicles in the IPPSF Following an 8 Hr Exposure to HD (Dose Response Study).

Treatment	Blisters	Microvesicles
10.0 mg/ml	4/5	5/5
5.0 mg/ml	2/4	3/4
0.2 mg/ml	1/4	1/4

Indirect immunohistochemistry

The IH of laminin, type IV collagen, fibronectin, BPA, and EBA and the IF of GB3 in normal pig skin (NPS) and in the IPPSF will be described below.

Laminin: The laminin antibody bound to NPS and formed a continuous linear label along the EDJ and along the capillary basement membrane (Figure 3-2A). The staining pattern within the ethanol IPPSFs was typically broader yet more intense than in the NPS (Figure 3-2B). No staining differences were observed between the ethanol control and the nonblistered areas of the HD-treated flaps. In blistered areas of HD-treated flaps, laminin stained the dermal side of the separation (blister floor), with occasional staining of the basal pole of the stratum basale cells (blister roof) (Figure 3-2C). Staining of the dermal interface was more intense in the blistered areas than in the adjacent nonblistered areas.

Type IV Collagen: In NPS, type IV collagen exhibited EDJ and capillary basement membrane staining similar to the linear pattern of laminin (Figure 3-3A). Type IV collagen had a higher EDJ binding affinity in the ethanol (Figure 3-3B) and in the nonblistered areas of the HD-treated IPPSFs than in the NPS. In all of the blistered areas of the HD-treated IPPSFs, staining was limited exclusively to the dermis and was more intense than the adjacent nonblistered areas (Figure 3-3C).

Fibronectin: Fibronectin stained a faint, fairly continuous band along the intact EDJ in NPS (Figure 3-4A), ethanol-treated flaps, and nonblistered HD-treated flaps (Figure 3-4B). No staining of the capillary basement membrane was detected. Staining was localized primarily to the dermis of HD-blistered flaps, with stained fragments attached to the basal pole of the stratum basale cells (Figure 3-4C).

GB3: The GB3 monoclonal antibody bound to the EDJ and stained an intense continuous band in NPS (Figure 3-5A), ethanol-treated (Figure 3-5B), and nonblistered areas of HD-treated flaps. In the HD-blistered areas, the staining was localized to the dermis (Figure 3-5C).

Bullous Pemphigoid Antibody: The BP antibody stained a faint, broken label along the EDJ of NPS (Figure 3-6A). In contrast, all ethanol flaps and HD-nonblistered areas (Figure 3-6B)

exhibited a more intense and continuous staining of the EDJ. Antibody staining of HD-blistered areas was limited to the basal pole of the stratum basale cells (Figure 3-6C).

Epidermolysis Bullosa Acquisita Antibody: The EBA antibody stained a continuous band along the EDJ in NPS (Figure 3-7A), ethanol-treated (Figure 3-7B), and HD-nonblistered areas of the IPPSF. In HD-blistered areas, the antibody bound to the dermis (Figure 3-7C).

L3d and 19-DEJ-1: No staining of NPS was noted by immunohistochemistry.

Normal serum controls of NPS, ethanol-treated, and HD-treated (nonblistered and blistered areas) IPPSFs revealed no specific staining within the EDJ or the capillary basement membrane.

Indirect immunoelectron microscopy

The ultrastructural mapping of the eight EDJ epitopes in NPS and the IPPSF is summarized in Table 3-II and illustrated in the following figures.

Laminin: Antibody binding in NPS exhibited a well defined, homogeneous pattern along the EDJ (Figure 3-8A) and around the dermal vasculature. All ethanol treatments and nonblistered areas of HD-treated IPPSFs (Figure 3-8B) produced a similar, but more diffuse and fragmented, staining pattern. In all flaps with HD-induced blisters, staining occurred predominately on the dermal interface with remnant staining on the basal pole of the stratum basale cells (Figure 3-8C).

Type IV Collagen: Type IV collagen binding in NPS formed a discrete, fairly continuous band along the EDJ (Figure 3-9A) and capillary basement membrane. In contrast, staining in all ethanol and HD-nonblistered areas was more diffuse (Figure 3-9B). Antibody localization in HD-blistered areas was limited to the dermal side of the split (Figure 3-9C).

Fibronectin: Although the cross-reactivity of fibronectin was extremely low, the slight antibody staining was found along the EDJ (Figure 3-10A), the upper papillary dermis, and the capillary basement membrane of NPS and HD-treated nonblistered areas of the IPPSF (Figure 3-10B). In HD-blistered areas of the IPPSF, fibronectin bound predominantly to the

dermis (Figure 3-10C) with discrete areas of epidermal staining. Fibronectin staining was much more intense in the HD-blistered areas of the IPPSF than in the nonblistered areas.

GB3: This antibody bound to the EDJ of NPS to form a discrete discontinuous pattern (Figure 3-11A). In most of the ethanol and nonblistered HD-treated IPPSFs (Figure 3-11B) staining was localized beneath the hemidesmosomes. In HD-blistered areas, staining was localized primarily to the dermis (Figure 3-11C), with occasional remnant staining of the basal pole of the stratum basale cells.

Bullous Pemphigoid Antibody: In NPS, BP stained a discrete discontinuous pattern along the EDJ (Figure 3-12A). A more continuous staining pattern was observed in most ethanol controls (Figure 3-12B) and nonblistered areas of HD-treated flaps. In the HD-induced blistered flaps, BPA was localized to discrete areas within the hemidesmosomes (Figure 3-12C).

Epidermolysis Bullosa Acquisita Antibody: EBA stained a diffuse band along the EDJ of NPS (Figure 3-13A), ethanol, and nonblistered HD-treated IPPSFs (Figure 3-13B). The antibody staining was better delineated in the flap than in NPS. In blistered HD IPPSFs, the antibody was bound exclusively to the dermis (Figure 3-13C).

L3d and 19-DEJ-1: No cross reactivity occurred in NPS with the mouse anti-human monoclonal antibodies L3d and 19-DEJ-1.

The normal control sera produced no staining in NPS, ethanol-treated IPPSFs, or nonblistered and blistered areas of HD-treated IPPSFs.

In summary, the HD-induced separation of the EDJ in the IPPSF is localized to the upper lamina lucida (Figure 3-14).

Table 3-II. Characterization of the Staining Patterns of Eight Epidermal-Dermal Junction Epitopes in HD-Induced Blisters in the IPPSF as Determined by Indirect Immunoelectron Microscopy.

Antigen	Localization[1]	Epidermis	Dermis	Capillary
Laminin	lamina lucida	fragmented	continuous (+++)	+++
Type IV	lamina densa	NA	continuous (+++)	+++
Fibronectin	lamina lucida	fragmented	continuous (+)	++
GB3	lamina lucida lamina densa	fragmented NA	continuous (++) continuous (++)	NA
BPA	hemidesmosomes	discontinuous (++)	NA	NA
EBA	lamina densa	NA	continuous (++)	NA
L3d	anchoring fibrils	*	*	*
19-DEJ-1	lamina lucida	*	*	*

[1] Normal human skin localization determined in historic studies.
* No antibody cross-reactivity in pig skin.
NA: not applicable
Staining intensity: (+++) = intense; (++) = moderate; (+) = slight.

Discussion

The EDJ of porcine skin has been described to be ultrastructurally similar to that of humans (Monteiro-Riviere, 1986; 1990). The EDJ consists of the basal cell plasma membrane (which includes the hemidesmosomes), the lamina lucida, the lamina densa (basal lamina), and the subbasal lamina. The antibodies chosen for this study have been localized within the EDJ of human skin and were found to cross-react with epitopes within the porcine EDJ. The authors are unaware of any extensive mapping studies within the EDJ of normal pig skin. Stanley et al. (1981) did report that laminin, type IV collagen, and BP bound to the EDJ of normal skin of weanling Yorkshire pigs. Another study (Rigale et al., 1991) found that porcine skin exhibited a high degree of cross-reactivity to murine laminin and to human type IV collagen and BPA. The mapping of additional antibodies within the EDJ allows further characterization of normal porcine skin and the IPPSF. In addition, the specificity of these antibodies within the EDJ of pig skin provide the precise localization of the HD-induced blister cleavage plane.

Foidart et al. (1980) originally reported that laminin was located within the lamina lucida of human skin. Other studies suggest laminin was found primarily (Fleischmajer et al., 1985) or exclusively (Laurie et al., 1982) within the lamina densa. It is now believed that the laminin molecule spans at least a portion of both layers (Briggaman, 1990; Horiguchi et al., 1991). Type IV collagen, the major structural protein of the EDJ (Briggaman, 1983), is localized within the lamina densa. Fibronectin, a macromolecule that may not be a true component of the EDJ (Clark, 1983), was originally demonstrated in the lamina lucida of fetal rodent skin and in the upper papillary dermis and around the vasculature in adult human skin. The monoclonal antibody GB3 was raised against human amnion and specifically binds to the lamina lucida (probably in association with hemidesmosomes) and the lamina densa (Verrando et al., 1987). The BP antigen is spatially associated with the hemidesmosomes of the cell membrane, although a portion of the molecule may cross into the lamina lucida (Fine et al., 1989). Woodley et al. (1984) defined the EBA antigen from autoantibodies in the sera of EBA

patients and localized the antigen to the lamina densa of the human basement membrane. The mouse monoclonal antibodies L3d and 19-DEJ-1 (Uncein) did not cross-react in NPS. In normal human skin, the L3d antibody binds an epitope on the carboxyl-terminal domain of type VII collagen immediately beneath the lamina densa located on the anchoring fibrils (Rusemko et al., 1989). The 19-DEJ-1 antibody binds within the midlamina lucida directly beneath the hemidesmosomes and may recognize an epitope on either a portion of the subbasal dense plate or the anchoring filaments (Fine,1991). The epitopes characterized by these monoclonal antibodies were not conserved in the skin of Yorkshire pigs.

In this present study, indirect immunohistochemical staining has shown that antibodies to laminin, type IV collagen, fibronectin, GB3, BP, and EBA cross-react with EDJ epitopes in normal pig skin and in the *in vitro* IPPSF model. Laminin, type IV collagen, and BP usually stained the EDJ in the IPPSF more intensely than in NPS. Immunoelectron microscopy, in general agreement with the immunohistochemistry, has shown that the staining patterns in NPS are similar, though more discrete than in the IPPSF. However, the GB3 antibody stained the EDJ in nonblistered flaps more discretely than in NPS. The more diffuse staining pattern typically found along the EDJ of most IPPSFs may be explained by a slight diffusion of the EDJ epitopes during perfusion. Fibronectin staining of NPS capillary basement membrane was noted by immunoelectron microscopy but not by immunohistochemistry due to extremely low cross-reactivity of this antibody.

HD (and its analog 2-chloroethyl methyl sulfide) and L caused the formation of gross blisters and microscopic EDJ separation in the IPPSF similar to that described in vesicant exposure of human skin (King et al., 1990; 1992; Monteiro-Riviere et al., 1991; 1993). Immunohistochemistry of HD-blistered and nonblistered areas from the IPPSF dosing site revealed a slight to intense antibody staining. No difference in antibody staining affinity was found between the IPPSF dosed with 0.2, 5.0, and 10.0 mg/ml HD and ethanol-dosed IPPSFs. Therefore, HD does not appear to effect the integrity of the EDJ epitopes. Epitope mapping of HD-blistered skin by IH localized the cleavage plane to be within the laminin and

fibronectin, above the type IV collagen, GB3, and EBA, and below the BP antigenic sites. Immunoelectron microscopy precisely defined the plane of epidermal-dermal cleavage. The laminin antibody bound primarily to the dermis with focal areas of attachment to the basal pole of the stratum basale cells. Woodley et al. (1983) described the same pattern using immunofluorescence in split human skin preparations. This indicates that the cleavage plane in the blistered HD-treated IPPSFs is localized to the upper portion of the lamina lucida. Type IV collagen, GB3, and EBA bound to the lamina densa and exclusively stained the dermal surface. Hemidesmosome-associated BPA stained only the epidermis. This is identical to the cleavage plane found in both experimental (suction, sodium chloride, heat shock, EDTA, various proteases) and diseased (junctional epidermolysis bullosa, autoimmune bullous diseases) states.

In conclusion, the characterization of the EDJ in normal pig skin and in the IPPSF was determined by the mapping of antibodies to laminin, type IV collagen, fibronectin, GB3, BP, and EBA. These six antibodies did cross-react with the EDJ epitopes in NPS while L3d and 19-DEJ-1 did not. Antibody staining in the IPPSF was similar though generally more diffuse than in NPS. No differences in antibody affinity were found between ethanol flaps and nonblistered areas of HD dosed flaps. The EDJ cleavage plane of the HD-blistered IPPSFs was within the upper lamina lucida, the weakest component of the EDJ. This data, coupled with historical morphological studies, proves that the pig skin EDJ has similarities to human skin and enhances the potential of the IPPSF as a model to study HD-induced vesication and blistering diseases.

References

Bartek, M.J., LaBudde, J.A., and Maibach, H.I. (1972). Skin permeability *in vivo*: Comparison in rat, rabbit, pig, and man. J. Invest. Dermatol. 58:114-123.

Bowman, K.F., Monteiro-Riviere, N.A., and Riviere, J.E. (1991). Development of surgical techniques for preparation of *in vitro* isolated perfused porcine skin flaps for percutaneous absorption studies. Am. J. Vet. Res. 52:75-82.

Briggaman, R.A. (1983). The epidermal-dermal junction and genetic disorders of this area. In Biochemistry and Physiology of the Skin, (Ed. L.A. Goldsmith). Oxford University Press, New York, NY, pp. 1001-1024.

Briggaman, R.A. (1990). Epidermal-dermal junction: Structure, composition, function and disease relationships. Prog. Dermatol. 24:1-8.

Carver, M.P., Williams, P.L., and Riviere, J.E. (1989). The isolated perfused porcine skin flap. III. Percutaneous absorption pharmacokinetics of organophosphates, steroids, benzoic acid, and caffeine. Toxicol. Appl. Pharmacol. 97:324-337.

Clark, R.A.F. (1983). Fibronectin in the skin. J. Invest. Dermatol. 8:475-479.

Fine, J.D., Horiguchi, Y., Jester, J., and Couchman, J.R. (1989). Detection and partial characterization of a midlamina lucida-hemidesmosome-associated antigen (19-DEJ-1) present within human skin. J. Invest. Dermatol. 92:825-830.

Fine, J.D. (1991). Structure and antigenicity of the skin basement membrane zone. J. Cutan. Pathol. 18:401-409.

Fleischmajer, R., Timpl, R., Dziadek, M., and Lebwohl, M. (1985). Basement membrane proteins, interstitial collagens, and fibronectin in neurofilibroma. J. Invest. Dermatol. 85:54-59.

Foidart, J.M., Bere, E.W., Yaar, M., Rennard, S.I., Gullino, M., Martin, G.R., and Katz, S.I. (1980). Distribution and immunoelectron microscopic localization of laminin, a noncollagenous basement membrane glycoprotein. Lab. Invest. 42:336-342.

Horiguchi, Y., Abrahamson, D.R., and Fine, J.D. (1991). Epitope mapping of the laminin molecule in murine skin basement membrane zone: Demonstration of spatial differences in ultrastructural localization. J. Invest. Dermatol. 96:309-313.

King, J.R., and Monteiro-Riviere, N.A. (1990). Cutaneous toxicity of 2-chloroethyl methyl sulfide in isolated perfused porcine skin. Toxicol. Appl. Pharmacol. 104:167-179.

King, J.R., Riviere, J.E., and Monteiro-Riviere, N.A. (1992). Characterization of lewisite toxicity in isolated perfused skin. Toxicol. Appl. Pharmacol. 116:189-201.

Laurie, G.W., LeBlond, C.P., and Martin, G.R. (1982). Localization of type IV collagen, laminin, heparan sulfate proteoglycan, and fibronectin to the basal lamina of basement membranes. J. Cell. Biol. 95:340-344.

Marlow, D.D., Mershon, M.M., Mitcheltree, L.W., Petrali, J.P., and Jaax, G.P. (1990). Sulfur mustard-induced skin injury in hairless guinea pigs. J. Toxicol.-Cut. & Occular Toxicol. 9:179-192.

Meyer, W., Schwarz, R., and Neurand, K. (1978). The skin of domestic mammals as a model for the human skin, with special reference to the domestic pig. Curr. Probl. Dermatol. 7:39-52.

Meyer, W., Gorgen, S., and Schlesinger, C. (1986). Structural and histochemical aspects of epidermis development of fetal porcine skin. Am. J. Anat. 176:207-219.

Mitcheltree, L.W., Mershon, M.M., Wall, H.G., Pulliam, J.D., and Manthei, J.H. (1989). Microblister formation in vesicant-exposed pig skin. J. Toxicol.-Cut. & Ocular Toxicol. 8:309-319.

Montagna, W., and Yun, J.S. (1964). The skin of the domestic pig. J. Invest. Dermatol. 43:11-21.

Monteiro-Riviere, N.A., and Stromberg, M.W. (1985). Ultrastructure of the integument of the domestic pig (*Sus scrofa*) from one through fourteen weeks of age. Anat. Histol. Embryol. 14:97-115.

Monteiro-Riviere, N.A. (1986). Ultrastructural evaluation of the porcine integument. In Swine in Biomedical Research, (Ed. M.E. Tumbleson), Plenum, New York, pp. 641-655.

Monteiro-Riviere, N.A., Bowman, K.L., Scheidt, V.J., and Riviere, J.E. (1987). The isolated perfused porcine skin flap (IPPSF). II. Ultrastructural and histological characterization of epidermal viability. In Vitro Toxicol. 1:241-252.

Monteiro-Riviere, N.A. (1990). Specialized technique: The isolated perfused porcine skin flap (IPPSF). In Methods for Skin Absorption, (Eds. B.W. Kemppainen and W.G.Reifenrath), CRC Press, Boca Raton, FL, pp. 175-189.

Monteiro-Riviere, N.A., King, J.R., and Riviere, J.E. (1991). Mustard-induced vesication in isolated perfused skin: Biochemical, physiological, and morphological studies. In Proceedings of the Medical Defense Bioscience Review. U.S. Army Medical Research Institute of Chemical Defense, Aberdeen Proving Ground, MD. pp. 159-162.

Monteiro-Riviere, N.A., Inman, A.O., Spoo, J.W., Rogers, R.A., Riviere, J.E. (1993). Studies on the pathogenesis of bis (2-chloroethyl) sulfide (HD) induced vesication in porcine skin. In Proceedings of the Medical Defense Bioscience Review. U.S. Army Medical Research Institute of Chemical Defense, Aberdeen Proving Ground, MD. pp. 31-40.

Monteiro-Riviere, N.A., and Inman, A.O. (1993). Histochemical localization of three basement membrane epitopes with sulfur mustard induced toxicity in porcine skin. Toxicologist. 13:58.

Papirmeister, B., Gross, C.L., Petrali, J.P., and Hixson, C.J. (1984a). Pathology produced by sulfur mustard in human skin grafts on athymic nude mice. I. Gross and light microscope changes. J. Toxicol.-Cut. & Ocular Toxicol. 3:371-391.

Papirmeister, B., Gross, C.L., Petrali, J.P., and Meier, H.L. (1984b). Pathology produced by sulfur mustard in human skin grafts on athymic nude mice. II. Ultrastructural changes. J. Toxicol.-Cut. & Ocular Toxicol. 3:393-408.

Petrali, J.P., Oglesby, S.B., and Mills, K.R. (1990). Ultrastructural correlates of sulfur mustard toxicity. J. Toxicol.-Cut. & Occular Toxicol. 9:193-214.

Reifenrath, W.G., Chellquist, E.M., Shipwash, E.A., and Jederberg, W.W. (1984). Evaluation of animal models for predicting skin penetration in man. Fundam. Appl. Toxicol. 4:S224-S230.

Renshaw, B. (1946). Mechanisms in production of cutaneous injuries by sulfur and nitrogen mustards. In Chemical Warfare Agents and Related Chemical Problems. Technical summary report, Vol. 1, Part III-VI, pp. 479-487.

Requena, L., Requena, C., Sanchez, M., Jaqueti, G., Aguilar, A., Sanchez-Yus, E., and Hernandez-Moro, B. (1988). Chemical warfare. Cutaneous lesions from mustard gas. J. Amer. Acad. Dermatol. 19:529-536.

Rigal, C., Pieraggi, M.T., Vincent ,C., Prost, C., Bouissou, H., and Serre, G. (1991). Healing of full-thickness cutaneous wounds in the pig. I. Immunohistochemical study of epidermo-dermal junction regeneration. J. Invest. Dermatol. 96:777-785.

Riviere, J.E., and Monteiro-Riviere, N.A. (1991). The isolated perfused porcine skin flap as an *in vitro* model for percutaneous absorption and cutaneous toxicology. CRC Crit. Rev. Toxicol. 21:329-344.

Rusenko, K.W., Gammon, W.R., Fine, J.D., and Briggaman, R.A. (1989). The carboxyl-terminal domain of type VII collagen is present at the basement membrane in recessive dystrophic epidermolysis bullosa. J. Invest. Dermatol. 92:623-627.

Stanley, J.R., Alvarez, O.M., Bere, E.W., Eaglstein, W.H., and Katz, S.I. (1981). Detection of basement membrane zone antigens during epidermal wound healing in pigs. J. Invest. Dermatol. 77:240-243.

Verrando, P., Hsi, B.L., Yeh, C.J., Pasani, A., Seriegs, N., and Ortonne, J.P. (1987). Monoclonal antibody GB3, a new probe for the study of human basement membranes and hemidesmosomes. Exp. Cell Res. 170:116-128.

Vogt, R.F. Jr, Dannenberg, A.M. Jr, Scofield, B.H., Hynes, N.A., and Papirmeister, B. (1984). Pathogenesis of skin lesions caused by sulfur mustard. Fundam. App. Toxicol. 4:S71-S83.

Wade, J.V., Mershon, M.M., Mitcheltree, L.W., and Woodard, C.L. (1989). The hairless guinea pig model and vesicant vapor exposures for bioassay purposes. In Proceedings of the Medical Defense Bioscience Review. U.S. Army Medical Research Institute of Chemical Defense, Aberdeen Proving Ground, MD. pp. 569-575.

Williams, P.L., Carver, M.P., and Riviere, J.E. (1990). A physiologically relevant pharmacokinetic model of xenobiotic percutaneous absorption utilizing the isolated perfused porcine skin flap. J. Pharm. Sci. 79:305-311.

Willems, J.L. (1989). Clinical management of mustard gas casualties. Annales Medionae Militaris. 3:1-61.

Woolina, U., Berger, U., and Mahrle, G. (1991). Immunohistochemistry of porcine skin. Acta Histochem. 90:87-91.

Woodley, D., Sauder, D., Talley, M.J., Silver, M., Grotendorst, G., and Qwarnstrom, E. (1983). Localization of basement membrane components after dermal-epidermal junction separation. J. Invest. Dermatol. 81:149-153.

Woodley, D., Briggaman, R.A., O'Keefe, E.J., Inman, A.O., Queen, L.L., and Gammon, W.R. (1984). Identification of the skin basement membrane autoantigen in epidermolysis bullosa acquisita. New Engl. J. Med. 30:1007-1013.

Yaoita, H., Gullino, M., and Katz, S.I. (1976). Herpes gestationis. Ultrastructure and ultrastructural localization of *in vivo*-bound complement: Modified tissue preparation and processing for horseradish peroxidase staining of skin. J. Invest. Dermatol. 66:383-388.

Figure 3-1. LM of IPPSF dosed with 10.0 mg/ml HD. Note EDJ separation (arrows). Epidermis (E), dermis (D). PAS. (X400).

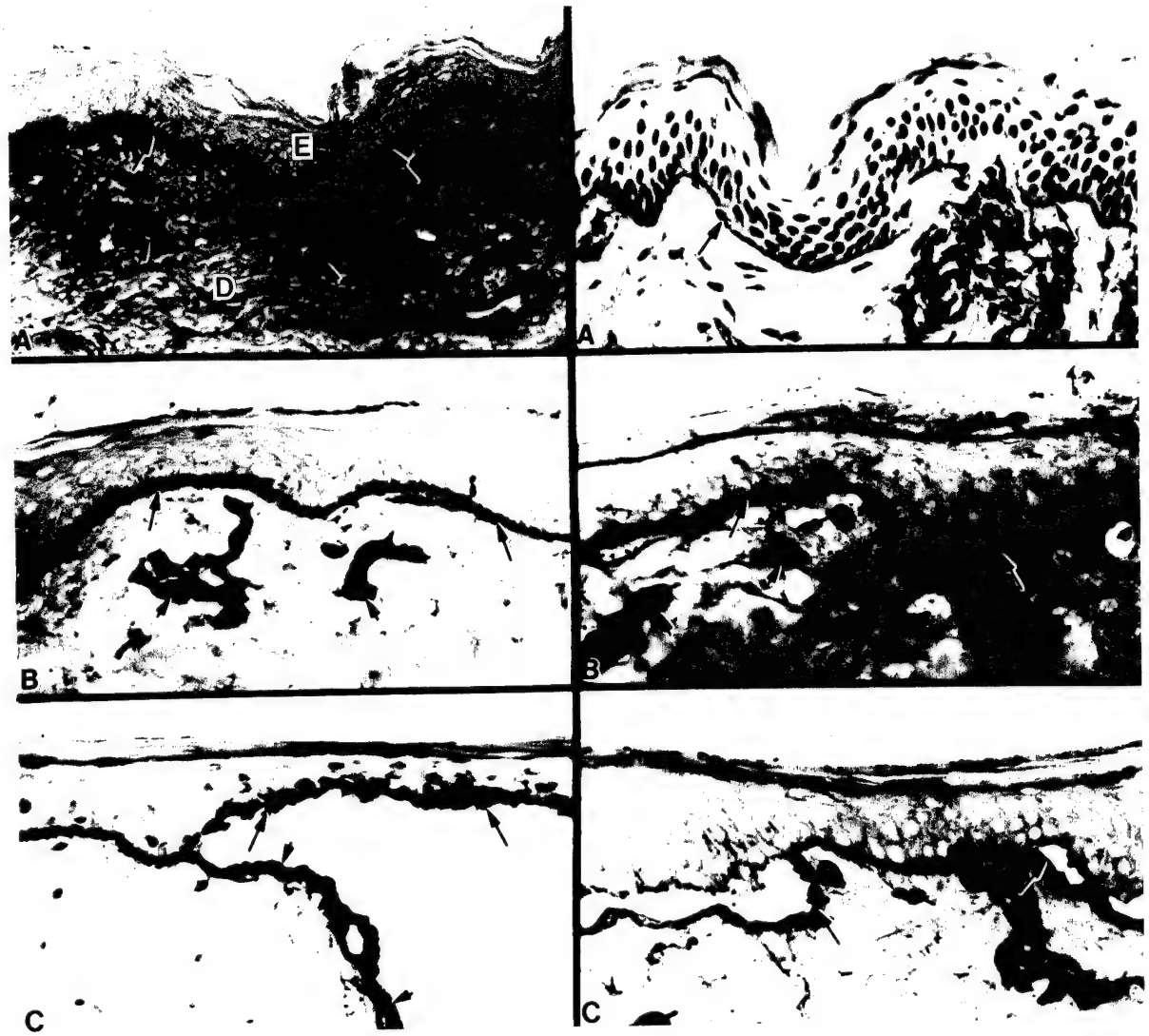

Figure 3-2. IH of the laminin antibody. A. Continuous EDJ (arrows) and capillary basement membrane (arrowheads) staining in NPS. Epidermis (E), dermis (D). (X200); B. Ethanol-treated IPPSF showing a continuous staining along the EDJ (arrows) and capillary basement membrane (arrowheads). (X280); C. A 5.0 mg/ml HD-induced blister with fragmented staining along the epidermal basal cells (arrows) and continuous staining along the dermal interface (arrowheads). (X300).

Figure 3-3. IH of the type IV collagen antibody. A. Continuous EDJ (arrows) and capillary basement membrane staining in NPS. (X300); B. Ethanol-treated IPPSF showing an intense continuous staining along the EDJ (arrows) and the capillary basement membrane (arrowheads). (X300); C. A 5.0 mg/ml HD-induced blister with staining along the dermal interface (arrows). (X275).

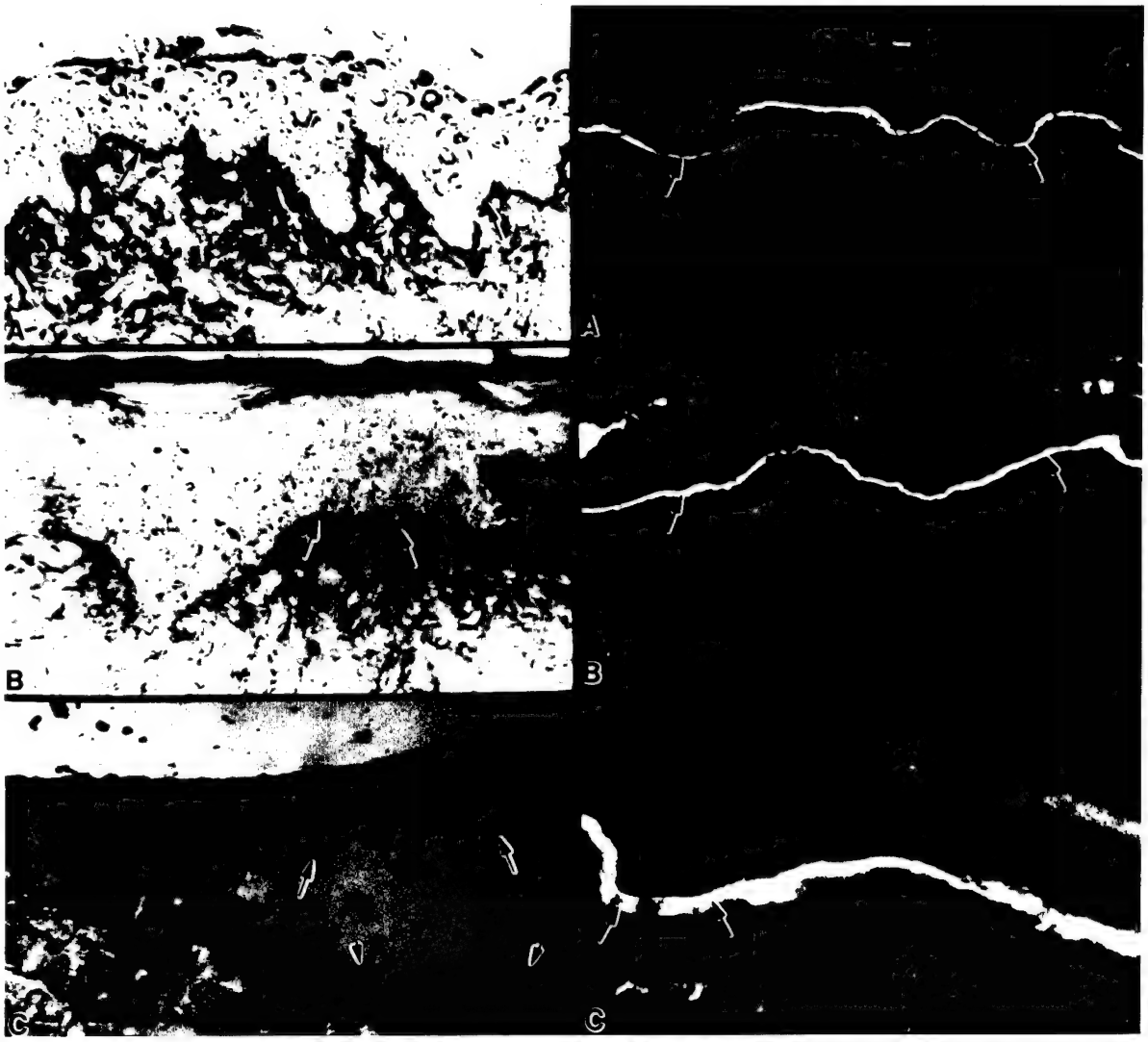

Figure 3-4. IH of fibronectin. A. Faint, inconsistent staining along the EDJ (arrows) in NPS. (X250); B. Inconsistent staining along the EDJ (arrows) of a nonblistered IPPSF dosed with 5.0 mg/ml HD. (X250); C. A 5.0 mg/ml HD-induced blister with fragmented staining along the epidermal basal cells (arrows) and fairly continuous staining along the dermal interface (arrowheads). (X300).

Figure 3-5. IF of the GB3 antibody. A. Continuous staining along the EDJ (arrows) in NPS. (X200); B. An ethanol-treated IPPSF showing EDJ staining by GB3 (arrows). (X200); C. A 10.0 mg/ml HD-induced blister with continuous staining along the dermal interface (arrows). (X270).

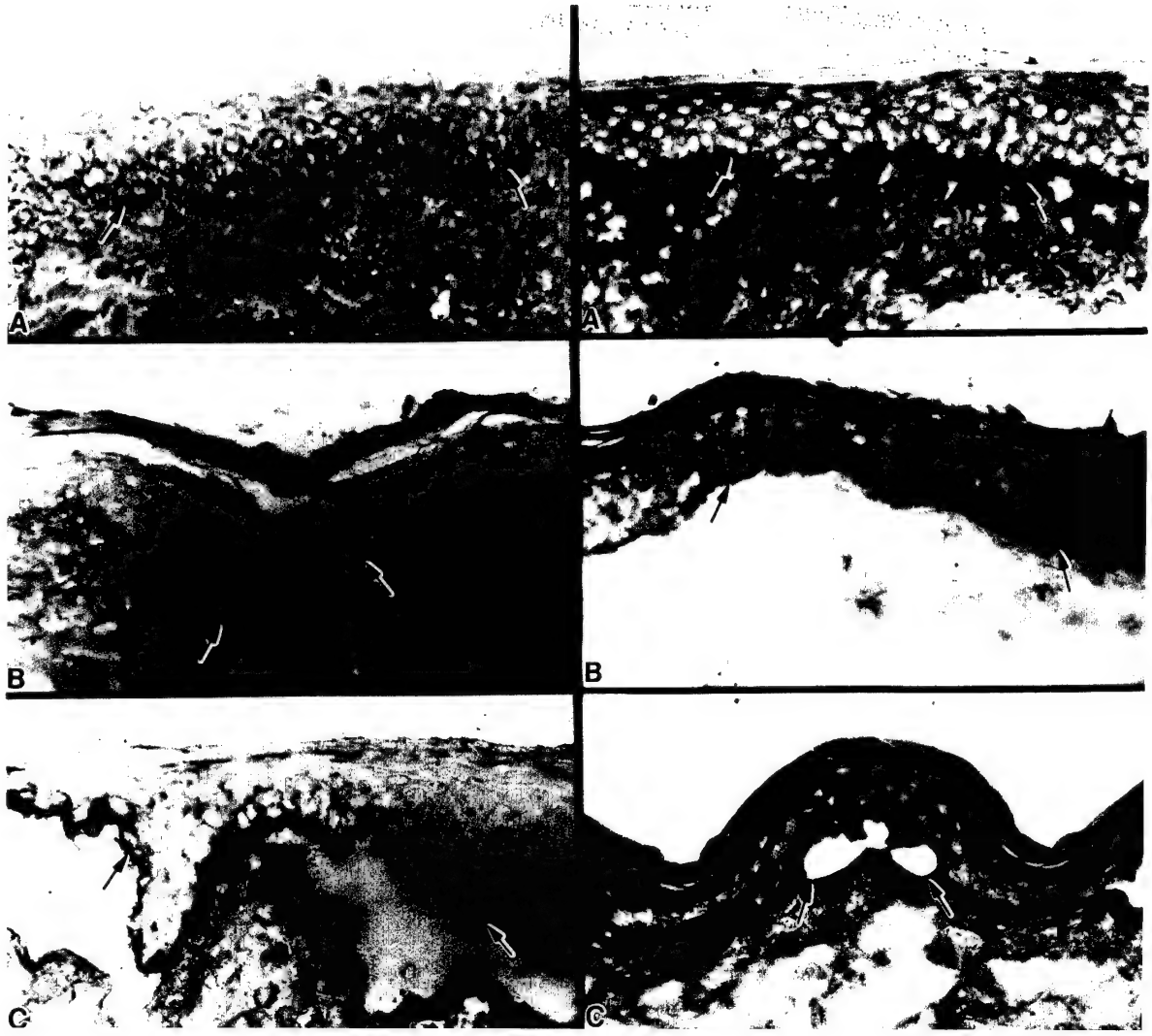

Figure 3-6. IH of the BP antibody. A. Faint, broken staining along the EDJ (arrows) in NPS. (X280); B. More intense and continuous staining along the nonblistered EDJ (arrows) in a 5.0 mg/ml dosed HD flap. (X225; C. A 10.0 mg/ml HD-induced blister with continuous staining along the epidermal basal cells (arrows). (X270).

Figure 3-7. IH of the EBA antibody. A. Continuous staining along the EDJ (arrows) in NPS. (X250); B. Continuous staining along the EDJ (arrows) in an ethanol-treated IPPSF. (X250); C. A 5.0 mg/ml HD-induced blister showing EDJ staining along the dermal interface (arrows). (X300).

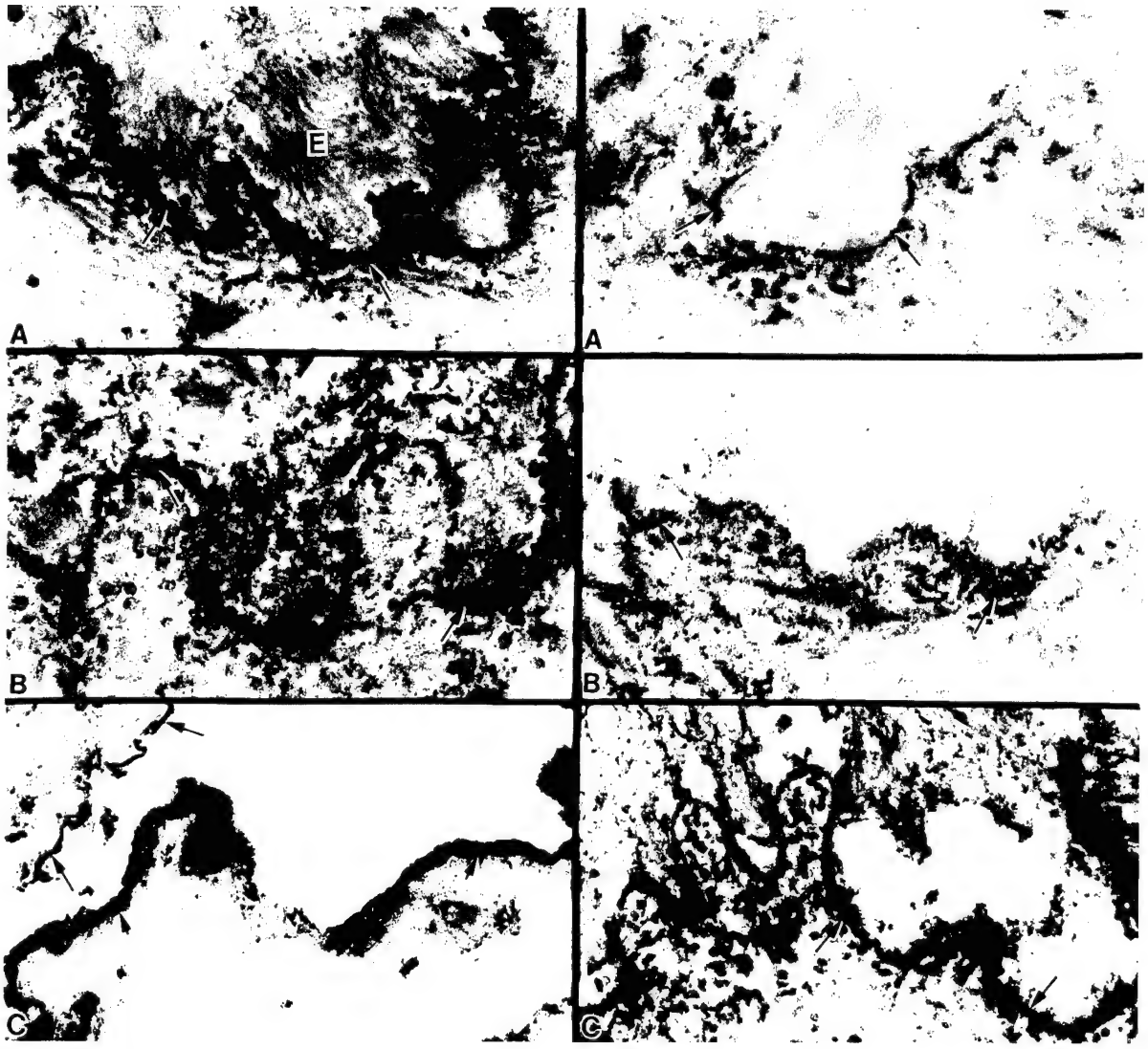

Figure 3-8. IEM of laminin. A. Well defined staining within the lamina lucida (arrows) of the EDJ in NPS. Epidermis (E), dermis (D). (X21,000); B. Diffuse and fragmented staining of the lamina lucida (arrows) of the IPPSF dosed with 0.2 mg/ml HD. (X26,500); C. Fragmented staining of the epidermal basal cells (arrows) and continuous staining of the dermal interface (arrowheads) in a blistered 10.0 mg/ml dosed flap. (X15,600).

Figure 3-9. IEM of type IV collagen. A. Discrete, fairly continuous staining in the lamina densa (arrows) of the EDJ in NPS. (X26,300); B. Nonblistered 0.2 mg/ml HD dosed IPPSF with diffuse staining in the lamina densa (arrows). (X26,300); C. Staining of a 10.0 mg/ml HD-induced blister showing strong dermal staining (arrows). (X18,000).

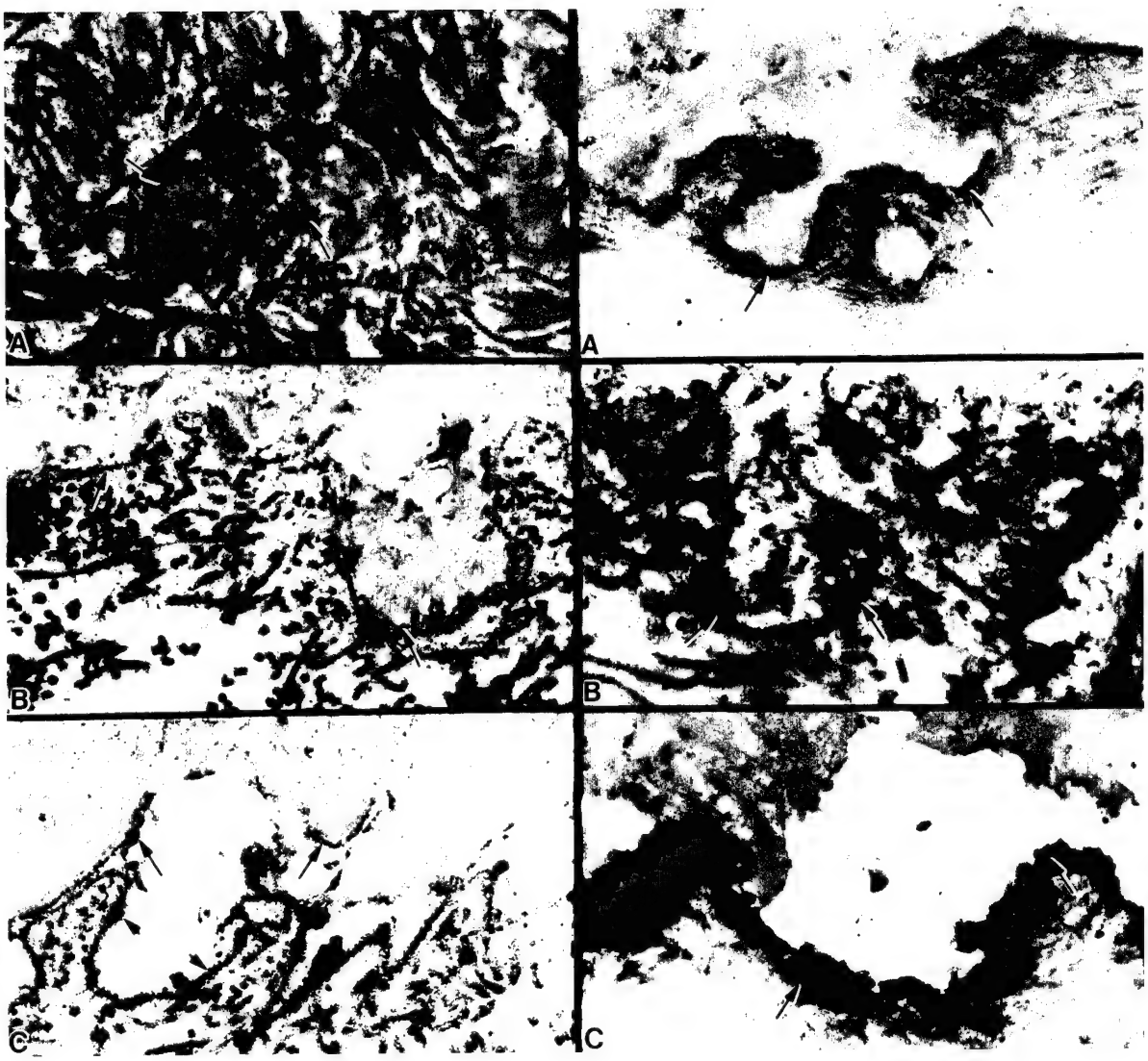

Figure 3-10. IEM of fibronectin. A. Cross-section of the EDJ in NPS showing slight antibody staining in the lamina lucida (arrows). (X16,900); B. Faint staining of the lamina lucida (arrows) in a nonblistered area of a 10.0 mg/ml dosed flap. (X18,350); C. A 10.0 mg/ml HD-induced blister showing dermal staining (arrowheads) and fragmented epidermal staining (arrows). (X18,000).

Figure 3-11. IEM of the GB3 antibody. A. Discontinuous staining in the lamina lucida and lamina densa region (arrows) of NPS. (X15,600); B. Antibody localized beneath the hemidesmosomes in the lamina lucida and lamina densa (arrows) in a nonblistered area of a 10.0 mg/ml HD-dosed IPPSF. (X25,350); C. Intense dermal staining (arrows) in a blistered area of a 10.0 mg/ml HD-dosed flap. (X14,500).

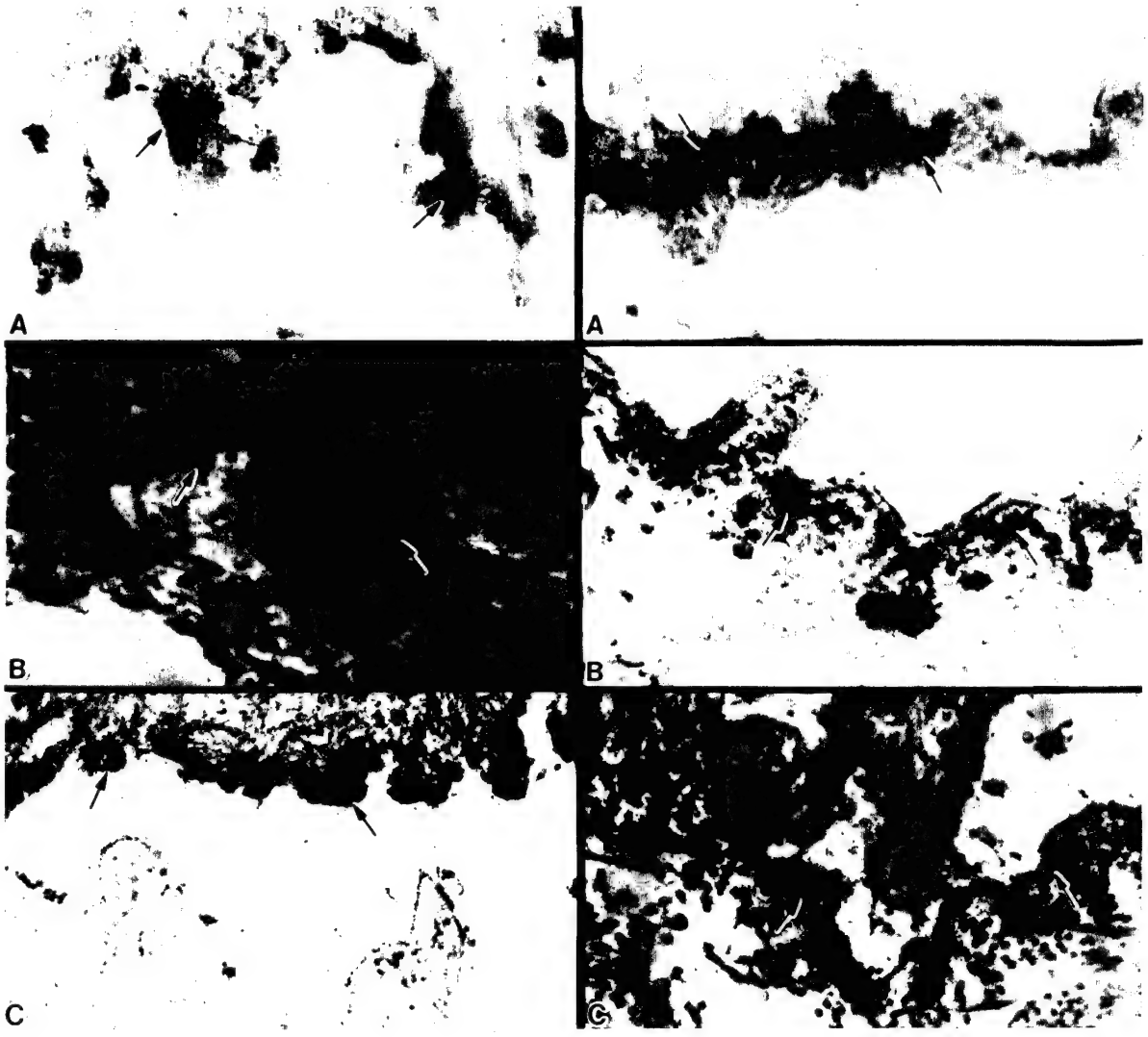

Figure 3-12. IEM of the BP antibody. A. Discontinuous staining pattern of the basal cell hemidesmosomes (arrows) of NPS. (X25,350); B. More continuous staining pattern (arrows) in an ethanol-treated flap. (X21,000); C. Discontinuous staining of epidermis (arrows) in a blistered 5.0 mg/ml HD-treated flap. (X15,600).

Figure 3-13. IEM of EBA. A. Diffuse stain encompassing the lamina densa (arrows) in NPS. (X15,800); B. Staining of the lamina densa (arrows) in a nonblistered area of a 10.0 mg/ml HD-dosed flap. (X22,200); C. Dermal staining (arrows) in a 10.0 mg/ml HD-induced blister (X18,000).

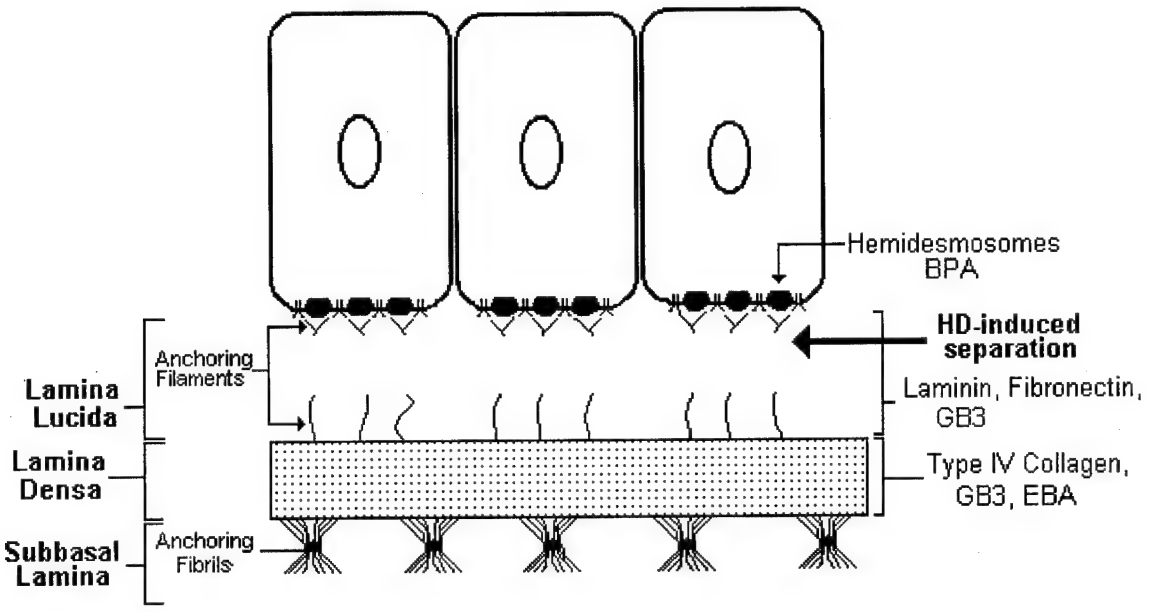

Figure 3-14. Schematic diagram showing HD-induced separation within the upper lamina lucida relative to six EDJ epitopes in the IPPSF.

4. ASSESSMENT OF SULFUR MUSTARD INTERACTION WITH BASEMENT MEMBRANE COMPONENTS

Zili Zhang, Barry P. Peters, and Nancy A. Monteiro-Riviere

Published in *Cell Biology and Toxicology* 11:89-101, 1995

Abstract

Bis-2-chloroethyl sulfide (sulfur mustard, HD) is a bifunctional alkylating agent which causes severe vesication characterized by slow wound healing. Our previous studies have shown that the vesicant, HD, disrupts the epidermal-dermal junction at the lamina lucida of the basement membrane. The purpose of this study was to examine whether HD directly modifies basement membrane components (BMCs), and to evaluate the effect of HD on the cell adhesive activity of BMCs. EHS laminin was incubated with ^{14}C-HD, and extracted by gel filtration. Analysis of the ^{14}C-HD-conjugated laminin fraction by a reduced sodium dodecyl sulfate-polyacrylamide gel electrophoresis (SDS-PAGE) revealed the incorporation of radioactivity into both laminin subunits and a laminin trimer resistant to dissociation in reduced SDS-PAGE sample buffer, suggesting direct alkylation and cross-linking of EHS laminin by ^{14}C-HD. Normal human foreskin epidermal keratinocytes (NHEK) were biosynthetically labeled with ^{35}S-cysteine. ^{35}S-labeled laminin isoforms, Ae.B1e.B2e. laminin and K.B1e.B2e. laminin, fibronectin, and heparan sulfate proteoglycan were isolated by immunoprecipitation from the cell culture medium, treated with HD or ethanol as control, and then analyzed by SDS-PAGE. On reduced SDS gels, these three BMCs not treated with HD showed the typical profile of dissociated subunits. However, HD treatment caused the appearance of higher molecular weight bands indicative of cross-linking of subunits within these BMCs. The HD scavengers sodium thiosulfate and cysteine prevented the cross-linking of BMC subunits by HD. Finally, tissue culture dishes coated with laminin or fibronectin were

treated with HD or ethanol as a control, and human keratinocytes were plated on the BMC-coated surfaces. After 20 hrs of incubation, it was observed that cell adhesion was decreased significantly on the BMC-coated surfaces treated with HD. As expected, the preincubation of HD with cysteine diminished the HD inhibition of cell adhesion. Thus, HD alkylates adhesive macromolecules of the basement membrane zone and inhibits their cell adhesive activity. These findings support the hypothesis that the alkylation of basement membrane components by HD destabilizes the epidermal-dermal junction in the process of HD-induced vesication. The failure of the HD-alkylated BMCs to support the attachment of keratinocytes might also contribute to the slow re-epithelialization of the wound site which is characteristic of HD-induced blistering.

Introduction

Bis-2-chloroethyl sulfide (sulfur mustard, HD) is a bifunctional agent which is highly reactive with many biological macromolecules, especially those containing nucleophilic groups such as the thiol group. HD is known for its severe cutaneous damage and systemic toxicity. The HD-induced dermal lesion is characterized by vesication and slow wound healing (Papirmeister et al., 1991). Our laboratory has shown that epidermal-dermal separation occurs at the lamina lucida of the cutaneous basement membrane in HD-induced dermal injury (Monteiro-Riviere et al., 1991; Monteiro-Riviere and Inman, 1993). No clear picture has emerged regarding the underlying mechanism of HD-induced vesication. It was thought that alkylation of DNA was the primary and initial event responsible for HD cutaneous toxicity (Papirmeister et al, 1991). Recently, however, results from several laboratories did not support

* We have used the nomenclature for laminin chains adopted recently by Engel and co-workers (Engel et al., 1991). Classic laminin (A.B1.B2.) is designated "Ae.B1e.B2e", where "e" reflects the origin of the laminin chains from the EHS tumor matrix or similar chains from other sources. K-laminin denotes the isoform of laminin described by Marinkovich (Marinkovich et al., 1992) in which the 190 kDa laminin K chain takes the place of the Ae chain in the assembled laminin molecule (K.B1e.B2e).

this initial hypothesis. It has been reported that higher dose of HD and shorter time are required to cause vesication than to alkylate DNA. Additionally, other DNA alkylating agents do not cause vesication and other pathological changes characterized by HD (Papirmeister, 1993). Therefore, alkylation of DNA may not be a primary biochemical event in acute cutaneous injury of HD, and HD may have its own unique molecular targets in the basement membrane zone of the skin. In order to explore the potential mechanisms of HD action, several pharmacological compounds have been tested for their ability to protect against HD toxicity. In several studies, reagents such as sodium thiosulfate and cysteine are shown to serve as HD scavengers that at least partially prevent HD toxicity. Observations of this type suggest that the chemical alkylation of intercellular and/or intracellular targets may contribute to local and systemic lesions induced by HD (Vojvodic et al., 1985; Zhang et al., 1994).

During the past decade, considerable information has accumulated regarding the structure of the cutaneous basement membrane (Timpl, 1989), a thin sheet of extracellular matrix located at the junction of the epidermis and dermis. It has been well documented that the basement membrane not only provides a mechanical support for epidermal-dermal interaction but also influences cell behavior and wound healing (Paulsson, 1992; Burgeson, 1993). Ultrastructurally, the basement membrane consists of the lamina lucida, lamina densa, and the subbasal lamina. Anchoring filaments, crossing the lamina lucida, bind keratinocytes to the lamina densa. Anchoring fibrils like type VII collagen link the lamina densa to the connective tissue of dermis. Two isoforms of laminin, Ae.B1e.B2e. laminin and K.B1e.B2e. laminin, type IV collagen, and heparan sulfate proteoglycan (HSPG) are among the major basement membrane components (BMCs) at the epidermal-dermal junction. Fibronectin is also present in this region, although its distribution extends from the basal cell layer across the epidermal-dermal junction and into the dermis (Fyrand, 1979). Defects in the structure of BMCs, evident in many of the inherited and autoimmune blister diseases (Fine, 1991), may weaken the basement membrane, rendering the skin susceptible to vesication. Although one study reported that HD reacts chemically with collagen (Goodlad, 1956), little research has

been performed on the chemical interaction of the extracellular matrix (ECM) with the vesicant HD. It is reasonable to think that chemical alkylation of BMCs by HD could destroy their cell adhesive activity and thereby, weaken the epidermal-dermal junction.

The purpose of this study was to examine the potential role of several proteins of the basement membrane zone as molecular targets for alkylation by HD. This was accomplished by (1) demonstrating the alkylation and bifunctional cross-linking of murine EHS laminin by HD, (2) demonstrating the bifunctional crosslinking by HD of human laminin isoforms, fibronectin, and HSPG produced by cultured keratinocytes, and (3) evaluating the inhibitory effect of HD on the ability of laminin and fibronectin to promote the adhesion of NHEK cells to BMC-coated culture surfaces. Our observations support the idea that HD alkylation of BMCs contributes to the vesication and may also contribute to the slow wound healing of skin exposed to HD.

Materials and Methods

Biosynthetic labeling and cell culture

Normal human keratinocytes (NHEK) were cultivated in keratinocyte growth medium (KGM) supplemented with bovine pituitary extract (Epipack, Clonetics Corp., San Diego, CA). Proliferating human UM-UC-9 bladder carcinoma cells were cultivated in Dulbecco's modified Eagle's medium containing D-glucose (4500 mg/liter) and supplemented with 10% FBS (Gibco BRL, Gaithersburg, MD). They were maintained in an atmosphere of 95% air / 5% CO_2 at 37°C, with fresh growth medium added every 1-2 days.

Cultures near confluence were biosynthetically labeled with L-^{35}S-cysteine (1113 Ci/mmole, ICN Biochemical, Costa Mesa, CA). The cells were preincubated in serum-free, cysteine-free, methionine-free Dulbecco's modified Eagle's medium (DME) for 30 min prior to labeling. Then, the NHEKs and UM-UC-9 cells were labeled with 100 μCi/ml of ^{35}S-cysteine in the cysteine-free DME medium (1 ml/5 cm^2). After a 4 hour labeling incubation, the labeling medium was removed, replaced with complete KGM or DME for chase incubation

intervals up to 20 hours. The medium was collected and floating cells were removed by centrifugation at 350 X g for 5 minutes. No visible pellets were obtained. The media were supplemented with 1/4 volume of cold (4°C) PBS containing 5% Triton X-100, 2.5% sodium deoxycholate, and 0.5% sodium dodecyl sulfate (PBS-TDS) and immunoprecipitated with antibodies against BMCs as described below.

Purification of basement membrane components by specific adsorption or immunoprecipitation

In order to purify BMCs produced by cultured keratinocytes, the antigens in the chase media were sequentially immunoprecipitated by treatment with antibodies against different BMCs. Sequential extraction of BMCs is disscussed in detail in each figure legend. Typically, fibronectin was first recovered from the chase media by adsorption to 160 μl/ml of gelatin-Sepharose (Sigma, St. Louis, MO) (Furie et al., 1980). The Ae.B1e.B2e. laminin isoform was then immunoprecipitated from the fibronectin-cleared media with a monoclonal antibody against human laminin A chain (Clone III, Gibco BRL, Gaithersburg, MD). Next, a polyclonal antibody (776) raised in rabbits against murine EHS tumor laminin (Gibco BRL) as the immunogen was used to extract the remaining K.B1e.B2e. laminin isoform from the Ae.B1e.B2e. laminin-depleted chase media. Finally, the immunoreactive HSPG was isolated by a polyclonal antibody (530) raised in rabbits against basement membrane HSPG isolated from UM-UC-9 human bladder carcinoma cells. One μl of antibody per ml of the medium was used to immunoprecipitate each of the basement membrane components. Recovery of the resulting immune complexes was accomplished by adsorption to protein A-Sepharose (Sigma, St. Louis, MO; 20 μl packed beads per μl antiserum per ml of labeling medium used for immunoprecipitation). The resulting protein A-Sepharose pellets were washed 3 times with PBS-TDS for SDS-PAGE. In order to degrade the heparan sulfate chains and release the core protein of the HSPG, HSPG immunoprecipitates were incubated for 24 hours at 37^0C with heparitinase (Sigma, 2 units) in 100 μl of 50 mM sodium acetate buffer (pH=7) with 2 mM calcium acetate.

Alkylation of EHS laminin by ^{14}C-HD

0.5 mg/0.5 ml of murine laminin purified from the murine Englebreth-Holm-Swarm (EHS) sarcoma (Gibco BRL) was treated with 25 µl of 10.0 mg/ml ^{14}C-HD or ETOH at ambient temperature for 2 hours. Stock ^{14}C-HD solution was obtained from the U.S. Army Medical Research and Development Command (0.5 mCi/mmole). Gel filtration was carried out to purify and desalt HD-alkylated EHS laminin from the reaction solution using a Sephadex G-10 column (31 cm X 1 cm). The column was equilibrated with 0.15 M sodium chloride and 0.01 M Tris-Cl, and one ml (5 min) column fractions were collected. ^{3}H-EHS laminin (NEN), used as a standard to calibrate the column, was eluted at 6-7 ml as detected by radioactive counting. Non-radioactive EHS laminin was also eluted in the same fraction, as determined by UV absorbance at 274 nm. Unconjugated ^{14}C-HD was effectively separated from the protein peak, being eluted from the column with 11-12 ml of buffer.

Incubation of basement membrane components with HD

NHEK BMCs absorbed to gelatin-Sepharose or protein A-Sepharose (20 µl packed volume) were suspended in 200 µl of 50 mM Tris-Cl buffer (pH 7.4), respectively, and were incubated at an ambient temperature for 2 hours with 10.0 µl of ethanol (ETOH), or 10.0 mg/ml HD in ETOH. Further, as a control, each sample of the BMC immunoprecipitates were treated with HD or ETOH in 200 µl of 50 mM Tris-Cl buffer (pH=7) containing HD scavengers, either 3 mM sodium thiosulfate or 30 mM cysteine under the same conditions described above. The criteria of choosing these concentrations was based on previous literature (Vojvodic et al., 1985) and pilot studies (Zhang et al., 1994).

Non-reduced and reduced SDS-PAGE

HD treated-BMCs were fractionated by both non-reduced and reduced sodium dodecyl sulfate-polyacrylamide gel electrophoresis (SDS-PAGE) using vertical slab gels (3-10% polyacrylamide gradient with a 3% stacking gel) in the Laemmli buffer system (Laemmli, 1970; Peters et al., 1985). Prior to fractionation, the samples were boiled for 5 minutes in an equal volume of 2-fold concentrated Laemmli sample buffer either with or without 2-

mercaptoethanol (2%) to reduce disulfide bonds. Gels were fixed, dried, and exposed to X-ray film to visualize the radioactive bands.

Cell adhesion assay

To test the cell adhesive ability on HD-alkylated BMCs, Biocoat® 6-well multiwell tissue culture plates coated with mouse EHS tumor laminin or fibronectin from human plasma (Becton Dickinson Labware, Bedford, MA) were treated with 50 µl of 10.0 mg/ml HD in ETOH, or ETOH alone as control for 2 hours at ambient temperature. In addition, cysteine was employed to determine if HD scavenger protects the adhesive activity of BMCs by preventing the direct chemical alkylation by HD. HD (50 µl of 10.0 mg/ml) was mixed with 50 µl of 30 mM cysteine in ETOH, and the mixed reaction solution was immediately applied to the plates coated with fibronectin, or laminin under the same conditions described above. Then the culture plates were washed three times with PBS to remove any residual HD. As a control, NHEK adhesion was also assessed on fibronectin, or laminin-coated plates treated with 30 mM cysteine in ETOH alone.

A suspension of NHEKs was prepared by trypsinization of confluent cells with 0.25 mg/ml trypsin in EDTA. The trypsin was quenched by adding trypsin neutralizing solution containing soybean trypsin inhibitor (Clonetics Corp., San Diego, CA) and the cells were pelleted by centrifugation and resuspended in KGM and then were plated onto the coated plates at a density of 3 x 10^6 per 0.2ml of medium per well. After a 20 hour incubation at 37°C, nonadherent cells were removed with two 2.0 ml PBS washes. Adherent cells were detached with trypsin and counted in a hemacytometer.

Statistical methods

Statistical comparisons were made for adherent cell number between HD-treated groups and control groups. Where significant differences were noted among treatment responses, multiple comparison tests were conducted using ANOVA *f* test at the 0.05 significance level.

Results

Chemical modification of basement membrane components by HD

Figure 4-1 reveals the covalent modification of EHS laminin by ^{14}C-HD. EHS laminin was incubated with ^{14}C-HD, and the reaction solution was applied to a gel filtration column in order to separate laminin-conjugated ^{14}C-HD from unreacted ^{14}C-HD and its hydrolytic products. A radioactive peak was eluted at 6-7 ml and was absent in the control incubation lacking of laminin (Figure 4-1). This peak of ^{14}C-HD-alkylated laminin was co-eluted with standard [^{3}H]-laminin and did not overlap the peak of unconjugated ^{14}C-HD, indicating the effective separation of the HD-laminin adduct from unconjugated HD. Analysis of the ^{14}C-HD-conjugated laminin fraction by SDS-PAGE revealed the incorporation of radioactivity into both Ae and Be laminin chains. HD-cross-linked laminin trimer, resistant to dissociation in reduced SDS-PAGE sample buffer, was also prominently visible on the gel. These results suggest that HD not only alkylates but also cross-links laminin subunits.

In light of these results using EHS laminin as a model compound, we wished to determine if laminin and other BMCs produced by human keratinocytes are alkylated by HD. However, due to the low specific activity of the ^{14}C-HD, and lack of milligram amounts of BMCs from the human keratinocyte culture, a different approach was used to assess their alkylation by HD. Our observation that HD, a bifunctional alkylating reagent, cross-linked the subunits of EHS laminin suggested that HD might also cross-link the subunits of NHEK laminin and fibronectin that have been biosynthetically labeled with ^{35}S-cysteine. If so, higher molecular weight bands corresponding to undissociated laminin and fibronectin should persist on SDS-PAGE, even after intersubunit disulfide bonds are broken with 2-mercaptoethanol. Such evidence for the bifunctional cross-linking of both laminin and fibronectin forms was visible on reduced SDS gels after HD treatment.

HD alkylates Ae.B1e.B2e. laminin

To determine if HD alkylates Ae.B1e.B2e. laminin synthesized by human cells, two human cell lines were chosen for the study, NHEK and UM-UC-9 cell. UM-UC-9 cell is a

richer source of the Ae.B1e.B2e. laminin. The Ae.B1e.B2e. laminin isoform from UM-UC-9 cells was immunoprecipitated with a polyclonal antibody against EHS laminin Ae chain, and subjected to HD exposure. As shown in Figure 4-2, laminin K chain was not produced seemingly in this type of cell line. On the reduced gel, dissociated laminin Ae and Be chains were similar to those of control laminin, showing the typical profile of laminin subunits at 400 kDa and 200 kDa. HD-treated UM-UC-9 laminin exhibited two new higher molecular weight bands on reduced SDS gels (Figure 4-2, Lane 2). These two higher molecular weight bands were located at 900 kDa and 600 kDa, corresponding to undissociated laminin trimer and a partially dissociated Ae.B1e.B2e. laminin form. Similar results were obtained with NHEK cells although HD-cross-linked NHEK Ae.B1e.B2e. laminin did not exhibit as apparent as that of UM-UC-9 cells (data not shown). These results demonstrate that HD covalently binds and cross-links the subunits of Ae.B1e.B2e. laminin synthesized by human cells.

HD alkylates K.B1e.B2e. laminin

Next, K.B1e.B2e. laminin isoform of NHEKs were immunoprecipitated with polyclonal anti-laminin antibody 776 after clearing out Ae.B1e.B2e. laminin isoform with A chain specific monoclonal antibody. Figure 4-3 illustrates the chemical modification of K.B1e.B2e. laminin by HD. The K.B1e.B2e. laminin precipitate treated with HD exhibited two new higher molecular weight bands on reduced SDS gels (Figure 4-3, Lane 3). Compared to control laminin that only showed the dissociated Be and K laminin subunits at 200 kDa and 190 kDa, respectively (Figure 4-3, Lane 2). The two new bands caused by HD treatment of K.B1e.B2e. laminin were not dissociated with 2-mercaptoethanol, and migrated similarly to nonreduced K.B1e.B2e. laminin trimer (Figure 4-3, Lane 1). This indicates that HD forms bifunctional cross-links between the K.B1e.B2e. laminin subunits.

HD cross-linked fibronectin

Analysis of the NHEK fibronectin by reduced and nonreduced SDS-PAGE is shown in Figure 4-4. After HD treatment, a higher molecular weight band resistant to dissociation in reduced SDS-PAGE sample buffer was observed above the fibronectin monomer (Figure 4-4,

Lane 3), This band was absent in the control sample lacking HD. All of the untreated control fibronectin was dissociated to monomer form on the reduced SDS gel (Figure 4-4, Lane 2). On a nonreduced SDS gel, control fibronectin migrated as a dimer form at 500 kDa and a monomer form at 250 kDa caused by the partial reduction of disulfide bonds due to the diffusion of 2-mercaptoethanol from neighboring gel lanes (Figure 4-4, Lane 1). The migration of the HD-cross-linked fibronectin (Figure 4-4, lane 3) on the SDS gel matched the dimer band of nonreduced fibronectin (Figure 4-4, Lane 1). This illustrates the intramolecular cross-linking of fibronectin subunits by HD.

HSPG core protein is cross-linked by HD

HSPG is another class macromolecule in the basement membrane. It is a polyanionic molecule consisting of heparan sulfate glycosaminoglycan chains linked covalently to a core protein. Although the quaternary structure of HSPG not known, HD might cross-link HSPG either to itself or to other BMCs, thereby exhibiting higher molecular weight bands similar to cross-linked subunits observed for the other BMCs discussed above. In this study, a polyclonal antibody against HSPG was used to immunoprecipitated HSPG along with fibronectin adventitiously attached to HSPG core protein. Figure 4-5 reveals the covalent modification of HSPG by HD. HD treatment diminished the HSPG heparitinase core protein band at 350 kDa position. Further, intensity of fibronectin was greatly reduced, and HD-cross-linked fibronectin dimer did not exhibit at 500 kDa position as we saw previously (Figure 4-5, Lane 2). Instead, a new higher molecular weight band that did not penetrate the gel was observed. In contrast, the core protein of HSPG was detected at 350 kDa position, and fibronectin on background was much more intense in the non HD treated sample (Figure 4-5, Lane 1). These results suggest a intermolecular cross-linking form of basement membrane proteins, including HSPG core protein and fibronectin, treated by HD. Although the classification and function of HSPG is not completely understood, most authors suggest that HSPG is a component of the lamina densa, and participates in the composition of the basement membrane. Studies in our laboratory showed that topically dosed ^{14}C-HD penetrated through the lamina lucida into the

dermis (Riviere et al., 1995), therefore HD can alkylate macromolecules within these zones as we described in this study. This result raises the possiblity that chemical modification of HSPG by HD may indirectly destablize the lamina lucida, leading to vesication.

Sodium thiosulfate and cysteine block the alkylation of BMCs by HD

The inhibitory effect of sodium thiosulfate and cysteine on HD alkylation and cross-linking of BMC was demonstrated in Figure 4-6. Both sodium thiosulfate and cysteine added to the BMC alkylation reaction prevented the formation of HD-cross-linked BMCs. For example, the band of HD-cross-linked fibronectin at 500 kDa was not present in the sodium thiosulfate or cysteine-treated samples (Figure 4-6, Lanes 1, 2, and 3). Similarly, HD-cross-linked laminin, migrating at 900 kDa position on reduced gel (Figure 4-6. Lane 4), was not observed, in sodium thiosulfate or cysteine treated samples (Figure 4-6, Lanes 5 and 6).

Cell adhesion to HD-treated basement membrane components

Culture surfaces coated with different BMCs were tested for their ability to promote cell adhesion with and without alkylation by HD. The results of the cell adhesion assay are shown in Figure 4-7. After 20 hours of incubation, NHEKs attached to untreated BMCs, whereas HD-treatment of the BMC-coated surfaces significantly inhibited NHEK adhesion. To determine if an HD scavenger destroys HD and protects the adhesive activity of BMCs, 10.0 mg/ml of HD was precubated with 30 mM cysteine, then applied to fibronectin or laminin-coated plates. As shown in Figure 4-7, cysteine-pretreated HD did not significantly inhibit NHEK adhesion to fibronectin and laminin, and cell adhesion was not affected on the BMC-coated surfaces treated with cysteine alone. In order to rule out the possibility that the failure of NHEKs attach to BMCs after HD treatment was due to cytotoxicity of residual HD and/or HD hydrolytic products, 10.0 mg/ml of HD was placed in KGM for 2 hours at ambient temperature. During this time, most, if not all, of the HD was hydrolyzed. NHEKs were then plated and incubated for 24 hours in the KGM medium containing HD hydrolysis products, no signs of cytotoxicity or cell detachment were observed, which indicated that residual HD or its

derivatives were not cytotoxic to NHEK cells. Rather, a direct chemical modification of the BMC-coated surface is necessary for HD to inhibit NHEK cell adhesion (data not shown).

Discussion

These experiments presented the hypothesis that HD decreases epidermal-dermal adhesion by alkylating cell adhesive cysteine-rich basement membrane proteins located at the site of epidermal-dermal separation in HD-induced blisters. HD is a highly toxic bifunctional alkylating agent with well described vesicant properties in the skin. However, the mechanism of HD cutaneous toxicity has not been clearly delineated. HD has long been known to react with a variety of other biomolecules, for example, alkylation of DNA by HD may play a role in HD cytotoxicity. However, these studies suggest that the genotoxicity of HD does not explain some of the acute cutaneous HD injury. Tissue injury requires a higher dose than does genotoxicity, takes less time to develop, and is not dependent on DNA cross-links. Furthermore, many DNA adducts or other cutaneous toxicants cause skin lesions without vesication. Our previous studies have shown HD-induced vesication in the upper lamina lucida of the basement membrane. Further, blisters and dark basal cells develop as early as 5 hours after HD exposure in our isolated perfused porcine skin flap model (Monteiro-Riviere et al., 1991). This raises the possibility of a direct chemical modification of proteins at the basement membrane zone by HD, leading to diminished stability of the epidermal-dermal junction in the process of its dermal toxicity and vesication.

The basement membrane is a complex structure composed of molecular components that stabilize the epidermal-dermal junction. The basement membrane zone is a major site of pathological changes associated with blister diseases. Defects in particular BMCs have been associated with blistering disease, thus suggesting their role in the process of vesication. For example, absence or diminution of type VII collagen and hemidesmosome-anchoring filaments are discovered in patients with epidermolysis bullosa (Fine, 1990; Fine et al., 1993). As mentioned above, immunohistochemical mapping of HD-induced vesication has been

accomplished and the epidermal-dermal separation was exclusively localized to the upper lamina lucida, just above the level of the prominent staining for laminin (Monteiro-Riviere and Inman, 1993; Monteiro-Riviere et al., 1993). This is precisely the location of laminin, fibronectin, and basement HSPG in skin and the site at which HD accumulates when administed topically in skin (Monteiro-Riviere et al., 1994). It is therefore plausible that the alkylation of these basement membrane components by HD may contribute to blister formation. Previous studies in our laboratory have shown that some of those components, such as laminin, may have free thiol groups available for alkylation (King et al., 1994), although HD is highly reactive with other nucleophiles as well.

In this study, incorporation of ^{14}C-HD into the A and B subunits of EHS laminin directly demonstrates that HD covalently alkylates laminin. This result strengthens our hypothesis that BMCs are the targets for HD modification in the process of vesication. Therefore, we further evaluated HD alkylation of the BMCs by incubation of biosynthetically labeled proteins from human cells (NHEKs and UM-UC-9 cells) with HD. Native laminin isoforms, Ae.B1e.B2e. laminin and K.B1e.B2e. laminin, and fibronectin are fully dissociated in SDS-PAGE under reduced conditions because of the breakage of intersubunit disulfide bonds. However, after HD treatment, undissociated higher molecular weight bands persist on the reduced SDS gels, the largest of which migrates similarly to the undissociated molecule. These bands signify the introduction of bifunctional covalent intramolecular cross-links between subunits of both laminin and fibronectin. In a similar manner, HD treatment caused the band of HSPG core protein to migrate at a higher molecular weight position. Thus, these results suggest that HD cross-links these BMCs intramolecularly and intermolecularly. Although the techniques employed in this study are not able to detect chemical reaction of HD other than cross-linking, it is worthy to mention that HD reacts with biomolecules not only bifunctionally but also monofunctionally, and that monofunctional modification of BMCs by HD or other vesicants such as hemimustard and lewisite may also contribute to blister formation (King and Monteiro-Riviere, 1990; King et al., 1994). Sodium thiosulfate and

cysteine have long been known to react with and detoxify HD. These two chemicals have been used to prevent HD from alkylating the crucial target molecules in cells and tissues, and their partial protective effects on HD toxicity were evident in several *in vitro* and *in vivo* studies (Vojvodic et al., 1985; Zhang et al., 1994). This study shows that these scavengers directly prevent fibronectin and laminin from HD alkylation and crosslinking, suggesting that nucleophilic groups such as the thiol group in BMCs are the primary targets for HD modification.

BMCs have a well defined role in maintaining epidermal-dermal interaction. In addition, recent studies show that BMCs are implicated in the regulation of cell differentiation and migration (Sakashiti et al., 1980; Kleinman et al., 1985; Goodman et al., 1989). Further, some BMCs are the earliest detectable proteins appearing at the wound site (Fine et al., 1987), suggesting a functional role of BMCs in tissue repair. So far, many functional domains of BMCs, such as cell binding sites, have been determined and sequenced. Not surprisingly, some of these domains are composed of cysteine-repeats (Sasaki et al., 1987; Sasaki and Yamada., 1987; Sasaki et al., 1988; Hartl et al., 1988). Thus, it is likely that HD may destroy the biological functions of BMCs by alkylating these domains, particularly, if they exist as free thiols.

Adhesion and spreading of cells on surfaces coated with BMC and the anchorage and migration of keratinocytes on BMC involves the participation of extracellular matrix receptors of integrins or possibly non-integrin types. This interaction between cells and BMCs is not completely understood. However, several integrins have been suggested as BMC receptors (Carter et al., 1990; Shimizu et al.; 1990; Hynes, 1992). These receptors may neither recognize nor respond to the BMCs modified by HD or other chemicals. Further, HD-alkylated BMCs may function as a receptor blocker preventing cell-cell and/or cell-matrix interaction. Our cell adhesive assay shows that HD-alkylated BMCs inhibits cell adhesion without any signs of cytotoxicity. Cysteine prevents HD inhibitory effect on cell adhesion to laminin and fibronectin, further suggesting the role of native BMCs in cell adhesion. In this

study, it could not be concluded which BMCs might be the most alkylatable by HD and/or responsible for cell adhesion. However, the results of this study have significant clinical implications in the pathogenesis of HD-induced cutaneous lesions.

In conclusion, we find that alkylation of BMCs may play a role in HD-induced vesication and this results in delayed wound healing which is characteristic of HD vesication. This study provides a new hypothesis regarding the mechanism of cutaneous toxicity caused by HD.

References

Burgeson, R.E. (1993). In Molecular and Cellular Aspects of the Basement Membrane. (Eds. D.H. Rohrbqehand and R. Timpl), Academic Press, Inc., San Diego, CA. pp. 49-66.

Carter, W.G., Wayner, E.A., Bouchard, T.S., and Kaur, P. (1990). The role of integrins $\alpha 2\beta 1$ and $\alpha 3\beta 1$ in cell-cell and cell-substrate adhesion of human epidermal cells. J. Cell Biol. 110:1387-1407.

Engel, J., Hunter, I., Schulthess, T., Beck, K., Dixon, T., and Parry, D. (1991). Assembly of laminin isoforms by triple- and double-stranded coiled-coil structure. Biochem. Soc. Trans. 19:839-843.

Fine, J-D., Redmar, D.A., and Goodman, A.L. (1987). Sequence of reconstitution of seven basement membrane components following split-thickness wound induction in primate skin. Arch. Dermatol. 123:1174-1178.

Fine, J-D. (1991). Structure and antigenicity of the skin basement membrane zone. J. Cutan. Pathol. 18:401-409.

Fine, J-D. (1990). 19-DEJ-1, a monoclonal antibody to the hemidesmosome-anchoring filment complex, is the only reliable immunohistochemical probe for all major forms of junctional epidermolysis bullsa. Arch. Dermatol. 126:1187-1190.

Fine, J-D., Johnson, L.B., Cronce, D., Wright, J.T., Leigh, I.M., Mccollough, M., and Briggaman, R.A. (1993). Intracytoplasmic retention of type VII collagen and dominant dystrophic epidermolysis bullosa: Reversal of defect following cessation of or marked improvement in disease activity. J. Invest. Dermatol. 101:232-236.

Furie, M.B., Frey, A.B., and Rifkin, D.B. (1980). Location of a gelatin-binding region of human plasma fibronectin. J. Biol. Chem. 255:4391-4394.

Fyrand, O. (1979). Studies on fibronectin in the skin. Brit. J. Dermatol. 101:263-270.

Goodlad, G.A.J. (1956). Cross-linking of collagen by S- and N-mustard. Chemical Defense Experimental Establishment, Porton, Wilts, CDE Technical Paper no. 573. DTIC, AD/119 934.

Goodman, S.L., Gundula, R., and Von Der Mark, K. (1989). The E8 subfragment of laminin promotes locomotion of myoblasts over extracellular matrix. J. Cell Biol. 109:799-809.

Hartl, L., Oberbaumer, I., and Deutzmann, R. (1988). The N terminus of laminin A chain is homologous to the B chains. Eur. J. Biochem. 173:629-635.

Hynes, R.O. (1992). Integrins: Versatility, modulation, and signaling in cell adhesion. Cell 69:11-25.

King, J.R., and Monteiro-Rivere, N.A. (1990). Cutaneous toxicity of 2-chloroethyl methyl sulfide in isolated perfused porcine skin. Toxicol. Appl. Pharmacol. 104:167-179.

King, J.R., Peters, B.P., and Monteiro-Rivere, N.A. (1994). Laminin in the cutaneous basement membrane as a potential target in lewisite vesication. Toxicol. Appl. Pharmacol. 126:164-173.

Kleinman, H.K., Cannon, F.B., Laurie, G.W., Hassel, J.R., Aumailley, M., Terranova, V.P., Martin, G.R. and Dubois-Dalca, M. (1985). Biological activities of laminin. J. Cell Biochem. 27:317-325.

Laemmli, U.K. (1970). Cleavage of structural proteins during assembly of the head of bacteriophage T4. Nature. 277:680-685.

Marinkovich, M.P., Lunstrum, G.P., Keene, D.R., and Burgeson, R.E. (1992). The dermal-epidermal junction of human skin contains a novel laminin variant. J. Cell Biol. 119:695-702.

Monteiro-Riviere, N.A., King, J.R., and Riviere, J.E. (1991). Mustard induced vesication in isolated perfused skin: Biochemical, physiological, and morphological studies. In Proceedings of the Medical Defense Bioscience Review, U.S.Army Medical Research Institute of Chemical Defense, Aberdeen Proving Ground, Maryland, pp. 159-162.

Monteiro-Riviere, N.A., and Inman, A.O. (1993). Histochemical localization of three basement membrane epitopes with sulfur mustard induced toxicity in porcine skin. Toxicologist. 13:58.

Monteiro-Riviere, N.A., Inman, A.O., Spoo, J.W., Rogers, R.A., and Riviere, J.E. (1993). Studies on the pathogenesis of bis (2-chloroethyl) sulfide (HD) induced vesication in porcine skin. In Proceedings of the Medical Defense Bioscience Review, U.S.Army Medical Research Institute of Chemical Defense, Aberdeen Proving Ground, Maryland, pp. 31-40.

Monteiro-Riviere, N.A., Zhang, J.Z., Inman, A.O., Brooks, J.D., and Riviere, J.E. (1994). Mechanisms of cutaneous vesication. DAMD17-92-C-2071, NTIS, ADA283085, pp. 42-55.

Papirmeister, B., Feister, A.J., Robinson, S.I., and Ford, R.D. (1991). Medical Defense Against Mustard Gas: Toxic Mechanisms and Pharmacological Implications, CRC Press, Boca Raton, FL.

Papirmeister, B. (1993). Excitement in vesicant research - Yesterday, today and tomorrow. In Proceedings of the Medical Defense Bioscience Review, U.S.Army Medical Research Institute of Chemical Defense, Aberdeen Proving Ground, Maryland, pp. 1-14.

Paulsson, M. (1992). Basement membrane proteins: Structure, assembly, and cellular interactions. Crit. Rev. Biochem. Mol. Biol. 27:93-127.

Peters, B.P., Hartle, R.J., Krzesicki, R.F., Kroll, T.G., Perini, F., Balun, J.E., Goldstein, I.J., and Ruddon, R.W. (1985). The biosynthesis, processing, and secretion of laminin by human choriaocarcinoma cells. J. Biol. Chem. 27:14732-14742.

Riviere, J.E, Brooks, J.D., Williams, P.L., and Monteiro-Riviere, N.A. (1995). Toxicokinetics of topical sulfur mustard penetration, disposition, and vascular toxicity in isolated perfused porcine skin. Toxicol. Appl. Pharmacol. 135:25-34.

Sakashiti, S., Engvall, E., and Ruoslahti, E. (1980). Basement membrane glycoprotein laminin binds to heparin. FEBS Lett. 116:243.

Sasaki, M., and Yamada, Y. (1987). The laminin B2 chain has a multidomain structure homologous to the B1 chain. J. Biol. Chem. 262:17111-17117.

Sasaki, M., Kato, S., Kohno, K., Martin, G.R., and Yamada, Y. (1987). Sequence of the cDNA encoding the laminin B1 chain reveals a multidomain protein containing cysteine-rich repeats. Proc. Natl. Acad. Sci. 84:935-939.

Sasaki, M., Kleinman, H.K., Huber, H., Deutzmann, R., and Yamada, Y. (1988). Laminin, a multidomain protein. The A chain has a unique globular domain and homology with the basement membrane proteoglycan and the laminin B chains. J. Biol. Chem. 263:16536-16544.

Shimizu, Y., Van Seventer, G.A., Horgan, K.J., and Shaw, S. (1990). Costimulation of proliferative responses of resting CD4+ T cells by the interaction of VLA-4 and VLA-5 with fibronectin or VLA-6 with laminin. J. Immunol. 145:59-67.

Timpl, R. (1989). Structure and biological activity of basement membrane proteins. Eur. J. Biochem. 180:487-502.

Vojvodic V., Moilosavljevic, Z., Boskovic, B., and Bojanic, N. (1985). The protective effect of different drugs in rats poisoned by sulfur and nitrogen mustard. Fundam. Appl. Toxicol. 5:S160-S168.

Zhang, Z., Riviere, J.E., and Monteiro-Riviere, N.A. (1995). Evaluation of protective effects of sodium thiosulfate, cysteine, niacinamide, and indomethacin on sulfur mustard-treated isolated perfused porcine skin. Chem. Biol. Interact. 96:249-262.

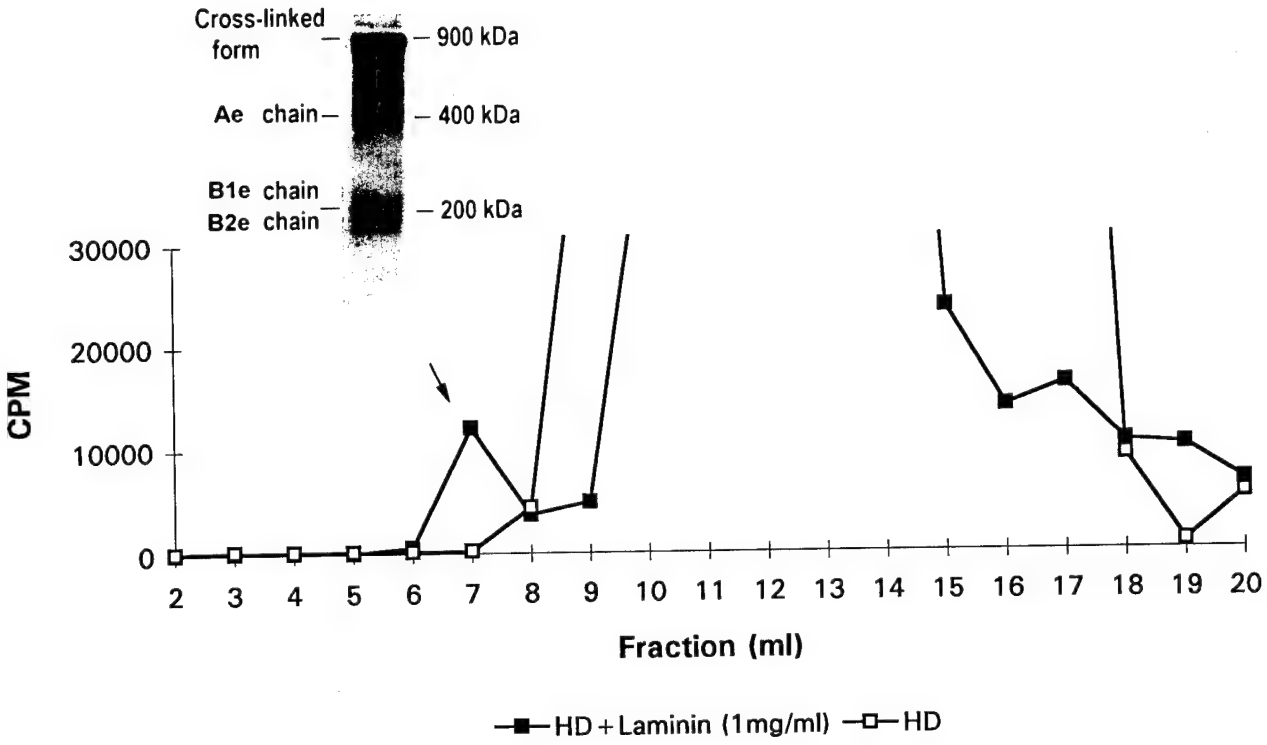

Figure 4-1. Covalent modification of EHS laminin by 14C-HD. 14C-HD was incubated with either EHS laminin in Tris-Cl buffer (■), or Tris-Cl buffer alone (□). 14C-HD-treated laminin was purified by gel filtration, and analyzed by reduced SDS-PAGE.

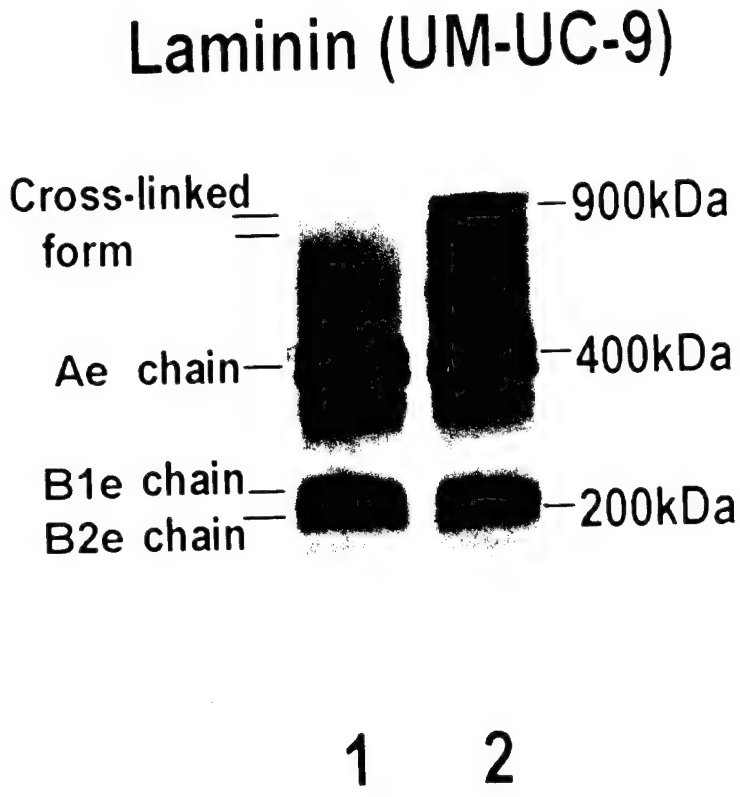

Figure 4-2. Reduced SDS-PAGE analysis of HD-treated UM-UC-9 laminin on a 3-10% acrylamide gradient gel. After clearing of fibronectin from the chase media twice, immunoprecipitation was initiated by a polyclonal antibody. Lane 1: laminin treated with ethanol; Lane 2: laminin treated with 10.0 mg/ml HD in ethanol.

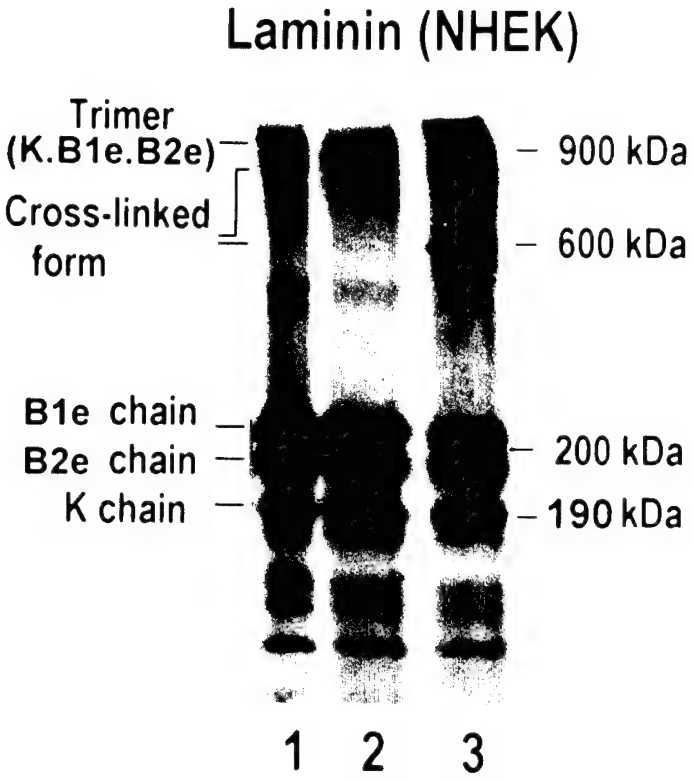

Figure 4-3. SDS-PAGE analysis of HD-treated NHEK laminin on a 3-10% acrylamide gradient gel. After clearing of fibronectin from the chase media twice, immunoprecipitation was initiated by a monoclonal antibody against laminin Ae chain, followed by a polyclonal antibody primarily against laminin Be chain. Lane 1: laminin treated with ethanol on non-reduced SDS gel; Lane 2: laminin treated with ethanol on reduced SDS gel; Lane 3: laminin treated with 10.0 mg/ml HD in ethanol on reduced SDS gel.

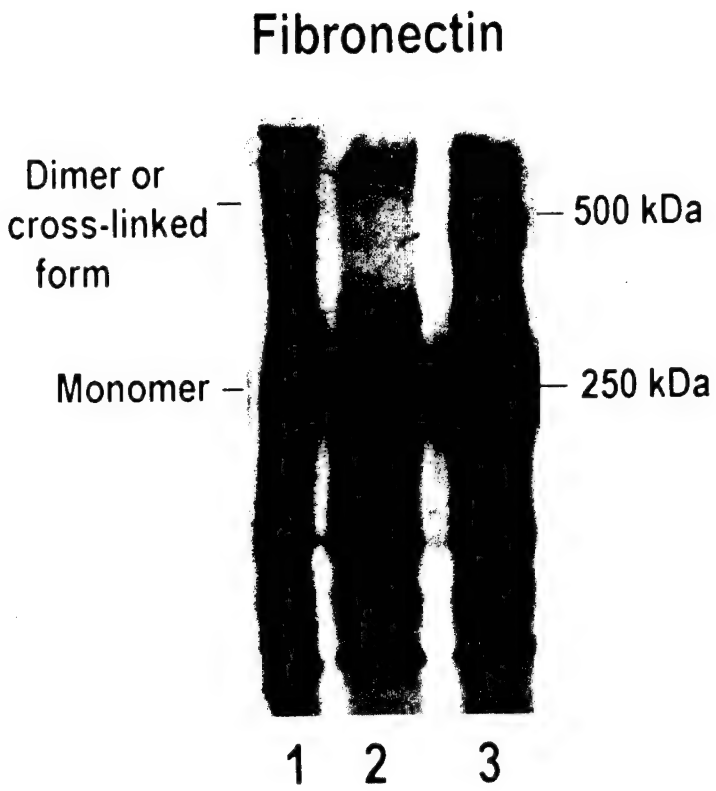

Figure 4-4. SDS-PAGE analysis of HD-treated NHEK fibronectin on a 3-10% acrylamide gradient gel. Fibronectin was recovered from the chasing media using gelatin-Sepharose. Lane 1: fibronectin treated with ethanol on non-reduced SDS gel; Lane 2: fibronectin treated with ethanol on reduced SDS gel; Lane 3: fibronectin treated with 10.0 mg/ml HD in ethanol on reduced SDS gel.

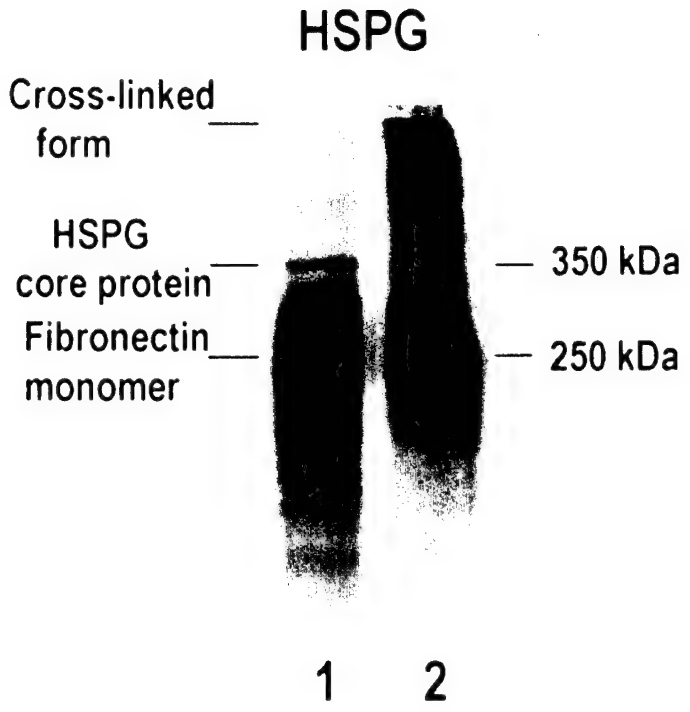

Figure 4-5. Reduced SDS-PAGE analysis of HD-treated NHEK heparan sulfate proteoglycan (HSPG) on a 3-10% acrylamide gradient gel. After clearing of fibronectin from the chase media once, immunoprecipitation was initiated by a polyclonal antibody primarily against laminin, followed by a polyclonal antibody against HSPG. Lane 1: HSPG treated with ethanol on reduced SDS gel; Lane 2: HSPG treated with 10.0 mg/ml HD in ethanol on reduced SDS gel.

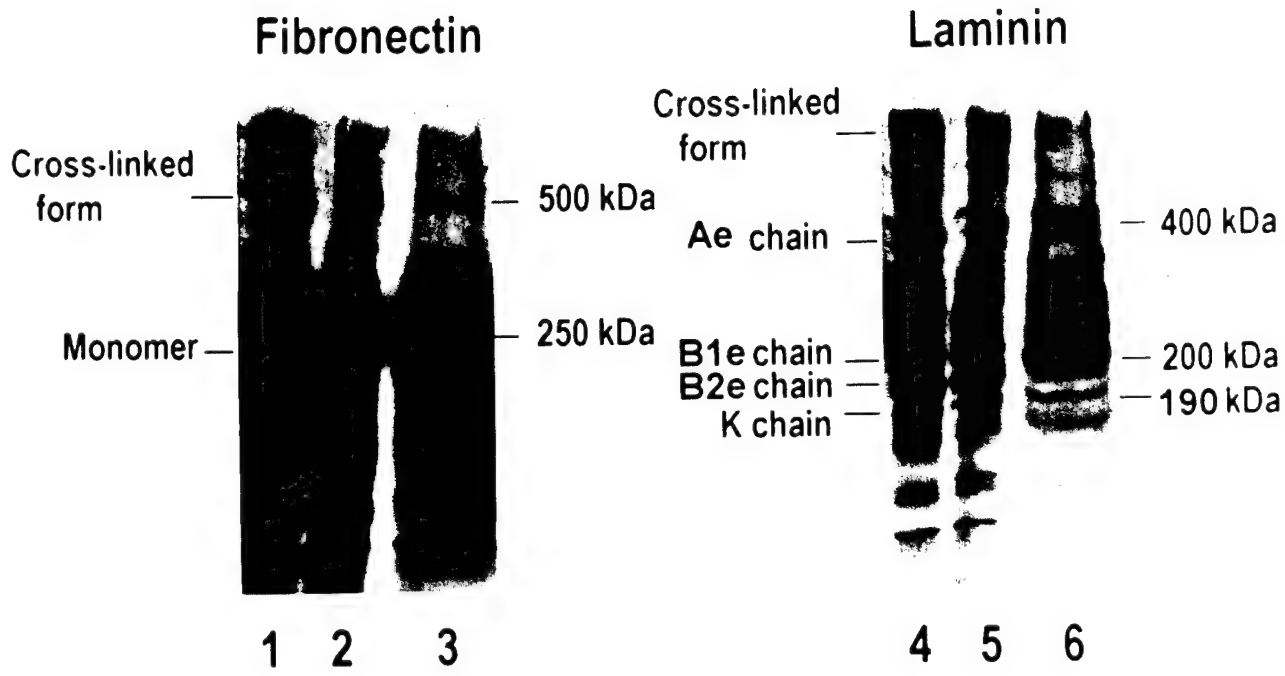

Figure 4-6. Reduced SDS-PAGE analysis of HD-treated NHEK basement membrane components in the presence or absence of HD scavengers on a 3-10% acrylamide gradient gel. Fibronectin was first recovered from the chase media using gelatin-Sepharose, laminin was then immunoprecipitated with a polyclonal antibody against laminin. Lane 1: fibronectin treated with 10.0 mg/ml HD in ethanol; Lane 2: fibronectin treated with 10.0 mg/ml HD in ethanol in the presence of 3 mM of sodium thiosulfate; Lane 3: fibronectin treated with 10.0 mg/ml HD in ethanol in the presence of 3 mM of cysteine. Lane 4: laminin treated with 10.0 mg/ml HD in ethanol; Lane 5: laminin treated with 10.0 mg/ml HD in ethanol in the presence of 3 mM of sodium thiosulfate; Lane 6: laminin treated with 10.0 mg/ml HD in ethanol in the presence of 3 mM of cysteine.

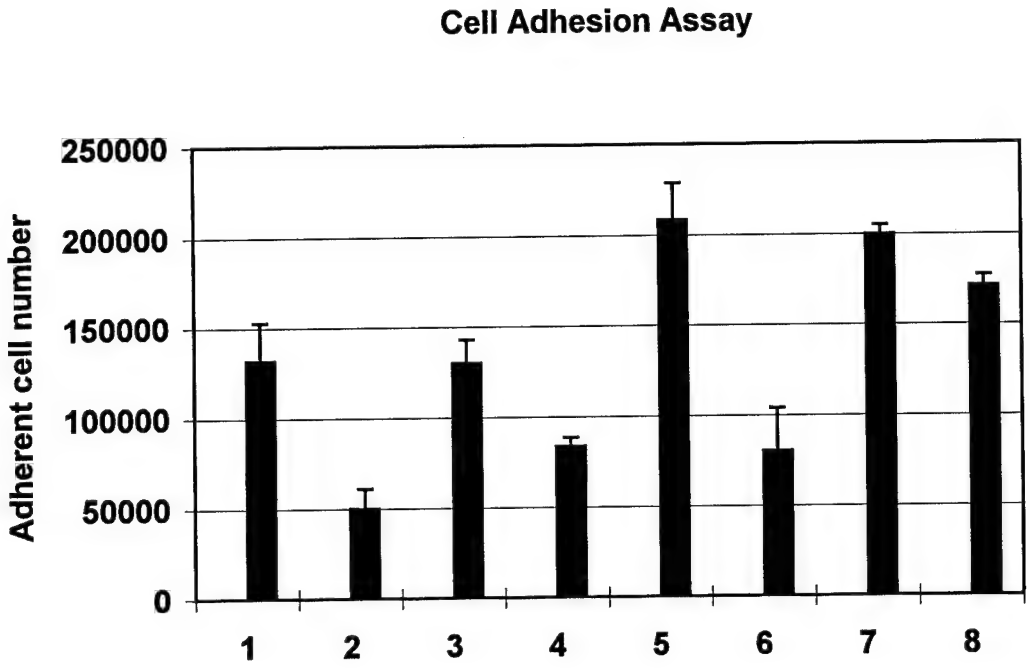

Figure 4-7. Effect of basement membrane components (BMC) and HD-treated BMCs on NHEK adhesion. Cell adhesion to ethanol-treated plates coated with laminin (Column 1); HD-treated plates coated with laminin (Column 2); ethanol-treated laminin plates in the presence of cysteine (Column 3); HD-treated laminin plates in the presence of cysteine (Column 4); ethanol-treated plates coated with fibronectin (Column 5); HD-treated plates coated with fibronectin (Column 6); ethanol-treated fibronectin plates in the presence of cysteine (Column 7); HD-treated fibronectin plates in the presence of cysteine (Column 8).

5. DETECTION OF SULFUR MUSTARD BIS (2-CHLOROETHYL) SULFIDE AND METABOLITES AFTER TOPICAL APPLICATION IN THE ISOLATED PERFUSED PORCINE SKIN FLAP

Jerry W. Spoo, Nancy A. Monteiro-Riviere and Jim E. Riviere

Published in *Life Sciences* 56:1385-1394,1995

Abstract

The purpose of this study was to develop an assay to study the flux of sulfur mustard (HD) through the skin and determine if metabolites are formed due to the epidermal metabolism of HD after topical exposure of the isolated perfused porcine skin flap (IPPSF) to ^{14}C-HD. Four IPPSFs were topically dosed with 2.85 mg of ^{14}C-HD in ethanol. Venous perfusate samples were collected and added to a 34% solution of NaCl and snap-frozen to inhibit the metabolism of HD until time for assay. Perfusate samples were extracted using a solid-phase extraction cartridge with ethyl acetate and then assayed using gas chromatography. Two of the 4 IPPSFs showed detectable levels of HD in the venous perfusate 15 min after dosing, with 1 of these 2 IPPSFs showing detectable levels of HD in the perfusate 2 hours after dosing. All 4 IPPSFs had no more than 3 metabolites of HD appearing in the perfusate throughout the 2 hr experiment, with one of those metabolites identified as thiodiglycol. These experiments showed that little, if any, HD appears in the venous perfusate intact after percutaneous absorption and that epidermal metabolism of HD does occur to a significant degree in the IPPSF.

Introduction

Sulfur mustard, bis (2-chloroethyl) sulfide (HD) has been used as an agent in chemical warfare intermittently throughout the 20th century. HD is a vesicating agent, causing the formation of painful fluid-filled blisters on the skin of humans and laboratory animal several hours or several days after the skin is exposed to the HD liquid. Other symptoms of HD poisoning, such as epigastric distress, ocular damage, and respiratory dysfunction can also occur (Wormser, 1991; Monteiro-Riviere et al., 1991). The mechanism of action of HD is not clearly understood although it was once thought to be related to its ability to alkylate DNA, however other theories on how HD produces its cytotoxic effects have been proposed (Papirmeister et al., 1985). HD metabolism has been studied extensively and many metabolites having been reported (Hambrook et al., 1992; Black et al., 1991; 1992; Roberts and Warwick, 1963; Black and Read, 1991; Davidson et al., 1961; Sandelowsky et al., 1992).

In order to better understand the mechanism of action of HD and determine how these cytotoxic events can be blocked, it is necessary to utilize a suitable *in vitro* model to better study the events associated with absorption, metabolism and the biochemical, physiologic and morphologic events that occur with HD toxicity. Previous studies performed in our laboratory have demonstrated that the isolated perfused porcine skin flap (IPPSF) produced gross fluid-filled blisters after exposure to the chemical vesicant HD. Transmission electron microscopy showed separation occurring at the upper lamina lucida of the basement membrane along with intracellular vacuolization and mitochondrial swelling in the stratum basale and stratum spinosum layers of the epidermis. These changes are similar to those lesions described in human exposures to HD and appears to be a relevant model for studying HD skin toxicity (Monteiro-Riviere et al., 1991).

Pig skin is histologically similar to human skin (Bartek et al., 1972; Monteiro-Riviere and Stromberg, 1985). The IPPSF model has an intact and viable epidermis, is similar to human skin, and possesses a functional microcirculation which is sensitive to pharmacologic and physiologic manipulations. The isolated perfused porcine skin flap (IPPSF) has been

utilized to study the cutaneous toxicity of several compounds (Riviere and Monteiro-Riviere, 1991; Srikrishna and Monteiro-Riviere, 1991; 1992; King and Monteiro-Riviere, 1990; Spoo et al., 1993; Monteiro-Riviere, 1990; Riviere et al., 1991; Riviere, 1991; King et al., 1992). The IPPSF model has been used to study the physiologic and biochemical effects of numerous compounds, including caffeine, parathion, testosterone, cisplatin, and various organic solvents (Riviere and Monteiro-Riviere, 1991; Srikrishna and Monteiro-Riviere, 1991; 1992; King and Monteiro-Riviere, 1990; 1991; Spoo et al., 1993; Monteiro-Riviere, 1990; Riviere et al., 1986; 1991; Riviere, 1991; King et al., 1992; Carver et al., 1989). All of these studies demonstrated that the IPPSF responds biochemically and physiologically similar to human skin.

The purpose of this study was to develop an assay to study the flux of HD through the skin and determine if metabolites are formed due to the epidermal metabolism of HD after topical exposure of the IPPSF to ^{14}C-HD.

Materials and Methods

IPPSF

Porcine skin flaps were created and harvested as described in previous reports (Riviere et al., 1986; Monteiro-Riviere, 1990; Bowman et al., 1991). In summary, 18-21 kg female Yorkshire pigs were acclimated in a controlled temperature facility (25°C) for at least one week prior to surgery. Pigs were housed singly with water provided *ad libitum*. Pig and sow pellets were fed once daily (Wayne Feeds Division, Chicago, IL). Prior to creating the skin flaps, each pig was given atropine sulfate (0.04 mg/kg) intramuscularly and anesthetized with intramuscular injections of xylazine hydrochloride (10 mg/kg) and ketamine hydrochloride (4 mg/kg). Each pig was then endotracheally intubated and general anesthesia maintained using halothane and oxygen. The skin in the inguinal areas of the pig are known to be primarily vascularized by the caudal superficial epigastric artery and its paired venous comitantes. A single-pedicle axial pattern island tubed skin flap was created in each inguinal area. Two days

after creation of the flaps (2 per pig), the arterial supply was cannulated and the flap removed from the pig. Each flap was gently flushed with heparinized physiologic saline solution via the arterial cannula to remove most of the blood from the flap vasculature and placed in a special chamber (providing relatively constant air temperature and humidity). Arterial and venous effluent samples were collected at hourly intervals, analyzed for glucose concentration, and glucose consumption calculated as an indictor of IPPSF viability. Arterial flow rate and pressure were monitored at periodic intervals to determine vascular resistance (VR = pressure ÷ flow). All values for GU and VR for each IPPSF were within acceptable limits throughout each experiment.

Each flap was routinely monitored for 1 hr prior to dosing to insure flap viability. Then, a flexible template (Stomahesive, ConvaTec-Squibb, Princeton, NJ) was attached to the top of the flap using Skin Bond (Pfizer Hospital Products, Inc., Largo, FL). Each of the four skin flaps were then dosed with 9.5 mg/ml ^{14}C-labeled HD in ethanol (specific activity = 0.53 mCi/mmole) on a 7.5 cm^2 dose site (2.85 mg total HD dose). Venous perfusate was collected immediately before dosing (time 0) and every 15 min after dosing for 2 hrs. To prevent the degradation of HD in venous perfusate after collection, each 1.0 ml sample of venous perfusate was mixed with 1.0 ml of 34% NaCl in double-distilled deionized water in a polypropylene tube at the time of perfusate collection (Sass and Steger, 1982; Vycudilik et al., 1985). The perfusate/NaCl mixture (final NaCl concentration ~ 17%) was gently vortexed and then immersed in a dry-ice/ethanol bath to immediately snap-freeze the sample. All samples were then stored in a -80°C freezer until time for HD extraction and assay. An additional 1.0 ml sample of venous perfusate was simultaneously collected and frozen at -80°C for determination of ^{14}C activity.

HD gas chromatography assay

All venous perfusate samples were assayed for HD using a combination of solid-phase cartridge extraction and gas chromatography through modifications originally described by Maisonneuve *et al.* (1992). Each perfusate sample was thawed in a room temperature water

bath, placed in a 3 ml polypropylene syringe connected to a tandem set of C_{18} extraction cartridges (Sep-Pak® Plus, Waters-Millipore, Cambridge, MA), and slowly passed through these cartridges using a multiple sample vacuum-driven extraction device at a flow rate of 1 ml/min. Room air was then passed through the cartridges at a high air flow rate (>20 ml/min) for 10 min to remove any excess liquid. Finally, 3 ml of HPLC-grade ethyl acetate (Fisher Scientific, Atlanta, GA) was passed at a flow rate of 1 ml/min and the eluent (containing the HD) collected in polypropylene tubes, placed in a refrigerated vacuum centrifugation device (Speed-Vac™, Model AS160, Savant) and the samples taken to complete dryness. Each sample was then reconstituted with 250 µl of HPLC-grade ethyl acetate, vortexed, and the entire quantity pipetted into a clear 1 ml glass vial and sealed with a screw-top lid. A 5 µl sample was then injected in duplicate onto the gas chomatograph according to the protocol shown in Table 5-I, the chromatograph obtained and peaks integrated. Recoveries from perfusate samples spiked with known amounts of ^{14}CHD yielded extraction efficiencies ≥ 95%.

The concentration of HD in each sample was then determined using a 7 point standard curve that ranged from 2000 ng/ml (10 ng/5µl injection volume) to 60 ng/ml (0.3 ng/5µl injection volume) HD in HPLC grade ethyl acetate. Concentration *vs.* peak height was plotted and a linear regression line was calculated using MS Excel 4.0*a* for Windows spreadsheet program to interpolate sample concentrations of HD.

Thiodiglycol has been reported to be a major metabolite of the hydrolysis of HD in other models and was considered a likely HD metabolite in the IPPSF model as well. To determine if metabolism from HD to thiodiglycol occurs, it was necessary to determine the retention time of thiodiglycol using our GC protocol. Thiodiglycol (Sigma Chemical Co., St. Louis, MO) was obtained and a dilute thiodiglycol standard in ethyl acetate was injected onto the GC.

Table 5-I. Gas Chromatograph Method Specifications for the Determination of HD Content in Extracted Venous Perfusate Samples.

Gas Chromatograph Instrument:	Hewlett-Packard Model 5890A Series 2.
Column:	Hewlett-Packard Type HP-1 Methyl Silicone Gum.
Column Specifications:	10 meters x 0.53 mm id x 2.65 μm film thickness.
Gas Flow Rates:	Helium = 21 ml/min Hydrogen = 77 ml/min Air = 75 ml/min Nitrogen = None
Detector:	Flame Photometric (in sulfur detect mode).
Detector Temperature:	200°C
Injector Temperature:	200°C
Initial Oven Temperature:	35°C
Initial Time:	0.5 min
Initial Temperature Rate:	2°/min
Final Oven Temperature:	50°C
Ramp A:	20°/min
Ramp A Final Oven Temperature:	150°C
Integrator	Hewlett-Packard Model 3396 Series II
Chart Speed	0.5 cm/min
Injection Volume:	5 μl

Determination of perfusate radioactivity

Two hundred and fifty microliters of perfusate sample was thawed and then oxidized using a Packard Model 306 open-flame tissue oxidizer (Packard Instrument Co., Downers Grove, IL). Samples then had their radioactivity (in Decompositions Per Minute (DPM)) determined over a 1 minute period using a Packard Model 1900 TR liquid scintillation counter. Counts were then corrected for background and plotted using MS Excel.

Results

Figure 5-1a shows a chromatogram of 1.0 ml of IPPSF venous perfusate spiked with 12 μg of HD, extracted and then assayed by our method. An identical HD-spiked sample was

allowed to sit at ambient temperature (~25°C) for 0.75 hrs before extraction and assayed (Figure 5-1b). Comparison of these two chromatograms shows that HD has a GC retention time of 10.74 min and that a 70% decomposition of HD occurs spontaneously within the IPPSF perfusate over 45 min at room temperature.

Figure 5-2a shows a chromatogram of 1.0 ml of IPPSF perfusate to which 1.0 ml of 34% NaCl solution was added to 1.0 ml of venous perfusate and then spiked with 10 μg of HD, extracted, and then assayed by our method. An identical HD-spiked sample was allowed to sit at ambient temperature for 0.75 hrs before extraction and assay (Figure 5-2b). Comparison of these chromatograms show only a 7% degradation of HD that occurred within 45 min at room temperature, indicating that the addition of NaCl significantly impairs but did not totally inhibit the degradation of HD in the IPPSF venous perfusate samples.

Figure 5-3 shows a graph of the ^{14}C radioactivity in venous perfusate at 15 minute intervals following a 2.85 mg topical dose of HD. All IPPSFs had ^{14}C venous fluxes that were at least 5 times above normal background for the entire 2 hr experiment. Peak radioactive flux in all flaps occurred at or before 20 min after dosing, however there was a substantial amount of variation of the overall amount of ^{14}C radioactive flux between IPPSFs. These data confirm that some flux of the ^{14}C-labelled dosing solution does penetrate the skin and can be absorbed into the systemic circulation, however it is impossible to determine from this data whether the ^{14}C activity is associated solely with parent compound, metabolite(s), or a combination of the two.

Figure 5-4 shows the typical flatline chromatogram that occurs between 4 and 20 min after sample injection of an extracted venous perfusate sample obtained immediately prior to the application of HD to the skin surface (*ie.* no HD or metabolites present in the extracted perfusate sample). Figure 5-5 shows a typical chromatogram for all of the extracted perfusate samples collected after the topical application of HD to the IPPSF. The retention times of the 4 peaks in the extracted perfusate samples (if present), occurring at 10.74 (HD), 10.82, 11.27 and 12.63 min, are consistent between each sample from the same IPPSF and between

individual IPPSFs. Thiodiglycol was found to have a retention time of 10.80 min using the HD GC assay method (data not shown), indicating that peak 2 on the chromatogram shown in Figure 5-5 is likely thiodiglycol.

Hemi-mustard (2-chloroethyl methylsulfide) has also been reported to be a metabolic product of HD and was thought to appear intact in our venous perfusate samples. Previous studies in our laboratory have shown that topically applied hemi-mustard behaves biochemically, physiologically, and morphologically similar to that of HD in the IPPSF (King and Monteiro-Riviere, 1990). Dilute hemi-mustard solutions in ethyl acetate were assayed using our gas chromatography method and found to have a retention time of 2.85 min (data not shown). No peaks at this time point were observed in any of our extracted samples, indicating that hemi-mustard either did not co-extract with the HD and other metabolites or was not present in detectable quantities in the venous perfusate samples.

Table 5-II compares each of these 4 peak heights for venous perfusate samples collected at 0.25, 1.0 and 2.0 hrs after dosing. Of the 4 IPPSFs dosed with topical HD, 2 IPPSFs had detectable (albeit very low) concentrations of HD 0.25 hrs after dosing, with only one IPPSF having detectable levels of HD at both 1 and 2 hours after dosing, although the peak heights were far below the lowest standard on our HD standard curve. All 4 IPPSFs had relatively high concentrations of thiodiglycol 0.25 hrs after dosing, while 3 of the 4 IPPSFs had detectable concentrations of thiodiglycol at 1 hr after dosing. Only 2 of those 3 IPPSFs showed thiodiglycol levels 2 hrs after dosing, however wide variations in concentrations of thiodiglycol was demonstrated to occurred between each IPPSFs, indicating possible alternative cutaneous metabolic pathways present in that IPPSF. Peaks 3 and 4 are likely to be other metabolites of HD containing a sulfur moiety in its chemical structure, however GC-mass spectrometry or other chemical identification methods would be needed to positively identify those metabolites.

Table 5-II. Mean Peak Heights of Parent ^{14}CHD (Peak 1) and HD, TDG (Peak 2), and Other Metabolites Containing a Sulfur Moiety (Peaks 3 And 4) At 0.25, 1, and 2 Hrs After a 2.85 Mg Topical Dose of HD in Ethanol. Peak Numbers Shown in the Table Correspond to the Peak Numbers Shown in Figure 5-5.

IPPSF No.	0.25 Hours After Dosing				1.0 Hour After Dosing				2.0 Hours After Dosing			
	Peak 1: (HD)	*Peak 2: (TDG)*	*Peak 3:*	*Peak 4:*	*Peak 1: (HD)*	*Peak 2: (TDG)*	*Peak 3:*	*Peak 4:*	*Peak 1: (HD)*	*Peak 2: (TDG)*	*Peak 3:*	*Peak 4:*
2000	80882	185354	NP	27334	17811	107125	NP	23926	11885	77216	NP	16955
2001	11186	22486	248207	NP	NP	NP	118559	8815	NP	NP	35547	10614
2002	NP	321226	NP	27860	NP	580434	NP	23086	NP	738331	NP	10362
2003	NP	81334	NP	15596	NP	44827	NP	10204	NP	NP	39461	2583

NP = No Peak

Discussion

Using a ^{14}C-radiolabeled form of HD, it was found that the peak flux of the dosing solution occurred within 20 min after application to the IPPSF skin surface and that the flux of ^{14}C varied greatly between IPPSFs. The degradation of HD into metabolites via hydrolysis has been reported to occur *in vitro* as well as *in vivo*. Based solely on this ^{14}C flux data, it would be difficult to determine if the total ^{14}C activity was associated with the parent HD or with the plethora of metabolites reported, two of which being hemi-mustard and thiodiglycol. It was also not known whether the ^{14}C activity would be associated with only a few or with all of those HD metabolites reported in the open literature. Given these problems of metabolism and non-specificity of the ^{14}C assay, it was therefore necessary to devise a way to inhibit or stop the metabolism of HD in the venous perfusate and then assay this matrix for parent HD as well as any metabolites that may be present in this model.

HD was demonstrated to degrade rather quickly over a short (0.75 hr) period of time in the venous IPPSF perfusate when left undisturbed at ambient temperature, indicating that if the

34% NaCl solution had not been added at the time of sample collection, a skewed picture of parent HD flux and subsequent metabolite formation would have been reported. In contrast, the addition of large amounts of Cl^- ions from NaCl was clearly demonstrated to inhibit the degradation of HD in the IPPSF venous perfusate samples, presumably due to the lack of formation of the ethylenesulphonium ion, the rate-limiting step in HD hydrolysis (Sass and Steger, 1982). Snap-freezing the samples also likely contributed to slowing the process of degradation of HD in our samples to <5%. Due to the susceptible nature of HD to degrade in aqueous media, it was imperative to retard the degradation of HD in the IPPSF perfusate prior to extraction. A large quantity of the IPPSF perfusion media is water and protein, therefore retarding the degradation of HD and then extracting the IPPSF perfusate samples into ethyl acetate prior to injection onto the GC allowed the removal of unwanted chemical contaminants containing sulfur moieties (*ie.* proteins, metabolic products of skin metabolism, etc.) and the retention of >95% of the parent HD and apparently some (but perhaps not all) of HD metabolites. It was not our intent to positively identify all of the HD metabolites produced by porcine skin. Our goal in this study was to obtain a "snap-shot" of HD content in the venous perfusate samples and to affirm that metabolites do exist and that metabolism is halted once the perfusate exited from the IPPSF.

As seen in Table 5-II, the most intriguing finding was that only 2 of the 4 IPPSFs studied showed any detectable venous flux of parent ^{14}CHD within 0.25 hrs after dosing, added to the fact that the flux of HD in those IPPSFs was extremely small and beyond the limits of our assay technique to determine a quantitative concentration of HD. Interestingly, only 1 IPPSF showed any detectable level of HD for the entire 2 hr experiment, further supporting the variable overall flux data seen in the ^{14}C radiolabelled portion of this study. It appears from this data that pig skin, like human skin, has the ability to metabolize a vast majority of the HD presented to it in the lower layers of the epidermis. This statement is supported by the observation that the majority of the peaks observed were those of HD metabolites, one of which was identified as thiodiglycol.

This experiment detected small quantities of parent HD permeates through pig skin and into the venous perfusate in the IPPSF model. This study also demonstrated that HD metabolic capabilities are present in the pig skin of the IPPSF and that metabolites of HD, one of which was thiodiglycol, may be the only measurable component of HD percutaneous penetration in the IPPSF. Therefore, the IPPSF model appears to be an acceptable alternative *in vitro* model for studying the percutaneous absorption and metabolism of HD in skin.

REFERENCES

Bartek, M.J., Labudde, J.A., and Maibach, H.I. (1972). Skin permeability *in* vivo: Comparison in rat, rabbit, pig, and man. J. Invest. Dermatol. 58:114-123.

Black, R.M., and Read, R.W. (1991). Methods for the analysis of thiodiglycol sulphoxide, a metabolite of sulphur mustard, in urine using gas chromatography-mass spectrometry. J. Chromat. 558:393-404.

Black, R.M., Clark, R. J., and Read, R.W. (1991). Analysis of 1,1'-sulphonylbis[2-(methyl sulphinyl)ethane] and 1-methylsulphinyl -2-[2-(methylthio)ethylsulphonyl]ethane, metabolites of sulphur mustard, in urine using gas chromatography-mass spectrometry. J. Chromat. 558:405-414.

Black, R.M., Hambrook, J.L., Howells, D.J., and Read, R.W. (1992). Biological fate of sulfur mustard, 1,1'-thiobis(2-chloroethane). Urinary excretion profiles of hydrolysis products and β-lyase metabolites of sulfur mustard after cutaneous application in rats. J. Analytical Toxicol. 16:79-84.

Bowman, K.F., Monteiro-Riviere, N.A., and Riviere, J.E. (1991). Development of surgical techniques for preparation of *in vitro* isolated perfused porcine skin flaps for percutaneous absorption studies. Am. J. Vet. Res. 52:75-82.

Carver, M.P., Williams, P.L., and Riviere, J.E. (1989). The isolated perfused porcine skin flap. III. Percutaneous absorption pharmacokinetics of organophosphates, steroids, benzoic acid, and caffeine. Toxicol. Appl. Pharmacol. 97:324-337.

Davidson, C., Rozman, R.S., and Smith, P.K. (1961). Metabolism of bis-ß-chloroethyl sulfide (sulfur mustard gas). Biochem. Pharmacol. 7:65-74.

Hambrook, J.L., Harrison, J.M., Howells, D.J., and Schock, C. (1992). Biological fate of sulphur mustard (1,1'-thiobis(2-chloroethane)): Urinary and faecal excretion of ^{35}S by rat after injection or cutaneous application of ^{35}S-labelled sulphur mustard. Xenobiotica. 22:65-75.

King, J.R., and Monteiro-Riviere, N.A. (1990). Cutaneous toxicity of 2-chloroethyl methyl sulfide in isolated perfused porcine skin. Toxicol. Appl. Pharmacol. 104:167-179.

King, J.R., and Monteiro-Riviere, N.A. (1991). Effects of organic solvent vehicles on the viability and morphology of isolated perfused porcine skin. Toxicol. 69:11-26.

King, J.R., Riviere, J.E., and Monteiro-Riviere, N.A. (1992). Characterization of lewisite toxicity in isolated perfused skin. Toxicol. Appl. Pharmacol. 116:189-201.

Maisonneuve, A., Callebat, I., Debordes, L., and Coppet, L. (1992) Specific and sensitive quantitation of 2,2- dichlorodiethyl sulphide (sulphur mustard) in water, plasma and blood: Application to toxicokinetic study in the rat after intravenous intoxication. J Chromat. 583:155-165.

Monteiro-Riviere, N.A. (1990). Altered epidermal morphology secondary to lidocaine iontophoresis: *In vitro* and *in vivo* studies in porcine skin. Fundam. Appl. Toxicol. 15:174-185.

Monteiro-Riviere, N.A. (1990). Specialized technique: The isolated perfused porcine skin flap (IPPSF). In Methods for Skin Absorption, (Eds. B.W. Kemppainen and W.G. Reifenrath). CRC Press, Boca Raton, FL., pp. 175-189.

Monteiro-Riviere, N.A., and Stromberg, M.W. (1985). Ultrastructure of the integument of the domestic pig (*Sus scrofa*) from one through fourteen weeks of age. Anat. Histol. Embryol. 14:97-115.

Monteiro-Riviere, N.A., King, J.R., and Riviere, J.E. (1991). Mustard induced vesication in isolated perfused skin: biochemical, physiological, and morphological studies. In Proceedings of the Medical Defense Bioscience Review, U.S. Army Medical Research Institute of Chemical Defense, Aberdeen Proving Ground, MD. pp. 159-162.

Papirmeister, B., Gross, C.L., Meier, H.L., Petrali, J.P., and Johnson, J.B. (1985). Molecular basis for mustard-induced vesication. Fundam. and Appl. Toxicol. 5:S134-S149.

Riviere, J.E., Bowman, K.F., Monteiro-Riviere, N.A., Carver, M.P., and Dix, L.P. (1986). The isolated perfused porcine skin flap (IPPSF). I. A novel *in vitro* model for percutaneous absorption and cutaneous toxicology studies. Fundam. Appl. Toxicol. 7:444-453.

Riviere, J.E., Sage, B.S., and Williams, P.L. (1990). The effects of vasoactive drugs on transdermal lidocaine iontophoresis. J. Pharm. Sci. 80:615-620.

Riviere, J.E. (1991). *In* vitro absorption skin flap model. In *In Vitro* Percutaneous Absorption: Principles, Fundamentals, and Applications. (Eds. R.L. Bronaugh and H.I. Maibach), CRC Press, Boca Raton, FL, pp. 207-222.

Riviere, J.E. and Monteiro-Riviere, N.A. (1991). The isolated perfused porcine skin flap as an *in vitro* model for percutaneous absorption and cutaneous toxicology. CRC Crit. Rev. Toxicol. 21:329-344.

Roberts, J.J., and Warwick, G.P. (1963). Studies of the mode of action of alkylating agents VI: The metabolism of bis-2-chloroethylsulphide (mustard gas) and related compounds. Biochem. Pharmacol. 12:1329-1334.

Sandelowsky, I., Simon, G.A., Bel, P., Barak, R., and Vincze, A. (1992). N^1-(2-hydroxyethylthioethyl)-4-methyl imidazole (4-met-1-imid-thiodiglycol) in plasma and urine: A novel metabolite following dermal exposure to sulphur mustard. Arch. Toxicol. 66:296-297.

Sass, S., and Steger, R.J. (1982). Gas chromatographic differentiation and estimation of some sulfur and nitrogen mustards using a multidetector technique. J. Chromat. 238:121-132.

Srikrishna, V., and Monteiro-Riviere, N.A. (1991). The effects of sodium hydroxide and hydrochloric acid on the isolated perfused porcine skin flap. In Vitro Toxicol. 4:207-215.

Srikrishna, V., Riviere, J.E., and Monteiro-Riviere, N.A. (1992). Cutaneous toxicity and absorption of paraquat in porcine skin. Toxicol. Appl. Pharmacol. 115:89-97.

Vycudilik, W. (1985). Detection of mustard gas bis(2-chloroethyl)-sulfide in urine. Foren. Sci. International. 28:131-136.

Wormser, U. (1991) Toxicology of mustard gas. TIPS. 12:164-167.

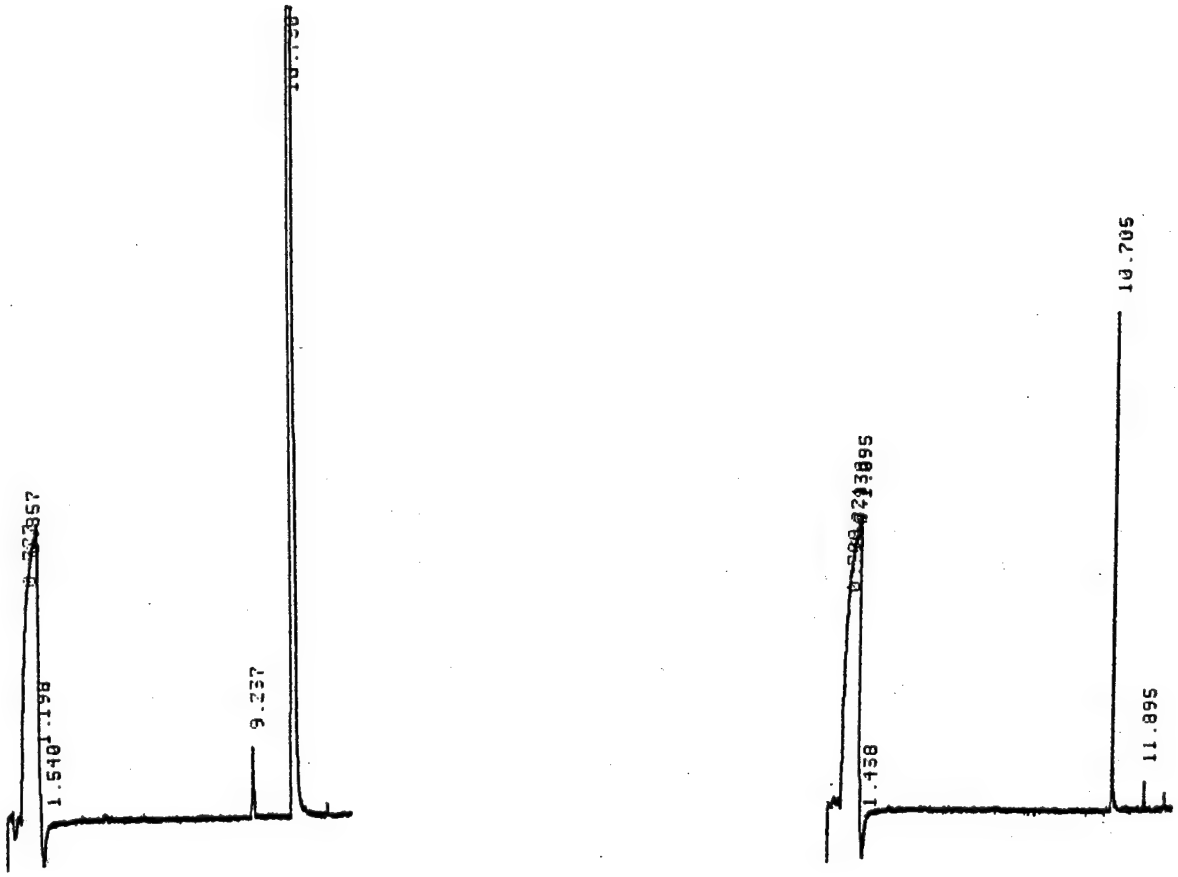

Figure 5-1. Gas chromatogram of (a) an IPPSF perfusate sample spiked with 12 μg/ml HD, then immediately extracted and assayed, and (b) an identical sample allowed to sit at ambient temperature for 0.75 hr before extraction and assay (calculated concentration = 3.6 μg/ml).

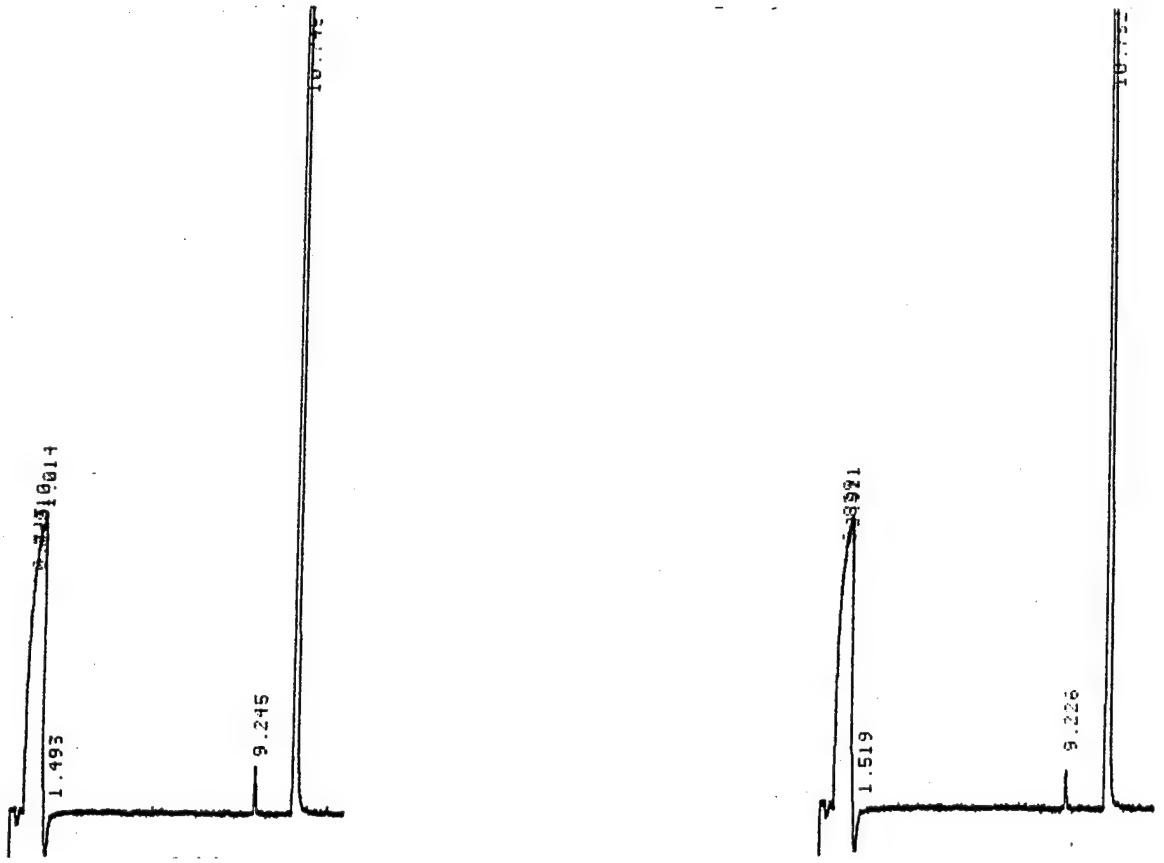

Figure 5-2. Gas chromatogram of (a) an IPPSF perfusate sample spiked with 12 μg/ml HD with 34% NaCl added, then immediately extracted and assayed, and (b) an identical sample allowed to sit at ambient temperature for 0.75 hr before extraction and assay (calculated concentration = 11.1 μg/ml).

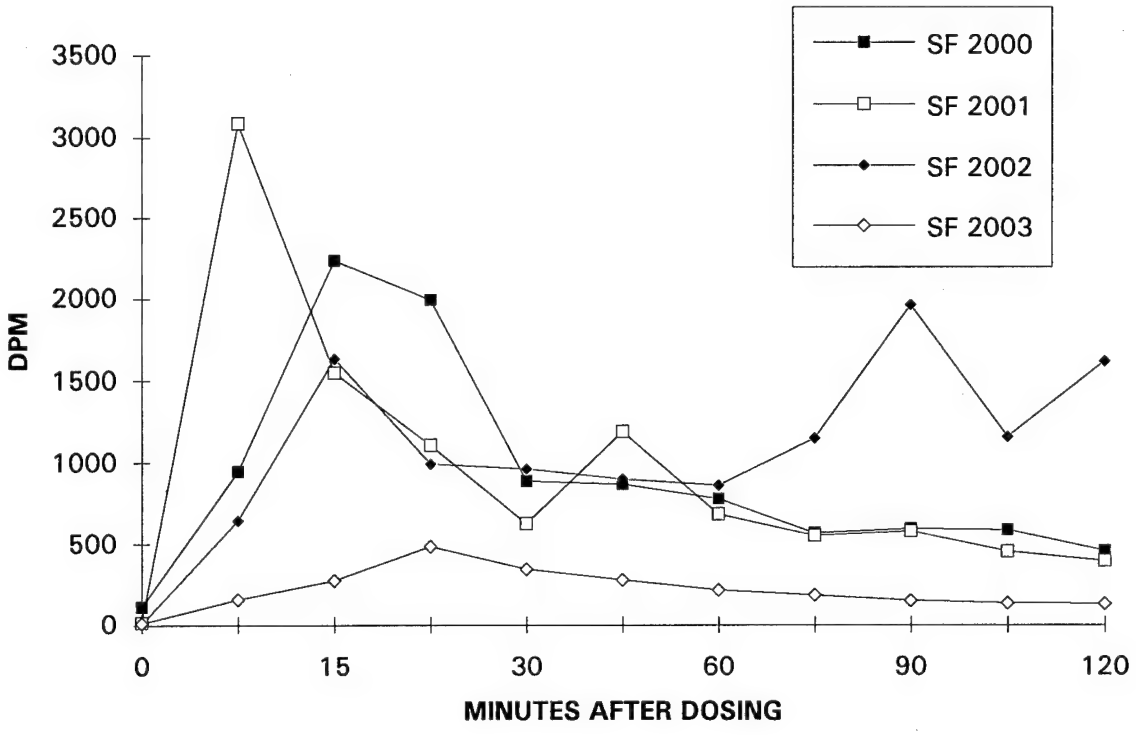

Figure 5-3. Graph of ^{14}C activity in 250 µl of venous perfusate after a 2.85 mg topical dose of ^{14}C-HD.

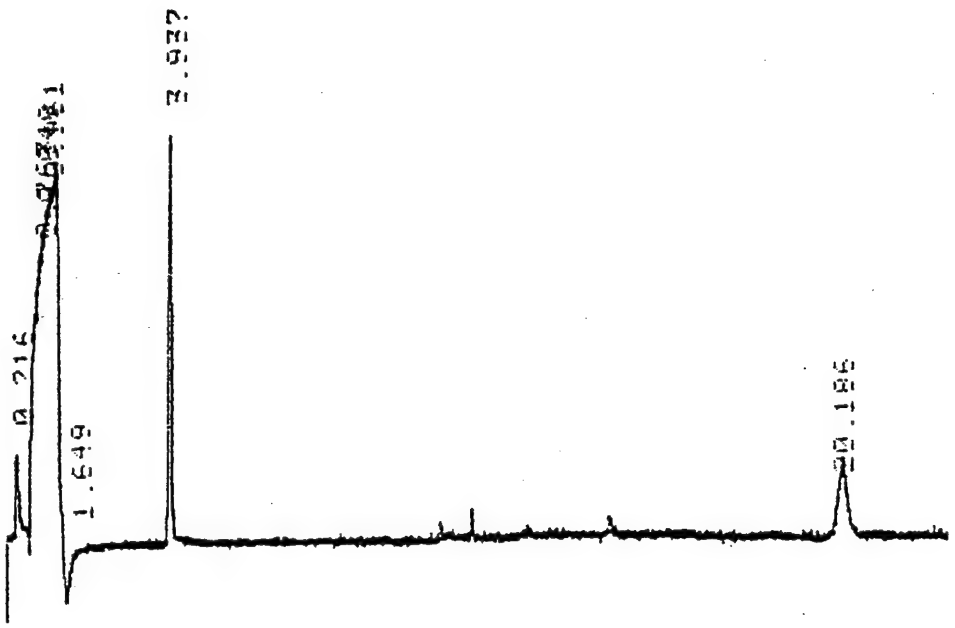

Figure 5-4. Typical gas chromatogram of an extracted IPPSF perfusate sample prior to dosing with HD.

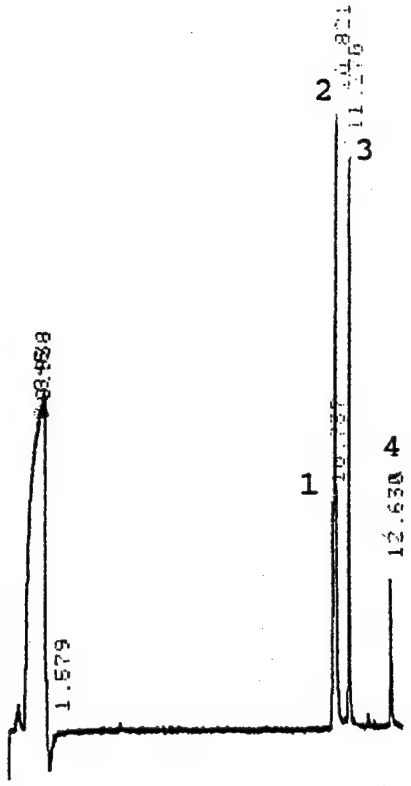

Figure 5-5. Typical gas chromatogram of an extracted IPPSF perfusate sample after the IPPSF received a 2.85 mg topical dose of ^{14}CHD in ethanol. Each of the 4 labeled peaks corresponds to the peak heights described in Table 5-II.

6. TOXICOKINETICS OF TOPICAL SULFUR MUSTARD PENETRATION, DISPOSITION, AND VASCULAR TOXICITY IN ISOLATED PERFUSED PORCINE SKIN

J.E. Riviere, J.D. Brooks, P.L. Williams, and N.A. Monteiro-Riviere

Published in *Toxicology and Applied Pharmacology* 135:25-34, 1995

Abstract

Sulfur mustard bis-(2-chloroethyl) sulfide (HD) is a bifunctional alkylating agent that causes cutaneous vesication. The isolated perfused porcine skin flap (IPPSF) is an *in vitro* model that has been used to study this toxic response. The purpose of this study was to formulate a toxicokinetic model of HD penetration and cutaneous disposition as an aid in correlating critical steps in the pathogenesis of vesication to HD concentrations in different regions of skin. ^{14}C-HD was dosed topically in ethanol at 10.0 mg/ml in a 7.5 cm^2 dosing site and venous efflux samples collected over 2, 4, or 8 hr. At the termination of the experiment, stratum corneum tape strips, core biopsies for serial sections, and the entire skin flap were collected for radioassay. Peak ^{14}C radiolabel flux occurred within 5 to 60 min in all skin flaps, much earlier than signs of HD-induced toxicity. A toxicokinetic model was used to quantitate the time profile of HD disposition in different skin compartments. Estimates of vascular and extracellular volume changes due to topical HD toxicity were estimated using radiolabeled albumin and inulin infusions. A second toxicokinetic model, with a time-variant distribution rate, was used to simulate volume changes. In order to accurately predict HD disposition, it was necessary to add another compartment as a reservoir for slowly released metabolites of HD. This model provides a quantitative profile of the time course of HD (or metabolites) disposition within skin which would aid in the interpretation of mechanistic studies of vesication as well as in designing interventive antivesicant drug strategies.

Introduction

Sulfur mustard, bis-(2-chloroethyl) sulfide (HD), is an old chemical warfare agent that causes vesication upon exposure to skin. It is well documented for its severe cutaneous damage (Papirmeister et al., 1991). The isolated perfused porcine skin flap (IPPSF) was developed in our laboratory as a novel *in vitro* model for percutaneous absorption and cutaneous toxicity. Because traditional *in vitro* models used to study skin toxicity usually do not contain an intact anatomic structure, they fail to mimic the complex physiological responses to HD. The IPPSF has been used to evaluate dermally toxic compounds including vesicants (Riviere et al., 1986; Riviere and Monteiro-Riviere, 1991; Srikrishna et al., 1992; Monteiro-Riviere, 1993). This model demonstrated biochemical, vascular, and morphological changes when exposed to HD (Monteiro-Riviere et al., 1990, Zhang et al., 1995a), including the formation of macroscopic blisters, that were identical to human cutaneous exposure to HD (Requena et al., 1988), hemimustard (King and Monteiro-Riviere, 1990), and lewisite (King et al., 1992).

The purpose of this study was to characterize the dermato-toxicokinetic profile of topically applied HD in the IPPSF. There were three major components to this task which culminated in a toxicokinetic-toxicodynamic model (TK-TD) of HD action in the IPPSF. These are 1) formulation of a dermato-pharmacokinetic model based on an analysis of individual skin flap data; 2) determination of the change in vascular and extracellular volumes as an effect of HD absorption; and 3) formulation of a more general dermato-toxicokinetic model that accounts for time-variant distribution of HD resulting from dynamic changes in vascular volume.

The primary reason for conducting this study was to formulate a basic kinetic model to support the development of the more complex TK-TD model for vesication as an endpoint. The initial individual analyses presented assume that all toxicokinetic rate constants do not change over the course of an experiment. Based upon all of the physiological data presented, we know that this assumption cannot be true, thus the final model incorporates a time-variant

distribution rate from the dermis into the vasculature to simulate a change in vascular volume caused by HD absorption.

Materials and Methods

Phase 1: Mustard penetration study

Twelve IPPSFs were used in the study. The technique of IPPSF perfusion is fully described elsewhere (Riviere et al., 1986; Monteiro-Riviere, 1990; Riviere and Monteiro-Riviere, 1991). Following a 1 hr predosing period the skin flaps received a 300 µl dose of 10.0 mg/ml ^{14}C-labeled HD (0.53 mCi/mmol) (radiochemical purity of ^{14}C-HD was determined by GC with thermal conductance to be 92.8%) in ethanol which was obtained from the U.S. Army Medical Research and Development Command. Total dose for each skin flap was 10 µCi in a 1.25 cm x 6 cm (7.5 cm^2) Stomahesive® template (ConvaTec, Princeton, NJ). The templates were secured to the skin flaps using Skin-Bond (Pfizer Hospital, Inc., Largo, FL). Three skin flaps each were run for 2 hr and 4 hr; 6 skin flaps were run for 8 hr post-dosing. This is the same dosing condition used in our previous HD toxicology studies.

Sampling was identical for all skin flap experiments. Venous efflux samples were taken at 5, 10, 20, 30, 45, 60, 75, 90, 105, and 120 min, and then every 30 min for 4 or 8 hr to determine the absorption profiles. At termination, several steps were taken to determine location and mass balance of the labeled compound. The template which demarcated the dosing area was removed and soaked in a known volume of ethanol for subsequent radio-analysis. The dose area was swabbed twice with a soap solution (10% solution of Ivory®, Procter & Gamble, Cincinnati, OH) and gauze and then tape stripped 12 times with cellophane tape (3M, St. Paul, MN). The ventral side of the skin flap was rinsed to remove any label that had collected over the 8-hr perfusion period. The skin flap cradle was rinsed twice and all rinses were retained. The entire dose site was dissected from the skin flap with a razor blade and then a 1 cm x 1 cm core sample was removed from the center and snap-frozen (see procedure below) for the penetration study. The remainder of the dose site was retained for

radio-analysis. The skin under the stomahesive template was dissected with a razor blade and separated from the subcutaneous fat after snap-freezing in liquid nitrogen. All the tissue samples (except the excised frozen core sample) and subcutaneous samples were dissolved individually in Soluene-350 (Packard Instrument Co., Downers Grove, IL). The leaks that resulted from the dissection of the skin flap, the fingertips of the gloves, and the instruments used during dissection were cleaned and the swabs retained for analysis.

Each 1.0 cm x 1.0 cm frozen core sample was placed with the epidermis side down in an aluminum foil boat and embedded in Tissue-Tek OCT (Miles, Inc., Diagnostics Division, Elkhart, IN), snap-frozen in an isopentane well immersed in liquid nitrogen, and stored at -80°C. Sectioning was performed on a Reichert-Jung Cryocut Model 1800 (Reichert Ophthalmic Instruments, Werner-Lambert Technologies, Inc., Buffalo, NY). Two 40 μm sections were combined for each sample taken from the frozen core. Samples from the cryostat were kept on dry ice until assayed to minimize evaporation of the radiolabeled compound.

All the above samples were assayed for radiolabel via a Packard Model 306 Tissue Oxidizer and samples counted on a Packard Model 1900TR Tri-Carb Liquid Scintillation Analyzer (Packard Instrument Co., Downers Grove, IL). The individual assay values were used in the subsequent modeling analysis.

Toxicokinetic model rate constants were estimated with the CONSAM computer program (Foster and Boston, 1983; Berman et al., 1983) using an iterative least-squares criterion. A multi-compartmental toxicokinetic model (Figure 6-1) was utilized to analyze this data. This model is based on similar studies previously reported by our group (Williams et al., 1990; Williams and Riviere, 1995).

The results of these assays from the IPPSF experiments were utilized as constraints for parameter estimation in several of the compartments in the multi-compartment passive topical kinetic model used to describe compound penetration and distribution. Compartment 8 (evaporative loss) is represented by unrecovered compound. Compartment 4 (surface) is represented by the swabs used to remove the surface compound. Compartment 9 (stratum

corneum and upper epidermis) is represented by the tape-strips plus 75% of the first 80 μm cryostat core sample. Compartment 2 (basal epidermis and basement membrane (BM) region excluding all stratum corneum) is represented by 25% of the first 80 μm frozen core sample. This is an important section since it contains both putative targets of HD, basal epidermal cells and the basement membrane region. These thicknesses are based on previously published IPPSF data (Monteiro-Riviere et al., 1987). All core samples were normalized to the entire dose area--i.e., multiplied by 7.5. Compartment 3 (dermis) is represented by the label found in the frozen core samples from 80 μm through 1100 μm. Compartment 5 (subcutaneous fat) is represented by the label found in the fat plus the remainder of the cryostat core samples. Compartment 12 (total skin) is the sum of compartments 1 + 2 + 3 + 9. This corresponds to the whole flap measure, excluding fat--that is, the tape strips plus all the skin measures (including the frozen core samples) and the leaks. Effluent is the cumulative amount of label measured in the venous effluent samples. Finally, recent work in our laboratory (Spoo et al., 1995) and that of others indicated that HD is metabolized in skin. Although metabolites were not assayed, this process was taken into account in a second modeling exercise.

Phase 2: Vascular and extracellular volume study

A total of 11 skin flaps were used for the vascular and extracellular volume of distribution study. All skin flaps were dosed intra-arterially in perfused IPPSF media with ^{125}I-labeled bovine serum albumin (45 mg/ml BSA) and ^{14}C-labeled inulin (3.5 μg/ml inulin). Five of the skin flaps received 300 μl of absolute ethanol (control, 0.0 mg/ml HD), 3 received 300 μl of 5.0 mg/ml of HD in ethanol, and 3 received 300 μl of 10.0 mg/ml of HD in ethanol. All topical doses were administered within a 1.25 cm x 6.0 cm (7.5 cm^2) dosing area. The ^{125}I-labeled BSA (4.01 mCi/mg) and the ^{14}C-labeled inulin (2.59 mCi/g) were both purchased from NEN Research Products, Wilmington, DE.

Arterial samples (the media before it entered the skin flap) and venous efflux samples were taken at 5, 10, 15, 20, 25, 30, 40, 50, 60, 75, 90, and 120 min, and then every 30 min for 6 hr to determine the absorption profiles. At termination (6 hr), similar steps were taken to

determine location and mass balance of the infused labeled compounds as in the topically-dosed study.

All of the above samples were assayed for ^{14}C-radiolabel via a Packard Model 306 Tissue Oxidizer and the samples were counted on a Packard Model 1900TR Tri-Carb Liquid Scintillation Analyzer (Packard Instrument Co., Downers Grove, IL). All of the above samples were assayed for ^{125}I-radiolabel via an LKB Model 1272 CliniGamma (Pharmacia LKB Biotechnology, Inc., Gaithersberg, MD). The individual assay values were used in the subsequent analysis.

Extracellular and vascular volumes of distribution were calculated as follows: Concentrations were calculated by converting DPMs to μg using specific activity. Flux was calculated by multiplying concentration by the flow rate over time. The volumes of distribution for both inulin (extracellular) and BSA (vascular) spaces were estimated using equation 1.

$$V(T) = M(T)/C_V(T) \qquad (1)$$

where: T = length of infusion (experiment length).

$M(T)$ = estimated mass of radiolabel in skin flap at t=T.

$C_V(T)$ = concentration of radiolabel emerging at t=T.

The estimation of M(T) was calculated using equation 2.

$$M(T) = \int_0^T J_A(t)dt - \int_0^T J_V(t)dt \qquad (2)$$

where: $J_A(t)$ = calculated arterial flux at time t.

$J_V(t)$ = calculated venous flux at time t.

Each value was divided by the individual skin flap mass. The integrals were approximated using the trapezoidal rule. Therefore, the extracellular volume of distribution change was calculated from the mass of the inulin remaining in the skin flap over time, and the vascular volume of distribution change was calculated from the mass of the BSA remaining in the skin flap over time. The values were then normalized to the fraction of the initial volumes of distribution. The above method has been published in detail elsewhere (Williams and Riviere, 1989). Linear regression analysis using statistical analysis software (SAS Institute Inc., Cary, NC) was performed to determine statistically the existence of non-zero slopes.

Results

Phase 1: Mustard penetration study

Table 6-I lists the results in percentage of the initial dose (mean $\pm$ SD) for the twelve IPPSF experiments. Listed are the total number of hr of each experiment, the number of replicates for each, the penetration, the absorption, the time of peak flux, and the observed peak flux listed in μg/min and percent-dose/min. Absorption is the amount of label detected in the venous efflux. Penetration is absorption plus the amount of label detected in the skin samples, the frozen core sample, the subcutaneous fat, and the leaks resulting from skin flap dissection.

The mean linear rate constants for the IPPSF experiments and the standard deviation are listed in Table 6-II. The final column in the table is the linear rate constants resulting from the application of CONSAM to the mean of twelve constraints for each compartment. The multiple constraints (2 hr, 4 hr, and 8 hr) allowed for more accurate curve fitting. That is, a single observed data point at termination cannot accurately describe a curve, while several points along that curve can offer some indication of curve shape. Figure 6-2 illustrates the result from the fit of the mean constraints of the twelve IPPSFs and shows the good agreement between the calculated and the mean observed ($\pm$ SEM) masses. Illustrated are a) the calculated and observed venous flux; b) the calculated and observed surface and evaporative

loss masses; c) the calculated and observed stratum corneum/upper epidermis and total skin masses; d) the calculated and observed dermis and effluent masses; (e) the calculated and observed fat mass; and (f) the calculated and observed basal epidermis/BM region mass. All skin flaps received the same dose: 3000 µg of ^{14}C-HD in ethanol.

Table 6-I. HD Penetration Results in Percentage of Dose [Dose(d) = 400 µg/cm^2].

IPPSF (mean±SD)	Dose Time (hr)	Penetration (%d)	Absorption (%d)	Time of Peak Flux (min)	Observed Peak Flux (ug/min)	Observed Peak Flux (%d/min)
1828	8-hr	7.0	4.7	15	1.78	0.059
1829	8-hr	10.5	6.0	30	0.97	0.032
1834	8-hr	3.4	2.1	5	1.74	0.058
1835	8-hr	10.3	6.0	45	1.33	0.044
1836	8-hr	2.6	1.7	25	0.94	0.031
1837	8-hr	4.9	3.3	60	1.13	0.038
Mean	8-hr	6.5	4.0	30.0	1.3	0.044
SD	(n=6)	3.4	1.9	20.0	0.4	0.012
1888	4-hr	1.8	0.7	45	0.14	0.005
1889	4-hr	6.6	2.8	45	0.64	0.021
1890	4-hr	11.9	3.6	45	1.20	0.040
Mean	4-hr	6.7	2.4	45.0	0.7	0.022
SD	(n=3)	5.0	1.5	0.0	0.5	0.018
2000	2-hr	3.8	1.7	10	0.91	0.030
2001	2-hr	2.9	1.5	10	0.83	0.028
2003	2-hr	1.9	0.5	15	0.24	0.008
Mean	2-hr	2.9	1.2	11.7	0.7	0.022
SD	(n=3)	0.9	0.7	2.9	0.4	0.012

Table 6-II. Passive Topical Kinetic Model Linear Rate Constants (/min).

Dose time (hr)	8 hr (n = 6) Mean	SD	4 hr (n = 3) Mean	SD	2 hr (n = 3) Mean	SD	Fit Mean Constraints (n = 12)
k_{48}	0.28	0.06	0.25	0.09	0.34	0.03	0.26
k_{49}	0.38	0.13	0.16	0.05	0.30	0.04	0.31
k_{94}	0.37	0.12	0.11	0.01	0.32	0.06	0.36
k_{92}	0.39	0.16	0.11	0.01	0.24	0.04	0.27
k_{29}	0.34	0.07	0.11	0.01	0.30	0.05	0.36
k_{23}	0.40	0.10	0.15	0.07	0.29	0.07	0.35
k_{32}	0.15	0.04	0.09	0.01	0.24	0.02	0.10
k_{31}	0.37	0.07	0.15	0.07	0.35	0.13	0.30
k_{13}	0.17	0.04	0.09	0.01	0.22	0.02	0.15
k_{35}	0.0014	0.0005	0.0020	0.0014	0.0025	0.0019	0.0029
k_{53}	0.0026	0.0012	0.0027	0.0021	0.0014	0.000	0.0040

Phase 2: Vascular and extracellular volume study

Table 6-III lists the accumulated changes (mean $\pm$ SD) in extracellular and vascular volumes of distribution over the course of the experiment for the eleven IPPSF studies. The tabulated data is the mean initial and mean final volumes of distribution in ml/g of skin flap tissue, and the mean changes in extracellular and vascular volumes of distribution. The volume of distribution changes were calculated from the individual final volumes divided by the initial volumes (fraction of the initial value). Note that the volume changes were calculated from individual skin flap data and not from the mean tabulated data.

Linear regression analysis of HD dose vs extracellular volume of distribution changes indicate a positive slope of 0.465 with a 95% probability that the slope is not zero ($p > 0.047$). Linear regression analysis of the vascular volume of distribution changes indicate a negative slope of -0.331 with a 97% probability that the slope is not zero ($p > 0.027$).

Figure 6-3a and 6-3b are graphic representations of the volume of distribution changes. The HD-treated skin flaps demonstrated different BSA and inulin profiles from the EtOH-treated control skin flaps, suggesting that HD alters the vascular permeability and extracellular fluid space of the IPPSF. The HD-treated skin flaps demonstrated an increase in extracellular volumes of distribution and a decrease in vascular volumes of distribution over the EtOH-

treated control skin flaps as a function of HD concentration (0.0 mg/ml HD vs 5.0 mg/ml HD vs 10.0 mg/ml HD).

Table 6-III. Accumulated Extracellular and Vascular Volume of Distribution Changes [Fractions of Initial Value].

	EtOH topical (n = 5)		**5 mg/ml HD (n = 3)**		**10 mg/ml HD (n = 3)**	
	Mean	SD	Mean	SD	Mean	SD
	INULIN - Extracellular volume of distribution changes					
Initial Vd (ml/g)	0.34	0.11	0.26	0.14	0.22	0.19
Final Vd (ml/g)	1.10	0.65	1.53	0.76	1.42	0.64
Vd change	3.79	2.61	6.13	3.06	8.43	3.48
	BSA - Vascular volume of distribution changes					
Initial Vd (ml/g)	0.07	0.04	0.15	0.08	0.12	0.06
Final Vd (ml/g)	0.57	0.27	1.07	0.48	0.57	0.23
Vd change	8.71	1.86	7.43	1.19	5.35	2.15

Phase 3: Use of a time-variant distribution rate to simulate change in vascular volume

In Figure 6-4, compartment 1 is drawn to suggest a decrease in vascular volume due to HD absorption. The distribution rate k_{31} is shown as a time-variant function as in equation 3. We feel that this distribution rate best reflects the change in vascular permeability reflected by the differential changes in inulin and albumin spaces. Selection of this equation is empirical to reflect the observed value changes and is not meant to be definitive at this stage of research.

$$k_{31} = ae^{-b*t} \qquad (3)$$

where: a = the maximum for the k_{31} distribution rate.

b = exponential constant.

An independent study in our laboratory suggests the occurrence of metabolism of HD in the skin (Spoo et al., 1995). No attempt has been made to determine which metabolites are present, however, compartment 22 is necessary to predict the slow release of radiolabel after the initial penetration occurring within the first hour. This slow release may also occur from

compartment 5 (fat) as more hydrophilic metabolites are partitioned from the fat. Figure 6-5 illustrates the same profiles as Figure 6-2, except the time-variant k_{31} distribution rate has been implemented, and a slow-releasing metabolism compartment 22 has been added. Note the excellent fit for this model. With the time-variant distribution rate and the slow release metabolism compartment 22, it was possible to more closely predict the venous flux profiles. The mean ($\pm$ SD) distribution rates for the twelve skin flaps, after implementation of the time-variant distribution rate and the slow-release metabolism compartment, are listed in Table 6-IV. Again, the final column in the table is the result of the application of CONSAM to the mean of 12 constraints for each compartment, and Figure 6-5 illustrates these calculated and observed results. Table 6-IV indicates a 14% decrease in the mean time-variant distribution rate k_{31}, (0.340 at t=0 compared to 0.294 at t=480).

The mean total recovery of radiolabel was 9.3% (range 3.8% to 17.7%). This indicates the volatility of HD. We made no attempt to trap the radiolabel, as this would cause an occluded condition which would deviate from the dosing conditions used in all HD toxicology studies. It must be stressed that the purpose of the study was to determine absorption, penetration, and distribution of HD under relevant exposure conditions and correlate to the previously conducted toxicologic studies.

Table 6-IV. Passive Topical Kinetic Model Rate Constants (/min) with Time- Variant k_{31} and Compartment 22 (/min).

Dose time (hr)	8 hr (n = 6) Mean	8 hr (n = 6) SD	4 hr (n = 3) Mean	4 hr (n = 3) SD	2 hr (n = 3) Mean	2 hr (n = 3) SD	Fit Mean Constraint (n=12)
k_{48}	0.34	0.03	0.33	0.08	0.35	0.02	0.34
k_{49}	0.29	0.03	0.18	0.07	0.26	0.01	0.25
k_{94}	0.36	0.13	0.08	0.00	0.35	0.09	0.23
k_{92}	0.29	0.10	0.11	0.03	0.26	0.05	0.26
k_{29}	0.35	0.08	0.08	0.00	0.35	0.09	0.22
$k_{2,22}$	0.11	0.02	0.10	0.01	0.17	0.02	0.12
$k_{22,2}$	0.006	0.004	0.004	0.004	0.028	0.003	0.007
k_{23}	0.35	0.07	0.13	0.01	0.27	0.06	0.24
k_{32}	0.15	0.04	0.06	0.00	0.27	0.05	0.12
k_{31} (t = 0) (*a*)[a]	0.40	0.10	0.16	0.05	0.34	0.10	0.33
k_{31} (t =480)[b]	0.363	0.087	0.153	0.051	0.294	0.083	0.315
(*b*)[c]	0.0002	0.0001	0.0001	0.0000	0.0003	0.0000	0.0001
k_{13}	0.16	0.03	0.06	0.00	0.24	0.03	0.12
k_{35}	0.0052	0.0015	0.0044	0.0038	0.0050	0.0040	0.0058
k_{53}	0.0036	0.0015	0.0046	0.0023	0.0006	0.0004	0.0060

[a] *(a)* Represents the initial value (t=0 min) of the time-variant distribution rate k_{31}

[b] Represents the terminal value (t=480, 240, or 120 min) of the time-variant dibution rate

[c] *(b)* Represents the exponential constant in the equation: $k_{31}=ae^{-b*t}$.

Discussion

IPPSFs were used to study absorption and distribution of HD. The bulk of the absorption occurs rapidly within 1 hr with a majority of the absorbed dose either penetrated into the skin or in the nous efflux. The rapid HD absorption and evaporative loss due to volatility is similar to that reported by other investigators (Nagy et al., 1946; Klain et al., 1988; Hambrook et al., 1992). This type of data is difficult to extract from many longer term *in vivo* studies (Davison et al., 1961; Black et al., 1992). Also, it demonstrates that at earlier time points a large fraction of the HD present in tissue (e.g. that determined in the core biopsies of the present study) is still mobile. It is probable that a large fraction of this radiolabel is not HD but one of numerous metabolites (Davison et al., 1961; Hambrook et al., 1992; Black et al., 1992; Sandelowsky et al., 1992; Spoo et al., 1995).

We were able to determine relative tissue concentrations of radiolabel. However, differentiation between bound parent and bound metabolite due to alkylation of tissues is not possible. The second model with the metabolism compartment indicates metabolism within the basal epidermis. This metabolism may also occur in other skin compartments. The percentage of metabolism indicated in our study is dependent upon this model. More invasive techniques would be required to fully identify these events, however it is beyond the scope of the present study. The profiles generated in these studies may now be correlated to histological, ultrastructural, enzyme histochemistry, and immunohistochemistry endpoints in these same tissue compartments to quantitatively delineate the mechanism of HD vessication. In this regard, the critical compartment would be the basal epidermis and BM region since these are the putative targets of HD vessication (Zhang et al., 1995a). This study would suggest that HD alkylation of BM components or direct basal epidermal cell toxicity could occur almost immediately.

The great difference in individual susceptibility to HD vesication has been widely acknowledged since the beginning of research in this area (Marshall et al., 1919). The first source of this variability must relate to the actual dose of topically exposed HD which reaches its target site within the skin. The quantity of applied HD which penetrates into the viable layers of skin is determined by its rate of surface loss in relation to its rate and extent of percutaneous absorption. As can be seen from these disposition studies (Table 6-I, amount penetrated), this is highly variable. Thus, the actual delivery of HD to its site of action is the first process which probably accounts for a significant amount of the variability in response to HD often reported.

It is evident that the extracellular volume of distribution significantly increased as a function of HD penetration. HD caused an overall decrease in vascular volume of distribution as a function of dose. These results confirm that significant changes in vascular permeability assessed by BSA space do occur.

This study provides the basic data for construction of a comprehensive dermato-toxicokinetic model. First, most of the compound absorption occurs within the first hour. This is toxicologically significant. Second, there is a significant change in BSA volume over the course of the experiment as a result of HD-induced vesication. This vascular change may be mediated by HD-induced release of prostaglandins (Zhang et al., 1995b).

The fact that BSA volume of distribution changes with time invalidates the assumptions inherent to constructing the toxicokinetic model which assumes constant volumes (Riviere and Williams, 1992). This point is critical. Since volumes are assumed constant, this actual change in volume is reflected in different parameter estimates for multiple parameters. HD is a potent toxicant which damages tissues upon exposure. This chemically induced change should thus alter the "toxicokinetic properties" of the tissue such that a dynamic PK model which incorporates these changes is really required to accurately model HD absorption. In fact, one could argue, that the difference between a pharmacokinetic and toxicokinetic model is not just the higher dose of the latter, but rather a model which directly incorporates toxicant-induced pathophysiology. This work is a step in that direction.

References

Berman, M., Beltz, W.F., Greif, P.C., Chabay, R., and Boston, R.C. (1983). *CONSAM User's Guide.* Laboratory of Mathematical Biology, U.S. Department of Health and Human Services, National Cancer Institute, National Institutes of Health, Bethesda, MD 20205.

Black, R.M., Hambrook, J.L., Howells, D.J., and Read, R.W. (1992). Biological fate of sulfur mustard, 1,1'-thiobis(2-chloroethane). Urinary excretion profiles of hydrolysis products and β-lyase metabolites of sulfur mustard after cutaneous application in rats. J. Analytical Toxicol. 16:79-84.

Davison, C., Rozman, R.S., and Smith, P.K. (1961). Metabolism of bis-β-chloroethyl sulfide (sulfur mustard gas). Biochem. Pharmacol. 7:65-74.

Foster, D.H., and Boston, R.C. (1983). The use of computers in compartmental analysis: The SAAM and CONSAM programs. In Compartmental Distribution of Radiotracers (J. Robertson, Ed.), pp. 73-142. CRC Press, Cleveland, OH.

Hambrook, J.L., Harrison, J.M., Howells, D.J., and Schock, C. (1992). Biological fate of sulphur mustard (1,1'-thiobis(2-chloroethane)): Urinary and faecal excretion of ^{35}S by rat after injection or cutaneous application of ^{35}S-labelled sulphur mustard. Xenobiotica. 22:65-75.

King, J.R., and Monteiro-Riviere, N.A. (1990). Cutaneous toxicity of 2-chloroethyl methyl sulfide in isolated perfused porcine skin. Toxicol. Appl. Pharmacol. 104:167-179.

King, J.R., Riviere, J.E., and Monteiro-Riviere, N.A. (1992). Characterization of lewisite toxicity in isolated perfused skin. Toxicol. Appl. Pharmacol. 116:189-201.

Klain, G.J., Bonner, S.J., and Omaye, S.T. (1988). Skin penetration and tissue distribution of ^{14}C Butyl 2-chloroethyl sulfide in the rat. J. Toxicol. Cut. & Ocular Toxicol. 7:255-261.

Marshall, E.K., Lynch, V., and Smith, H.W. (1919). On dichlorethylsulphide (mustard gas). II. Variations in susceptibility of the skin to dichlorethylsulphide. J. Pharmacol. Exp. Therap. 12:291-301.

Monteiro-Riviere, N.A., Bowman, K.F., Scheidt, V.J., and Riviere, J.E. (1987). The isolated perfused porcine skin flap (IPPSF): II. Ultrastructural and histological characterization of epidermal viability. In Vitro Toxicol. 1:241-252.

Monteiro-Riviere, N.A., King, J.R., and Riviere, J.E. (1990). Cutaneous toxicity of mustard and lewisite on the isolated perfused porcine skin flap. DAMD17-87-C-7139; NTIS, ADA229922, pp. 1-144.

Monteiro-Riviere, N.A., (1990). Specialized technique: The isolated perfused porcine skin flap (IPPSF). In Methods for Skin Absorption (B.W. Kemppainen and W.G. Reifenrath, Eds.), pp. 175-189. CRC Press, Boca Raton.

Monteiro-Riviere, N.A., (1993). Use of isolated perfused skin in dermatotoxicology. In Vitro Toxicol. 5:219-233.

Nagy, S.M., Golumbic, C., Stein, W.H., Fruton, J.S., and Bergmann, M. (1946). The penetration of vesicant vapors into human skin. J. Gen. Physiol. 29:441-469.

Papirmeister, B., Feister, A.J., Robinson, S.I., and Ford, R.D. (Eds.) (1991). Medical Defense Against Mustard Gas: Toxic Mechanisms and Pharmacological Implications, CRC Press, Boca Raton, FL.

Requena, L., Requena, C., Sanchez, M., Jaqueti, G., Aguilar, A., Sanchez-Yus, E., and Hernandez-Mow, B. (1988). Chemical warfare: Cutaneous lesions from mustard gas. J. Amer. Acad. Dermatol. 19:529-536.

Riviere, J.E., Bowman, K.F., Monteiro-Riviere, N.A., Carver, M.P., and Dix, L.P. (1986). The isolated perfused porcine skin flap (IPPSF). I. A novel *in vitro* model for percutaneous absorption and cutaneous toxicology studies. Fundam. Appl. Toxicol. 7:444-453.

Riviere, J.E., and Monteiro-Riviere, N.A. (1991). The isolated perfused porcine skin flap as an *in vitro* model for percutaneous absorption and cutaneous toxicology. CRC Crit. Rev. Toxicol. 21:329-344.

Riviere, J.E., and Williams, P.L. (1992). On the pharmacokinetic implications of changing blood flow in skin. J. Pharm. Sci. 81:601-602.

Sandelowsky, I., Simon, G.A., Bel, P., Barak, R., and Vincze, A. (1992). N^1-(2-hydroxyethylthioethyl)-4-methyl imidazole (4-met-1-imid-thiodiglycol) in plasma and urine: A novel metabolite following dermal exposure to sulphur mustard. Arch. Toxicol. 66:296-297.

Spoo, J.W., Monteiro-Riviere, N.A., and Riviere, J.E. (1995). Detection of sulfur mustard bis (2-chloroethyl) sulfide and metabolites after topical application in the isolated perfused porcine skin flap. Life Sci. 56:1385-1394.

Srikrishna, V., Riviere, J.E., and Monteiro-Riviere, N.A. (1992). Cutaneous toxicity and absorption of paraquat in porcine skin. Toxicol. Appl. Pharmacol. 115:89-97.

Williams, P.L., and Riviere, J.E. (1989). Estimation of physiological volumes in the isolated perfused porcine skin flap. Res. Commun. Chem. Pathol. Pharmacol. 66:145-158.

Williams, P.L., and Riviere, J.E. (1995). A biophysically-based dermatopharmacokinetic compartment model for quantifying percutaneous penetration and absorption of topically-applied agents. I. Theory. J. Pharm. Sci. 84:599-608.

Williams, P.L., Carver, M.P., and Riviere, J.E. (1990). A physiologically relevant pharmacokinetic model of xenobiotic percutaneous absorption utilizing the isolated perfused porcine skin flap. J. Pharm. Sci. 79:305-311.

Zhang, Z., Peters, B.P., and Monteiro-Riviere, N.A. (1995a). Assessment of sulfur mustard interaction with basement membrane components. Cell Biol. Toxicol. 11:89-101.

Zhang, Z., Riviere, J.E., and Monteiro-Riviere, N.A. (1995b). Evaluation of protective effects of sodium thiosulfate, cysteine, niacinamide, and indomethacin on sulfur-mustard-treated isolated perfused porcine skin. Chem.-Biol. Interactions. 96:249-262.

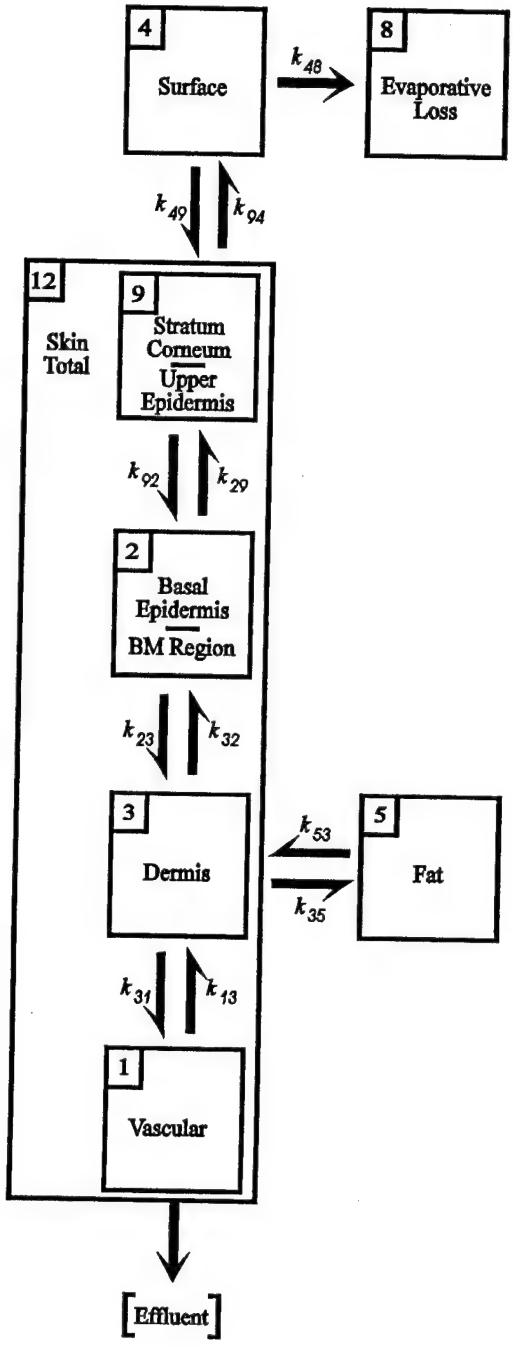

Figure 6-1. Multi-compartmental toxicokinetic model with linear rate constants used to predict HD penetration and distribution in the IPPSF.

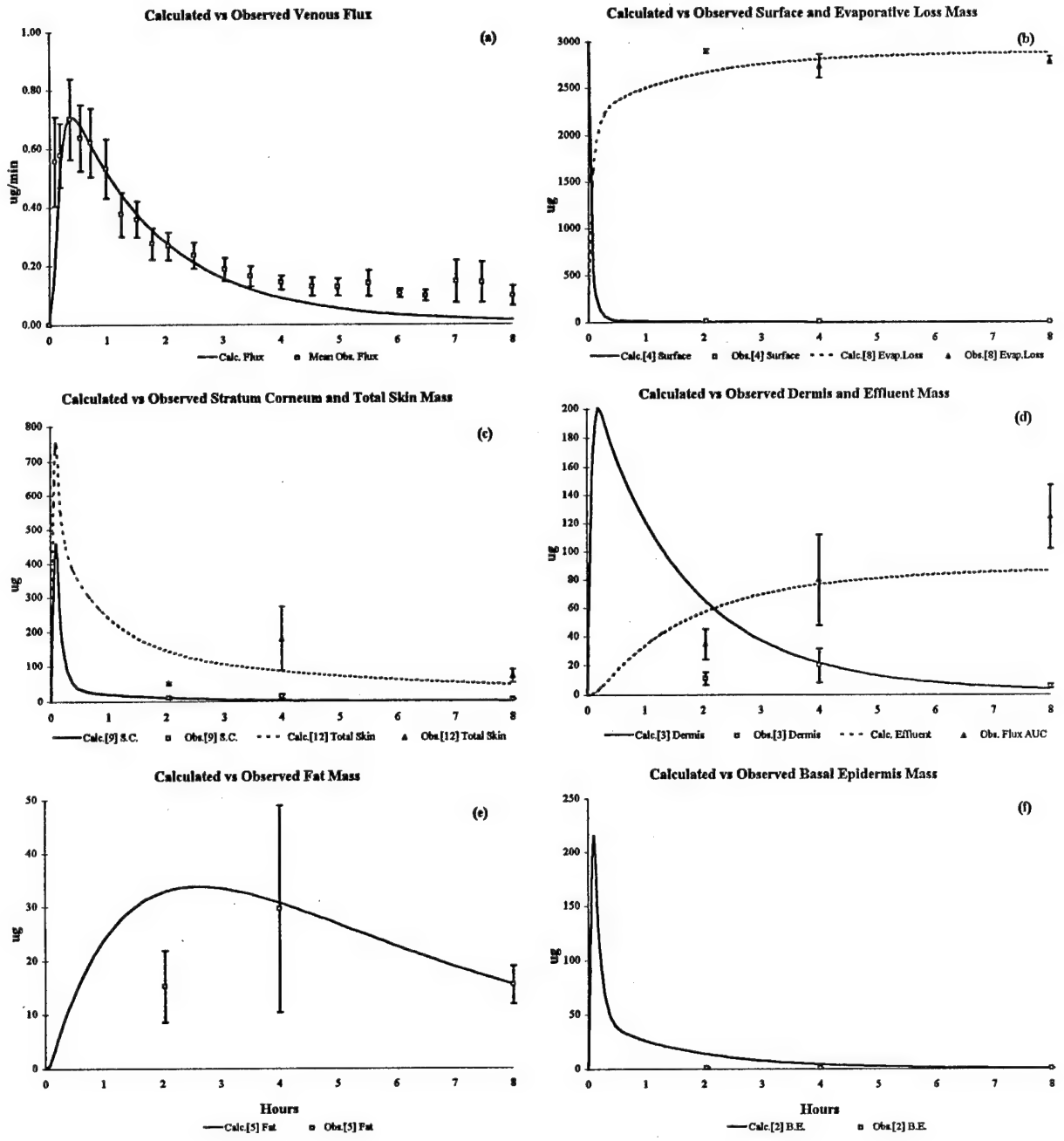

Figure 6-2. HD disposition profiles for twelve IPPSFs. Calculated with mean observed (± SEM) compartmental masses in (a) venous flux, (b) surface and evaporative loss, (c) stratum corneum/upper epidermis and total skin, (d) dermis and effluent, (e) fat, and (f) basal epidermis/basement membrane. Observed flux data is from the effluent samples. The observed compartmental data is the mass in the compartment at termination (8-hr, n=6; 4-hr, n=3; 2-hr, n=3).

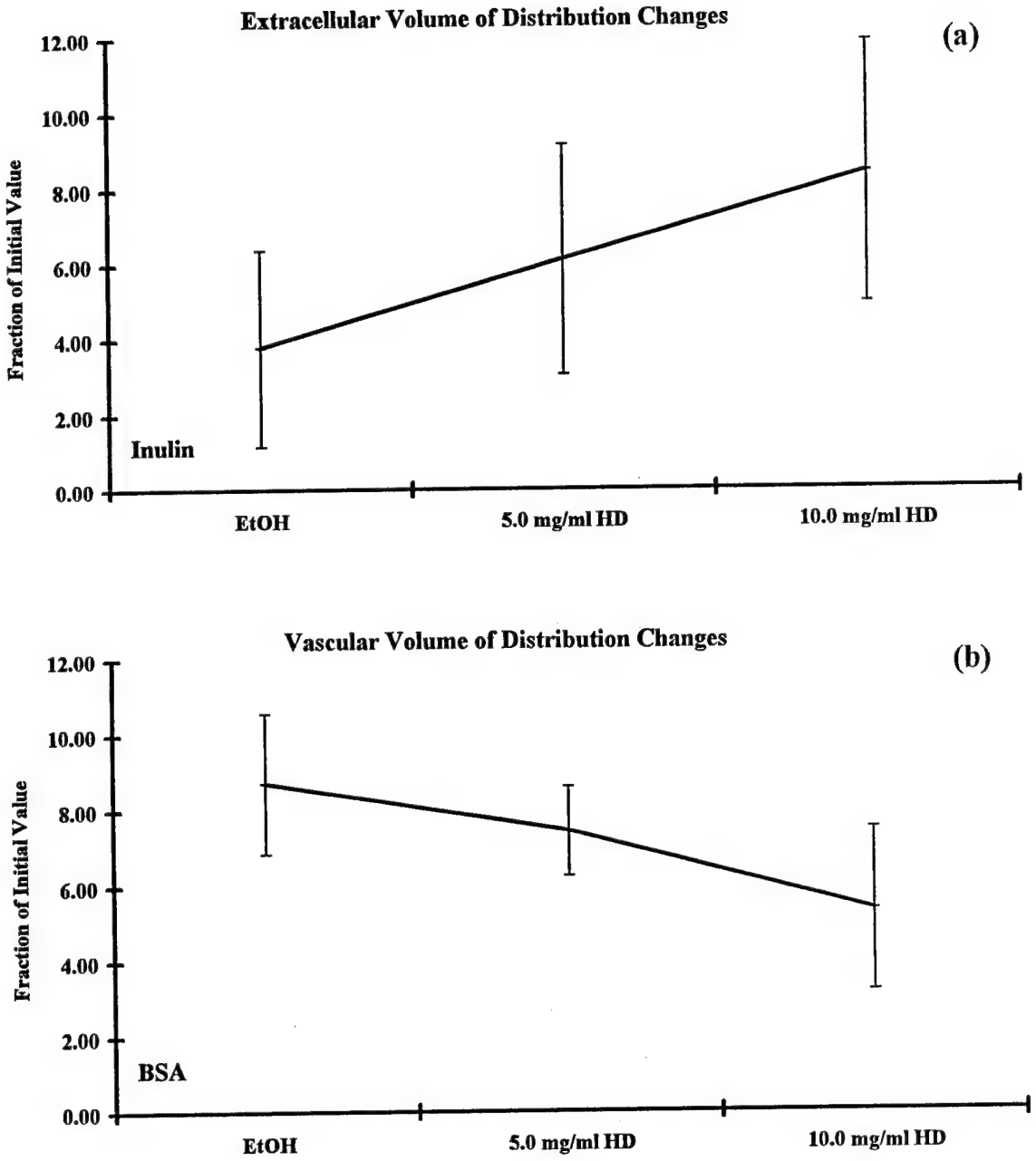

Figure 6-3. Graphic representation of (a) the extracellular volume of distribution changes and (b) the vascular volume of distribution changes (fraction of the initial volume) in the IPPSF following topical doses of ethanol, and 5.0 or 10.0 mg/ml HD. Data is listed in Table 6-III under extracellular and vascular volume of distribution changes.

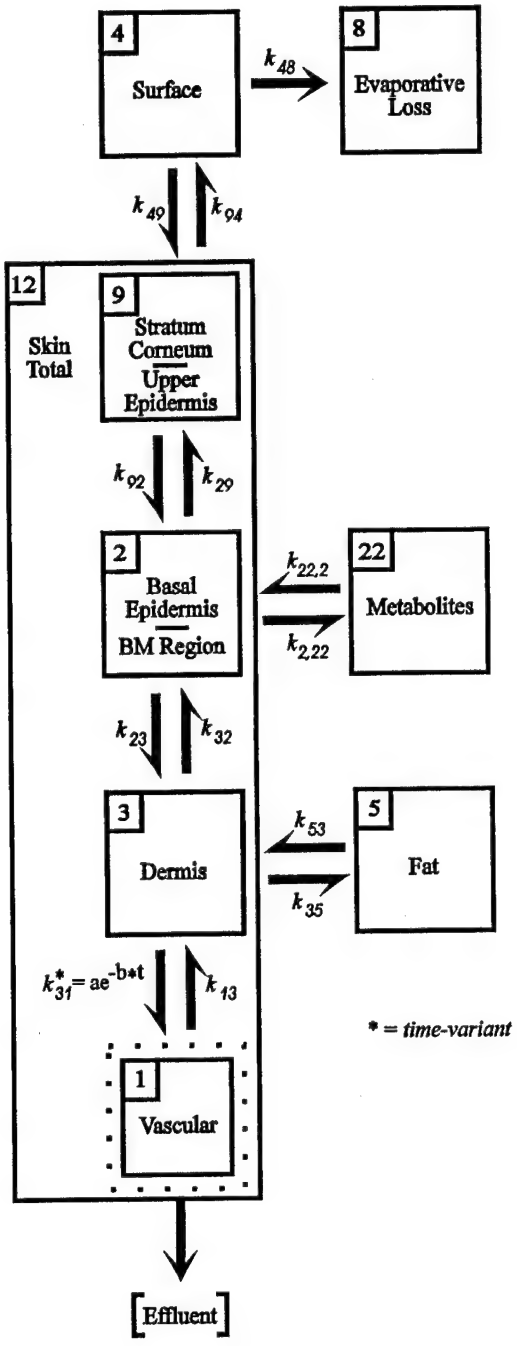

Figure 6-4. Multi-compartmental toxicokinetic model containing a time-variant distribution rate k_{31} used to predict HD penetration and distribution in the IPPSF. A decrease in vascular volume is depicted in compartment 1 vascular, and a metabolism compartment 22 allows a better fit to compartmental constraints.

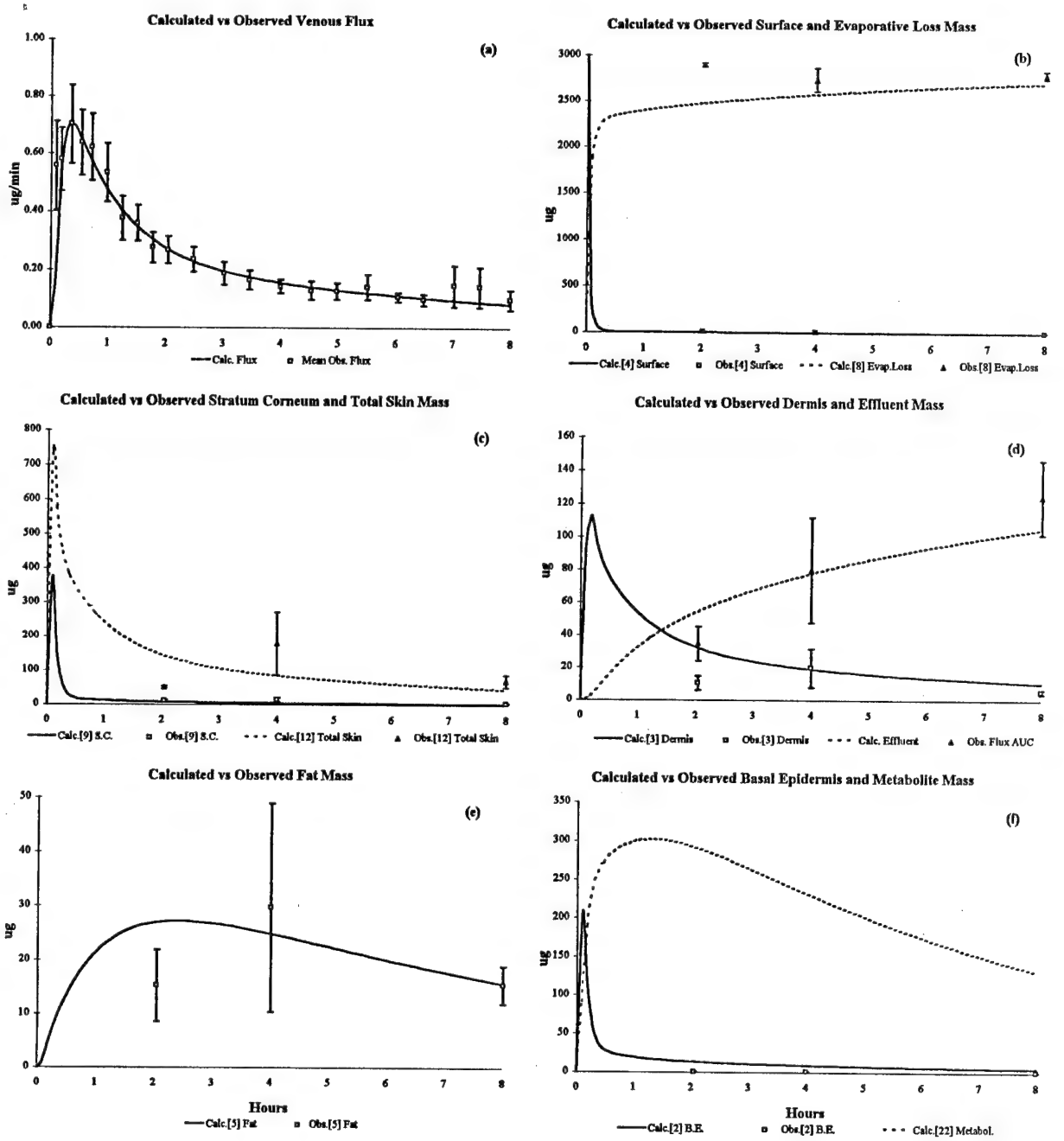

Figure 6-5. HD disposition profiles for twelve IPPSFs after implementation of a time-variant distribution rate and a metabolism compartment. Calculated with mean observed (± SEM) compartmental masses in (a) venous flux, (b) surface and evaporative loss, (c) stratum corneum/upper epidermis and total skin, (d) dermis and effluent, (e) fat, and (f) basal epidermis/basement membrane and metabolite. Observed flux data is from the effluent samples. The observed compartmental data is the mass in the compartment at termination (8-hr, n=6; 4-hr, n=3; 2-hr, n=3). Compartment 22 (metabolism) mass is calculated from the rate constants which allows the best fit of the other compartmental constraints.

CONCLUSIONS

The results reported in this final report offer significant insight into the pathogenesis of HD-induced vesication in the skin. Since HD-induced vesication is exclusively located at the epidermal-dermal junction, many current *in vitro* skin models are not suitable for HD vesication experiments, because they only possess some keratinocyte cell layers, do not have the correct lipid composition, nor adnexial structures, and lack a complete basement membrane. Study of HD-induced blister formation requires a skin model which contains an intact anatomical structure including the epidermis and the dermis. In addition, the importance of having a functional vasculature and other physiological responses in a skin model is necessary for the development of vesication, which is evident in the fact of failure to form gross blister and some epidermal-dermal separation in skin organ cultures. The IPPSF overcomes these limitations in most current *in vitro* skin models, showing its potential for studying different classifications of vesication. First, one must take into account that all of these studies were conducted in the IPPSF, an *in vitro* model whose inflammatory responses occur independent of any systemic influences. Thus HD-induced vesication in this model, which has previously been shown to be similar to *in vivo* human lesions, occurs in a milieu that is solely controlled by local cutaneous factors.

HD is a highly reactive toxic agent which can alkylate many biological molecules such as DNA, amino acids, carbohydrates, and lipids. It interferes with different cellular biological processes, and causes a variety of toxicological manifestations. Although both vesication as well as direct cytotoxicity including DNA alkylation and depletion of NAD^+ can be observed in the skin after HD exposure, it is not proper to make the conclusion that HD-induced

vesication must be caused by cytotoxicity or DNA alkylation. Alteration of cellular metabolism is a common consequence of cell injury,' and many toxic agents can cause similar cytotoxicity but are not vesicants. Furthermore, prevention of NAD^+ depletion is not correlated with blocking HD-induced vesication, and the anatomical location of HD-induced blister is different from blisters caused by most cytotoxic compounds. Accordingly, DNA alkylation, cytotoxicity, and vesication coexist in HD-induced skin injury, but this confluence does not dictate that DNA alkylation is responsible for the vesication. HD may cause blister formation by a different mechanism than what is involved in cytotoxicity. It is very important for mechanistic studies of HD-induced vesication to probe for the true underlying cause and dissect out confounding HD cytotoxicity which is unrelated to the mechanism of blister formation. That is, vesication occurs without the requisite involvement of blood-borne humoral or cellular elements of the immune system. With this knowledge at hand, these experiments attempted to define the potential mediators that are involved in modulating the vascular response (altered VR) seen after HD exposure. Inflammatory mediators including PGE_2, $PGF_{2\alpha}$, and IL-1α were released in the IPPSF after dose-specific treatment of HD. The 5.0 mg/ml of HD treatment significantly increased PGE_2 and $PGF_{2\alpha}$ release, however PGE_2 and $PGF_{2\alpha}$ were unaffected after the exposure of 10.0 mg/ml HD. In contrast, 10.0 mg/ml but not 5.0 mg/ml of HD treatment enhance the release of IL-1α. Unlike prostaglandins which are synthesized de novo, IL-1α is preformed and stored in cells. Thus, 10.0 mg/ml of HD may kill the cells to release more IL-1α, and inhibits the cells to produce PGE_2 and $PGF_{2\alpha}$. This is the most likely hypothesis to explain the HD dose specific pattern of inflammatory mediator profiles in the IPPSF. In addition, the correlation of inflammatory mediator and VR

profiles suggests that inflammatory mediator release may play a role in the IPPSF vascular response to HD.

In contrast, yet similar to that reported in human skin cultures, prostaglandins were not released at the higher exposure concentration in spite of the presence of epidermal-dermal separation. As discussed in Section 1 of the report, increased exposure to HD could result in cell death rather than injury, inhibition of arachidonic acid metabolism enzymes, or release of other classes of inflammatory mediators when more severe toxicity is seen. Additionally, direct endothelial cell injury could occur at higher HD concentrations which would ablate the vascular response to any mediator released. Changes in vascular volumes (BSA space) were detected at the 5.0 mg/ml and the 10.0 mg/ml of HD doses, suggesting that vascular involvement occurs at both doses. It must be pointed out that there is a confounding factor in assessing inflammatory mediator profiles in the IPPSF venous effluent. If mediators are locally released and as the vascular volume data suggests, tissue volume of distribution and permeability increases, there will be a local dilution of the mediator within the skin, which would tend to decrease the venous concentrations and confound interpretation of these profiles. Accompanying this vascular exudation is the increase in VR which causes edema and perfusion resistance. This vascular pooling would also lengthen the residence time of prostaglandins in the skin which, due to their lability, could result in degradation and again a decreased venous efflux in the face of increased tissue production.

In order to explore the potential mechanism of HD-induced vesication, the IPPSF was used to evaluate the antagonistic effects of the different pharmacological agents on three endpoints of HD-induced skin toxicity, including cytotoxicity, vesication and inflammation. As

cysteine, which are HD scavengers, niacinamide, an inhibitor of poly (ADP-ribose) polymerase, and indomethacin, a prostaglandin synthetase inhibitor. None of these tested agents were effective in completely blocking HD toxicity. Partial blocking of the cytotoxicity by sodium thiosulfate, cysteine and niacinamide did not correlate to the prevention of vesication, suggesting that cytotoxicity may not initiate HD-induced vesication. However, indomethacin blocked the vascular response and partially prevented the blister formation after HD treatment.

One of the most exciting results generated in the present study involves the molecular mechanism of HD-induced epidermal-dermal separation and vesication. The effect of HD exposure on six basement membrane epitopes in the IPPSF was characterized. As discussed in Section 3, these studies localized the HD-induced blister cleavage plane to be within the upper lamina lucida, above the type IV collagen, EBA and GB3, but below the BP antigenic sites. These data focus on the molecular mechanisms of direct HD action to the laminin and fibronectin. These morphological studies thus confirm the *in vitro* findings that laminin may be a primary target of HD action.

We have demonstrated in Section 4, that exposure of laminin to HD alters laminin structure, probably due to alkylation and cross-linking of laminin chains. Additionally, our studies suggest that HD-alkylated laminin inhibits cell adhesion in the absence of cytotoxicity. These data provide evidence for a direct role of HD-alkylation in the formation of a blister. However, once this blister forms, the HD-alkylated laminin is still present as a remnant at the basement membrane zone. Under normal wound-healing circumstances, normal laminin would promote epidermal cell adhesion to the dermal matrix. It is widely known that HD

blisters require a prolonged time interval for healing. Our data strongly suggest that one reason for this delayed wound healing would be the presence of HD-alkylated laminin in the wound surface which would tend to antagonize epidermal cell adhesion. Thus, the direct alkylation of laminin (and possibly other basement membrane molecules) and not HD-induced genotoxicity, may be the primary blockade to healing of HD blisters. This hypothesis would have major implications on the clinical management of HD blisters as compared to other bullous diseases and should be pursued further.

As discussed in Section 5, the flux of HD and metabolites through the skin was chartacterized and small quantities of parent HD actually permeates the skin into the venous perfusate in the IPPSF model. Also, this study demonstrated that HD metabolic capabilities are present in the IPPSF. Therefore, the IPPSF appears to be a suitable *in vitro* model for studying the percutaneous absorption and metabolism of HD in skin.

In Section 6, the final phase of this report involves formulating a comprehensive TK-TD model of HD absorption, penetration, and toxicologic effect. The first step in building such a model is to characterize, using classic compartmental modeling techniques, the time course of HD absorption in the IPPSF. These studies, based on tissue and venous efflux analyses, confirm previous worker's findings that HD is rapidly absorbed into skin. Also, they graphically illustrate the great deal of variability seen in HD absorption. This must be the proximate cause for the large variability seen in HD toxicity. However, the primary reason for conducting these initial studies was to formulate a basic kinetic model to beginning the more complex construction of a TK-TD model. These individual analyses presented in this report assume that all pharmacokinetic rate constants do not change over the course of an

experiment. Based upon all of the physiological data presented above, we know that this assumption cannot be true. In order to model this, we used the time course of vascular volume and VR changes to vary the volume of compartments 1,2, 3, and 7 of Figure 6-4 over the course of an experiment. This change will significantly impact on the value of all estimated rate constants. The profiles generated in these studies may now be correlated to histological, ultrastructural, enzyme histochemical, and immunohistochemical endpoints in these same tissue compartments to quantitatively delineate the mechanism of HD vesication. In this regard, the critical compartment would be the stratum basale cells of the epidermis and the basement membrane zone, since these are putative targets for HD vesication as mentioned in Section 4. This study suggests that HD alkylation of the basement membrane components or direct basal epidermal cell toxicity could occur almost immediately. This study provides the basic data for construction of a comprehensive dermato-toxicokinetic model. First, most of the compound absorption occurs within the first hour. This is toxicologically significant. Second, there is a significant change in BSA volume over the course of the experiment as a result of HD-induced vesication. This vascular change may be mediated by HD-induced release of prostaglandins that was discussed in Section 1. The ultimate goal would be to define the HD-concentration-response relationship at the level of the basement membrane and epidermis. This would allow a more quantitative evaluation of protective strategies which reduce HD flux across the stratum corneum and help evaluate the requirements for successful antivesicant therapy.

In conclusion, we feel that we have made significant progress in achieving the stated research goals of the present contract. All of these studies have confirmed the utility of the IPPSF to study the mechanism of HD vesication. The studies have validated our previous

reported findings and further characterize the response of the IPPSF to HD exposure and the disposition of HD within the model. This is a unique aspect of this particular model system for unlike many *in vitro* models, both absorption and toxicology studies can be done in the same model. The most exciting aspects of these results are the finding of a direct HD interaction with the laminin molecule and its implications to both the pathogenesis of HD vesication and the healing of the resulting wound.

APPENDIX

List of Publications

Monteiro-Riviere NA: The use of isolated perfused skin in dermatotoxicology. In Vitro Toxicology 5: 219-233, 1993.

Monteiro-Riviere NA, Inman AO, Spoo JW, Rogers RA, Riviere JE: Studies on the pathogenesis of bis (2-chloroethyl) sulfide (HD) induced vesication in porcine skin. In Proceedings of the 1993 Medical Defense Bioscience Review U.S. Army Medical Research Institute of Chemical Defense, Aberdeen Proving Ground, Maryland, pp. 31-40, 1993.

Monteiro-Riviere NA, Zhang JZ, Inman AO, Brooks JD, Riviere J.E. Mechanisms of Cutaneous Vesication.DAMD17-92-C-2071;NTIS,ADA283085, pp. 1-114, 1994.

Zhang JZ, Riviere JE, Monteiro-Riviere NA: Topical sulfur mustard induces changes in prostaglandins and interleukin-1α in isolated perfused porcine skin. In Vitro Toxicology 8: 149-158, 1995.

Zhang JZ, Riviere JE, Monteiro-Riviere NA: Evaluation of protective effects of sodium thiosulfate, cysteine, niacinamide, and indomethacin on sulfur mustard-treated isolated perfused porcine skin. Chemico-Biological Interactions 96:249-262,1995.

Spoo JW, Monteiro-Riviere NA, Riviere JE: Detection of sulfur mustard (bis-2-chloroethyl sulfide) and metabolites after topical application in the isolated perfused porcine skin flap. Life Sciences 56: 1385-1394, 1995.

Monteiro-Riviere NA and Inman AO: Indirect immunohistochemistry and immunoelectron microscopy distribution of eight epidermal-dermal junction epitopes in the pig and in isolated perfused skin treated with bis (2-chloroethyl) sulfide. Toxicologic Pathology 23:313-325, 1995.

Zhang JZ, Peters BP, Monteiro-Riviere NA: Assessment of sulfur mustard interaction with basement membrane components. Cell Biology and Toxicology 11:89-101, 1995.

Riviere JE, Brooks JD, Williams PL, Monteiro-Riviere NA: Toxicokinetics of topical sulfur mustard penetration, disposition, and vascular toxicity in isolated perfused porcine skin. Toxicology and Applied Pharmacology 135:25-34, 1995.

Monteiro-Riviere NA, Inman AO: Ultrastructural characterization of sulfur mustard-induced vesication in isolated perfused porcine skin. Microscopy Research and Technique (In Press).

Monteiro-Riviere NA, Riviere JE: The pig as a model for cutaneous pharmacology and toxicology research. In Swine In Biomedical Research,(Eds. ME Tumbleson and LB Schook), Plenum Publishing Corporation, New York, NY (In Press).

Monteiro-Riviere NA, Zhang JZ, Riviere JE: Pathogenesis and mechanisms of sulfur mustard. Critical Reviews in Toxicology (In Preparation-Invited Review, 1996)

Monteiro-Riviere NA, Inman AO: Characterization of mustard-induced toxicity by enzyme histochemistry in isolated perfused skin. (In preparation)

List of Published Abstracts:

Spoo SW, Riviere JE, Monteiro-Riviere NA: Prostaglandins in isolated perfused skin flaps treated with sulfur mustard. Pharmaceutical Research 9:232, 1992.

Monteiro-Riviere NA, Inman AO: Histochemical localization of three basement membrane epitopes with sulfur mustard induced toxicity in porcine skin.Toxicologist 13: 58, 1993.

Monteiro-Riviere NA, Inman AO, Spoo JW, Rogers RA, Riviere JE: Studies on the pathogenesis of bis (2-chloroethyl) sulfide (HD) induced vesication in porcine skin. In roceedings of the 1993 Medical Defense Bioscience Review pp.31-40, 1993.

Riviere JE, Monteiro-Riviere NA, Bowman KF: Development of *in vitro* isolated perfused porcine skin flaps for study of percutaneous absorption of xenobiotics. Medical Chemical Defense 6:15-16, 1993.

Monteiro-Riviere NA, Riviere JE: Cutaneous toxicity of mustard and lewisite on the isolated perfused skin flap. Medical Chemical Defense 6: 16, 1993.

Zhang Z, Peters BP, Monteiro-Riviere NA: Sulfur mustard alkylates laminin by cross linking. Toxicologist 14:428, 1994.

Riviere JE, Williams PL, Zhang Z, Monteiro-Riviere NA: Toxicokinetics of sulfur mustard cutaneous disposition and percutaneous absorption in isolated perfused porcine skin. Toxicologist 14:184, 1994.

Riviere JE, Williams PL, Zhang Z, Monteiro-Riviere NA: Toxicokinetics of sulfur mustard cutaneous disposition and percutaneous absorption in isolated perfused porcine skin. Toxicologist 14:184, 1994.

Zhang Z, Peters BP, Monteiro-Riviere NA: Assessment of the cutaneous basement membrane in sulfur mustard-induced toxicity. J. Invest. Dermatol. 103:855, 1994.

Monteiro-Riviere NA, Inman AO: Histochemical distribution of five epidermal-dermal junction epitopes in porcine skin treated with bis (2-chloroethyl) sulfide. Toxicologist 15:324, 1995.

Zhang Z, Riviere JE, Monteiro-Riviere NA: Protective effects of sodium thiosulfate, cysteine, niacinamide, and indomethacin on sulfur mustard treated isolated perfused porcine skin. Toxicologist 15:324, 1995.

List of Publications (continued)

Inman AO, Monteiro-Riviere, NA: An autoradiography study to evaluate the distribution of bis (2-chloroethyl) sulfide in the isolated perfused porcine skin flap. Toxicologist 15:324, 1995.

Monteiro-Riviere NA and Riviere JE: The pig as a model for cutaneous and pharmacology and toxicology research, Proceedings of the International Symposium on Swine in Biomedical Research, College Park, MD., p.77, 1995.

List of Posters:

Zhang Z, Peters BP, Monteiro-Riviere NA: Sulfur mustard alkylates laminin by cross linking. N.C. Society of Toxicology, Research Triangle Park, N.C. February 19, 1994.

Zhang Z, Peters BP, Monteiro-Riviere NA: Assessment of the Cutaneous Basement Membrane in Sulfur Mustard-Induced Toxicity. International Symposium on Epidermolysis Bullosa, The University of North Carolina at Chapel Hill, April 26, 1994.

Zhang Z, Riviere JE, Monteiro-Riviere NA: Protective effects of sodium thiosulfate, cysteine, niacinamide, and indomethacin on sulfur mustard treated isolated perfused porcine skin. North Carolin State University, College of Veterinary Medicine, Research Forum, April 21, 1995.